Figure

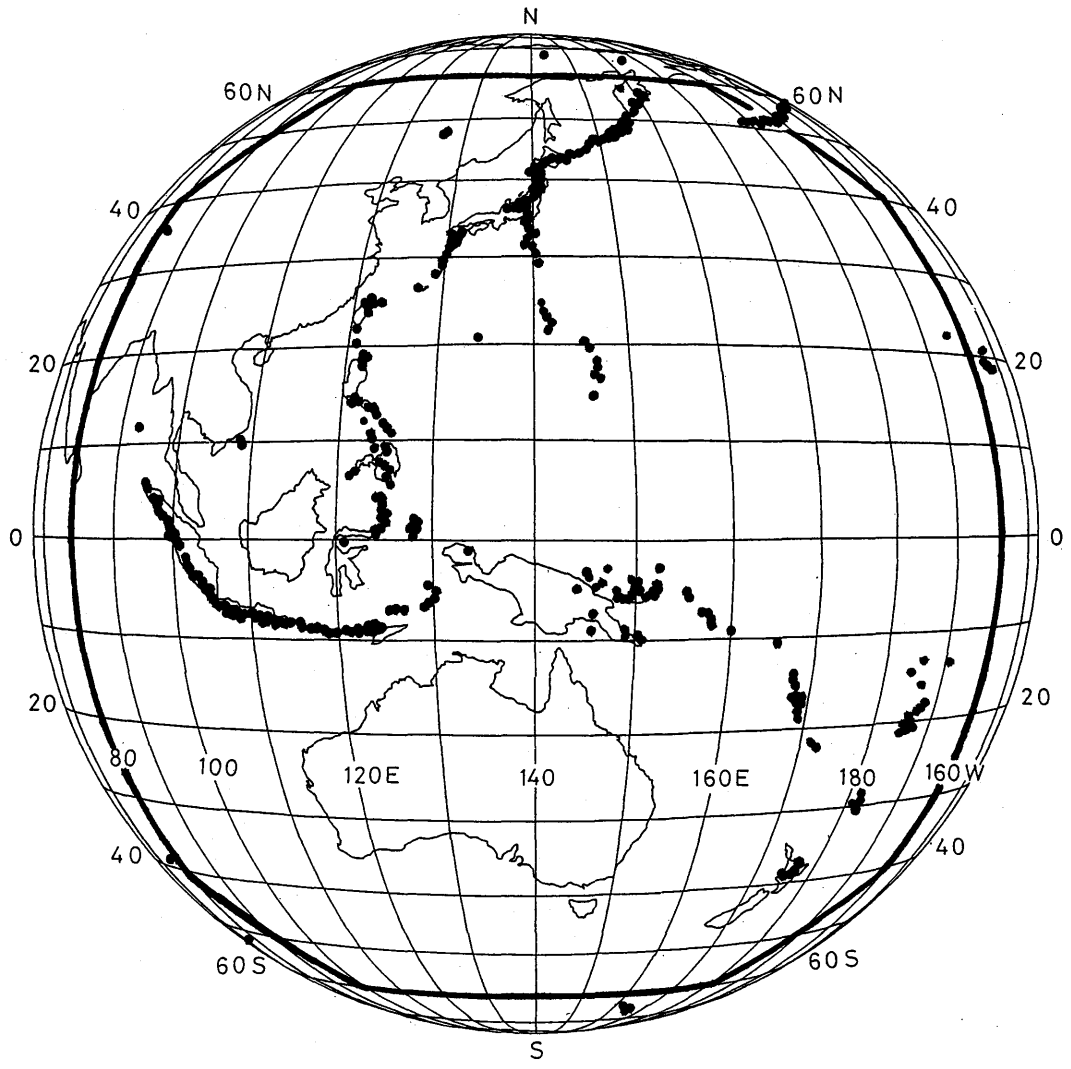

Fig. 1-1 Field of view of GMS and distribution of active volcanoes (solid circles) within the field of view encircled with bold line for this study.

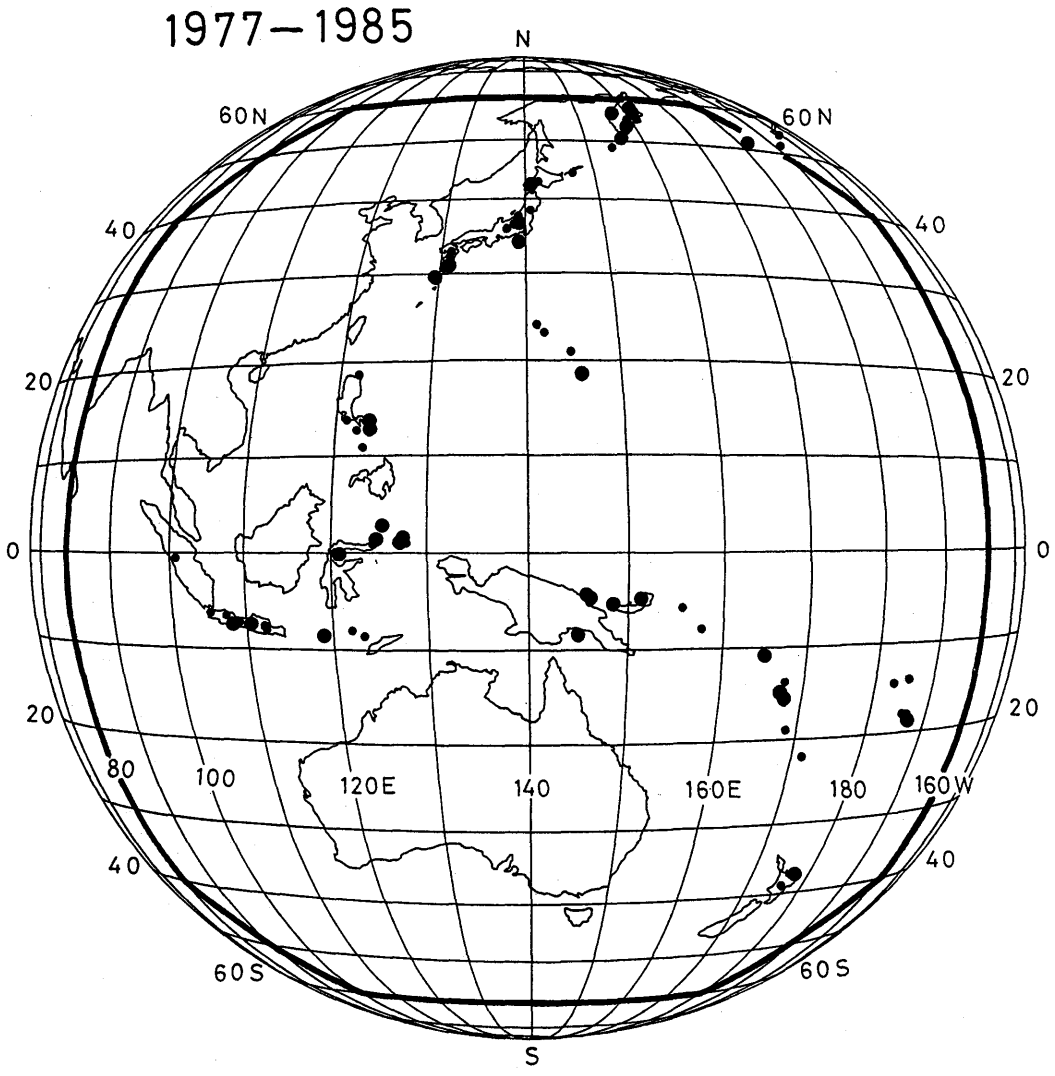

Fig. 2-1 Volcanoes which erupted during 1977-1985 within the field of view of GMS shown by bold line in Fig.1-1. Larger solid circle denotes volcano from which the eruption cloud rose higher than 4 km above the crater.

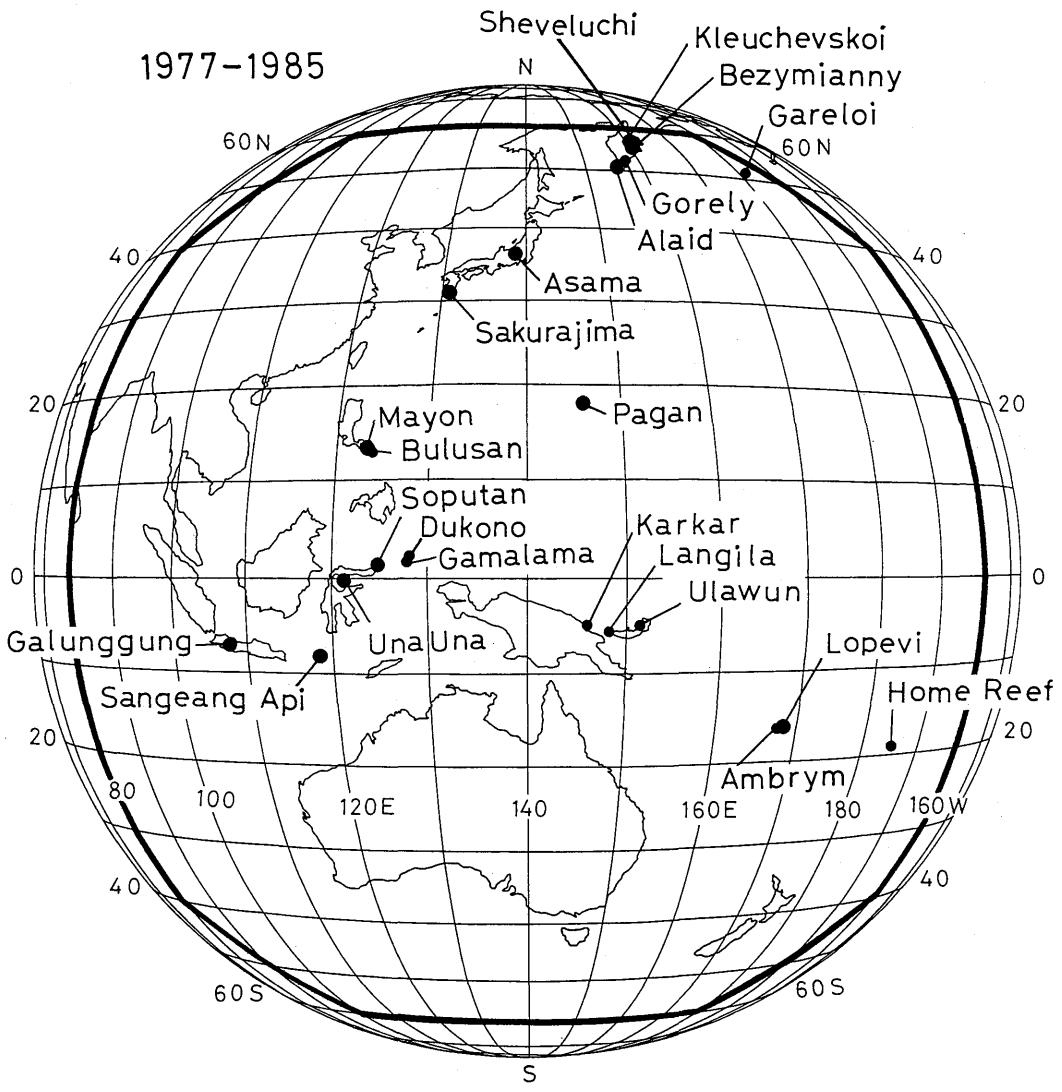

Fig. 2-2 Locations of volcanoes from which eruption clouds were detected by GMS images. Larger solid circles signify that good eruption cloud data were obtained without severe disturbances by surrounding atmospheric clouds.

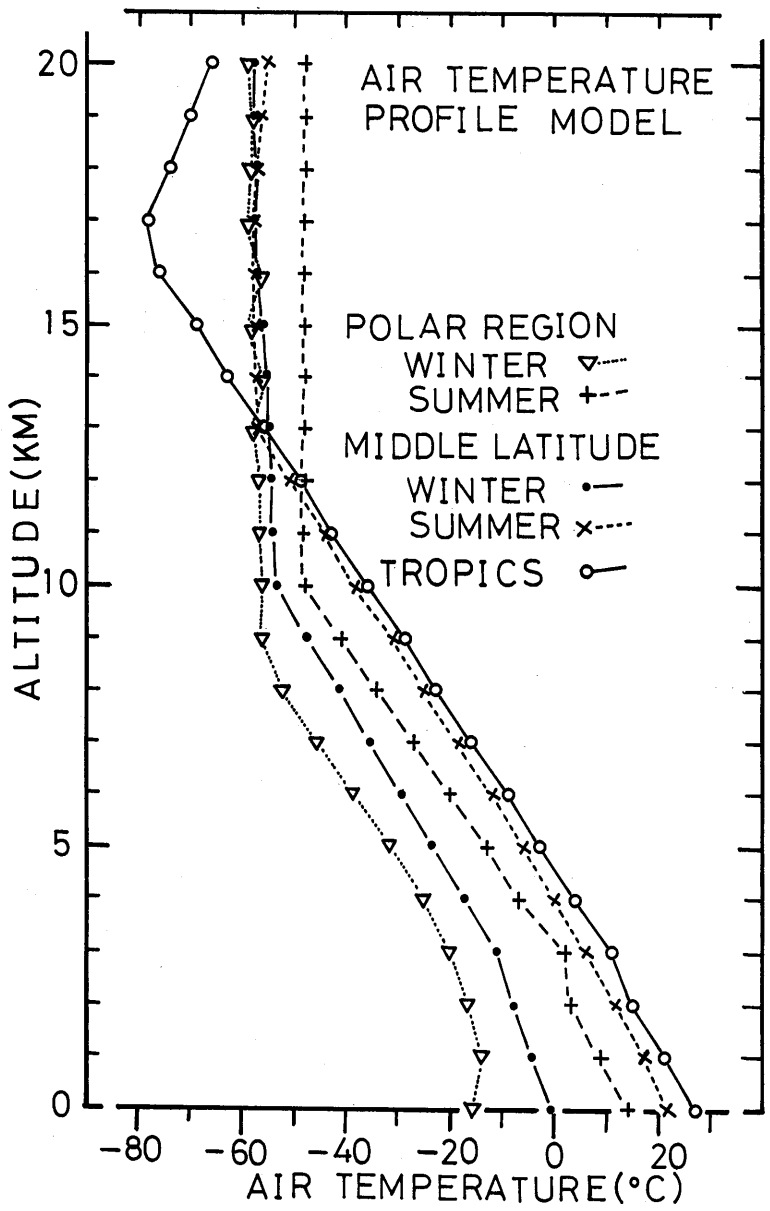

Fig. 3-1 Air-temperature profiles at three regions : polar region for winter and summer seasons, middle-latitude region for winter and summer and the tropics proposed by McClatchey et al. (1972). These data were tentatively used in this study for estimation of altitude of eruption clouds when radio-sounding materials around the volcanoes were not available.

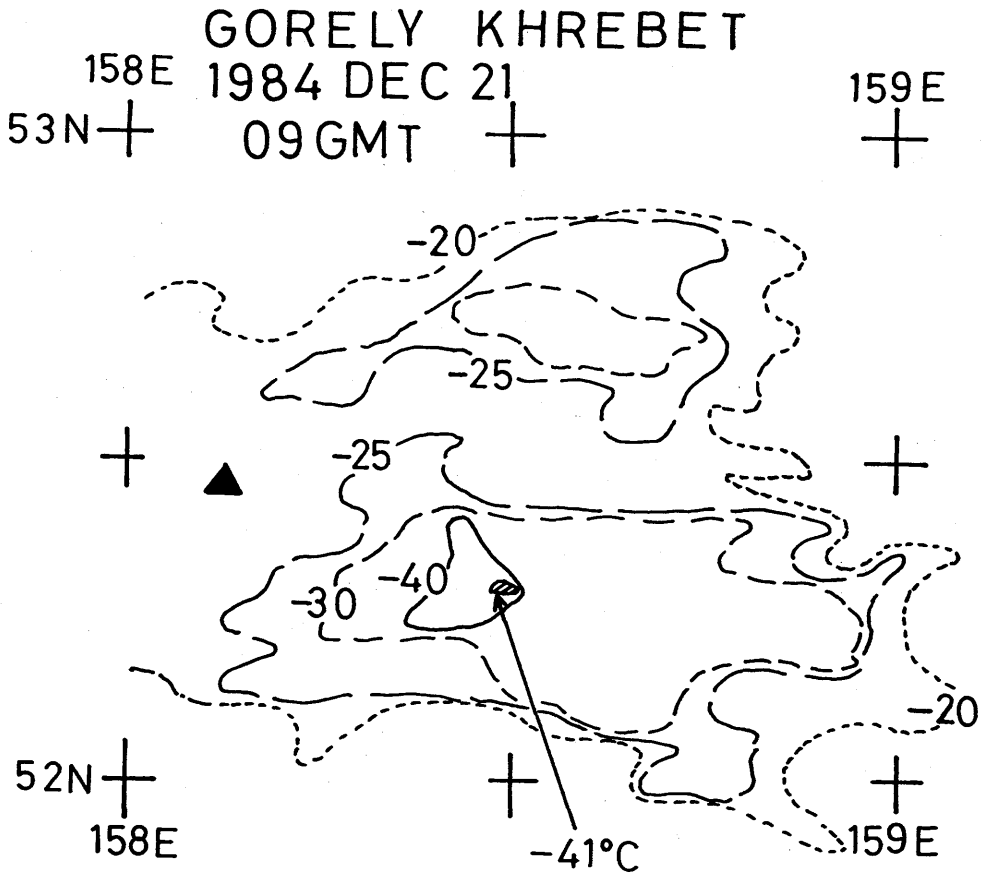

Fig. 3-2 Surface temperature distribution of the eruption cloud data from Gorely-Khrebet volcano at 09 GMT on December 21, 1984. Domain lower than -20°C is shown, the lowest being -41°C.

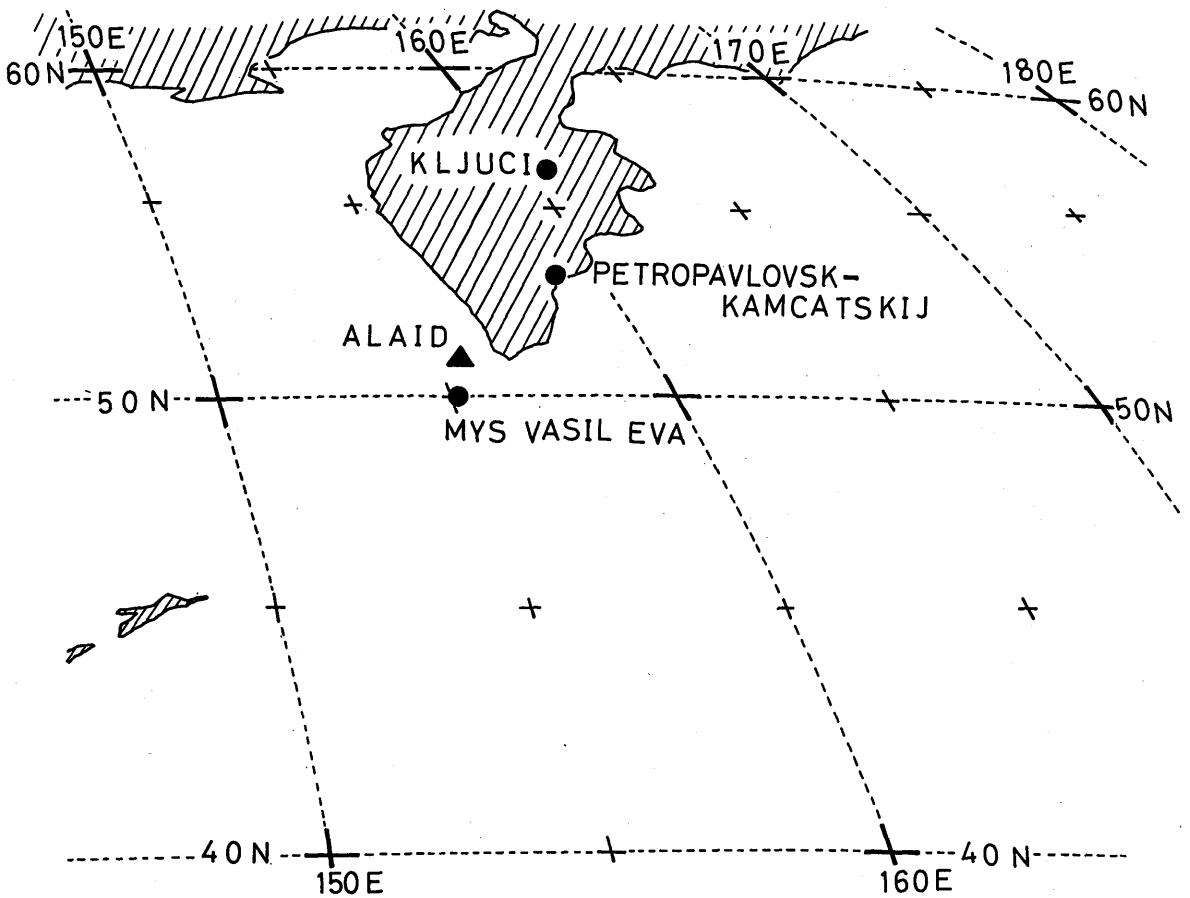

Fig. 3-3 Location of Alaid volcano indicated with a solid triangle. Solid circles denote three radio-sounding stations that provided observational materials used for estimation of altitudes of the eruption clouds.

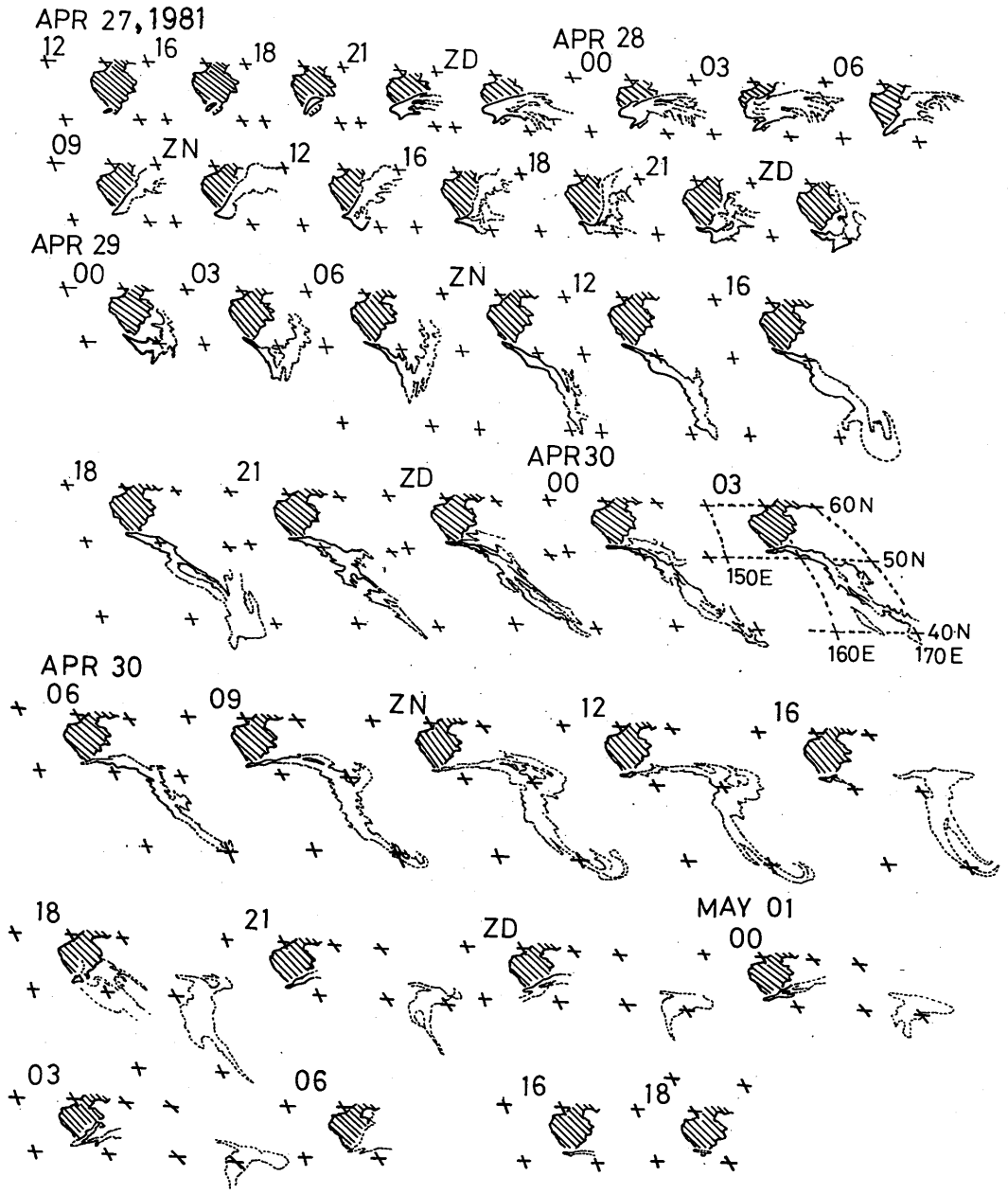

(a)

Fig. 3-4 (a)-(b)

Traced extent of eruption clouds from Alaid volcano in 1981 and 1982, detected in GMS's IR images. Eruption clouds are shown with solid lines in cases of distinct extent and with dotted ones in cases of indistinct margins.

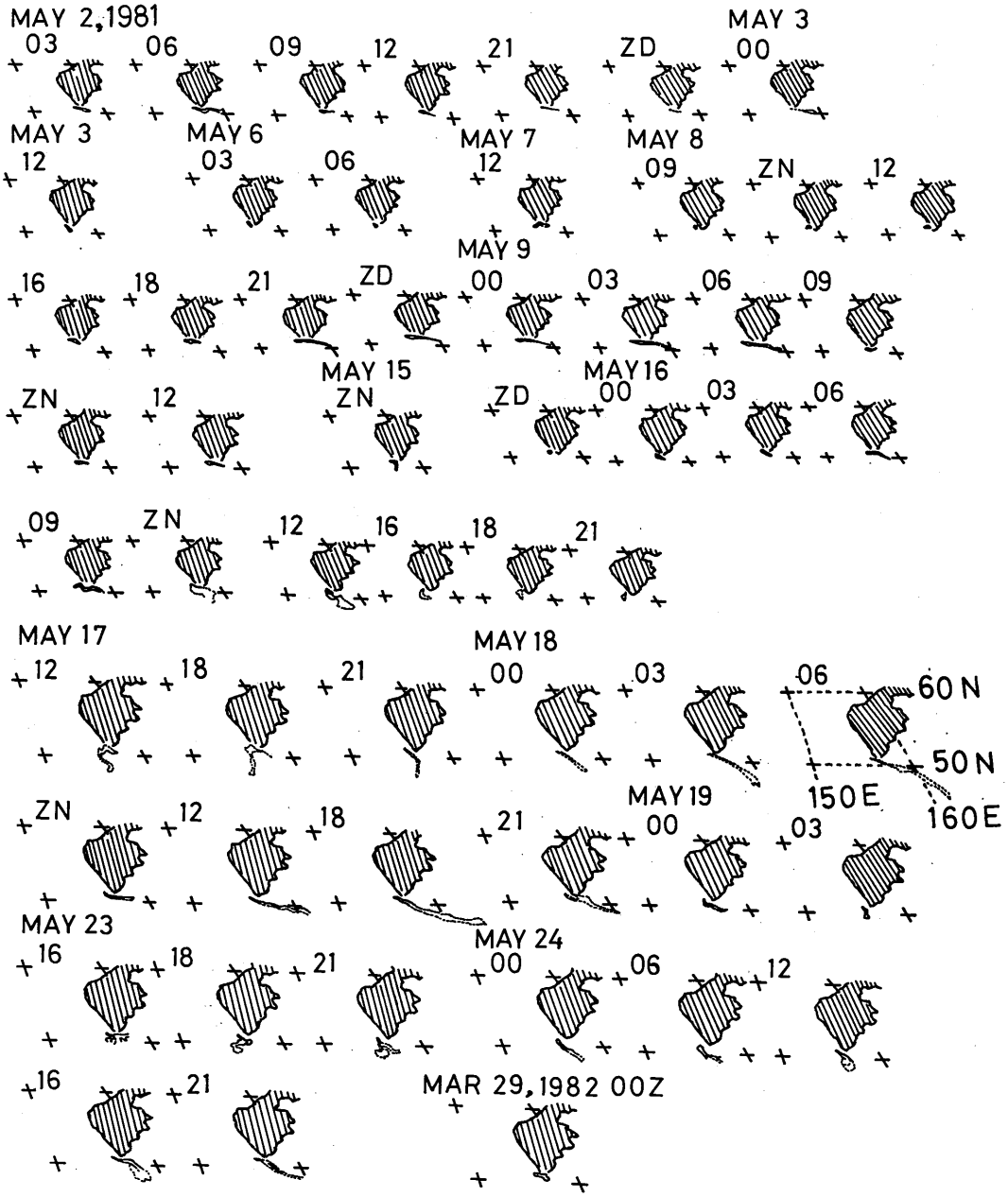
MAY 2, 1981
03
06
09
12
21
MAY 3
ZD
00
MAY 3
12
MAY 6
03
06
MAY 7
12
MAY 8
09
ZN
12
MAY 9
16
18
21
ZD
00
03
06
09
MAY 15
ZN
12
ZN
MAY 16
ZD
00
03
06
09
ZN
12
16
18
21
MAY 17
12
18
21
MAY 18
00
03
06
60 N
50 N
150 E
160 E
ZN
12
18
21
MAY 19
00
03
MAY 23
16
18
21
MAY 24
00
06
12
16
21
MAR 29, 1982 00Z

(b)

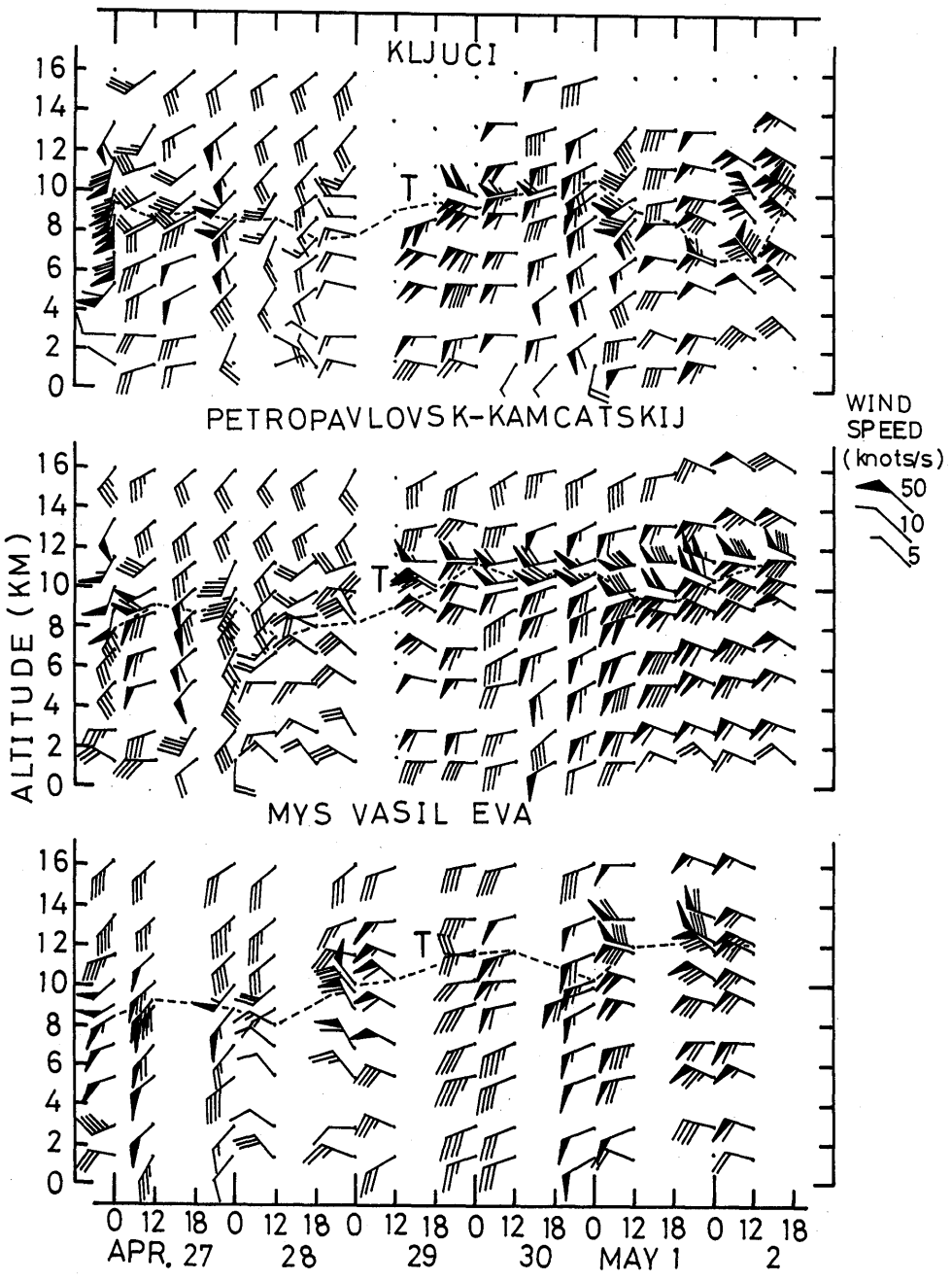

Fig. 3-5 Wind directions observed at three radio-sounding stations fo Kljuci, Petropavlovsk-Kamcatskij and Mys Vasil Eva, the locations of which are shown in Fig. 3-1. Wind speeds are expressed with international notations.

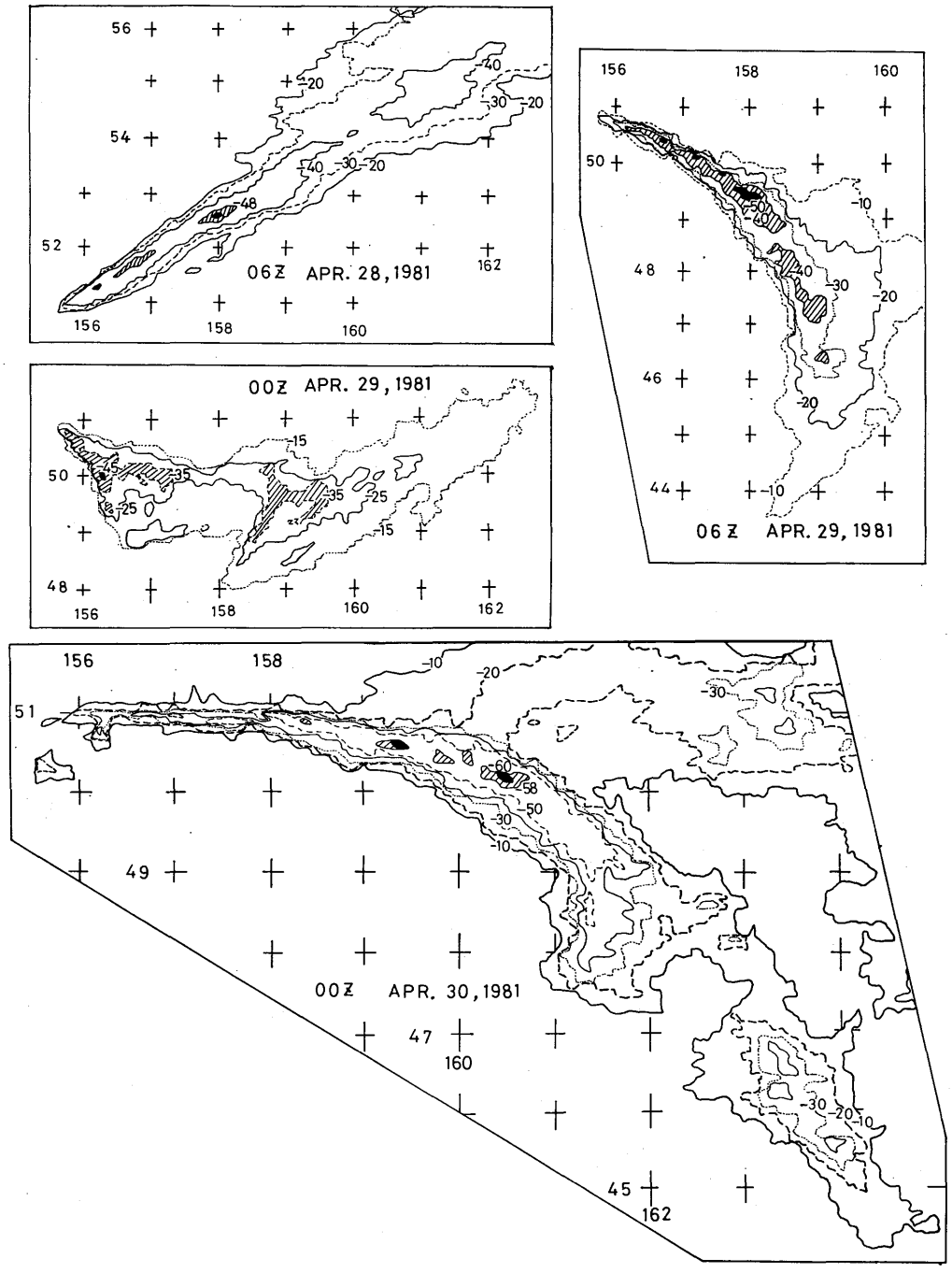

Fig. 3-6 Examples of surface temperature distribution based on IR digital image data processing. The lowest temperature areas are shown with black portions in the figures, and their values in Table 2-2.

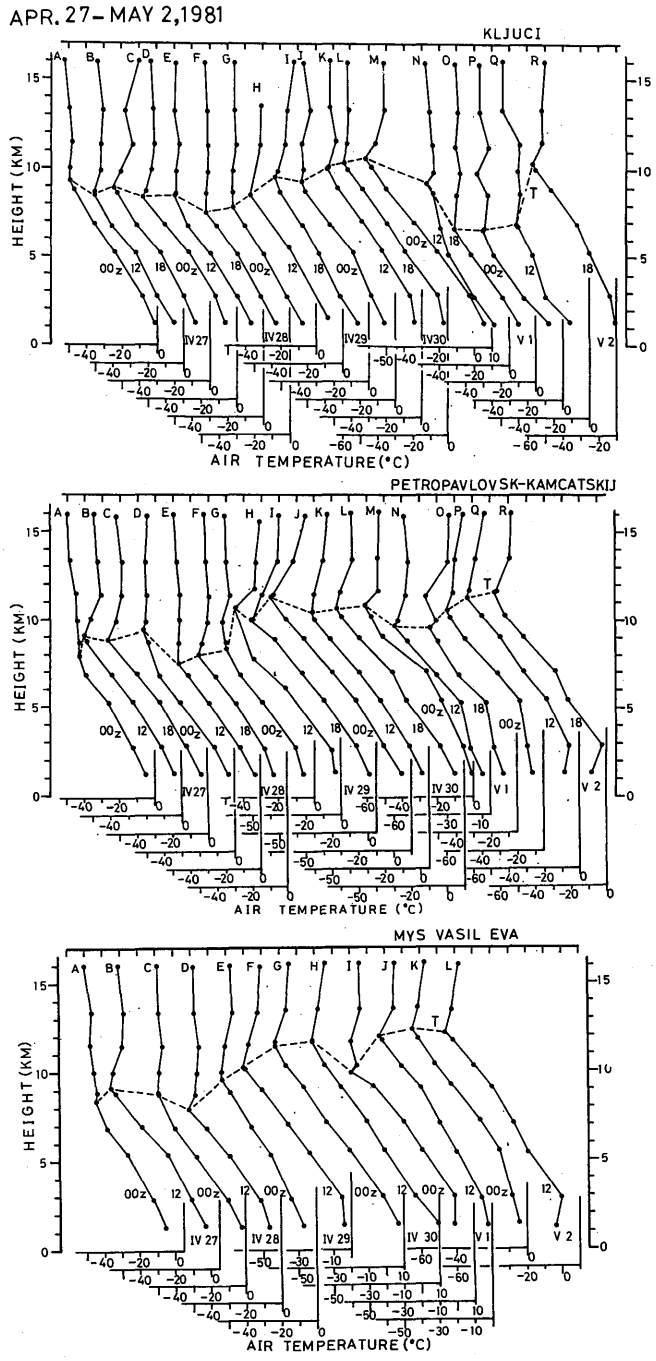

Fig. 3-7 Air-temperature profiles obtained by radio-sounding observations at Kljuci, Petropavlovsk-Kamcatskij and Mys Vasil Eva stations from top to bottom during the period from April 27 to May 2, 1981. T with dotted line denotes the altitude of the tropopause.

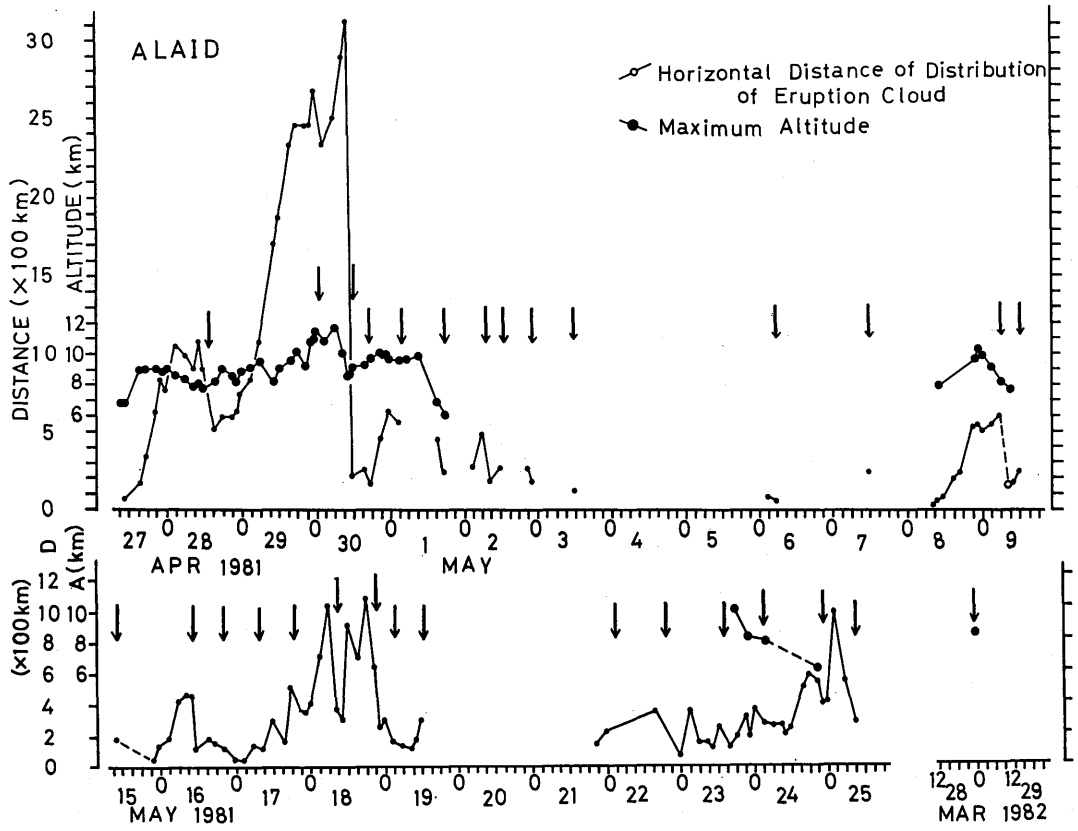

Fig. 3-8 Time variations of horizontal lengths (solid circles) along the long axes and the maximum altitudes estimated (smaller open circles) of Alaid eruption clouds. Black arrows denote the GMS image returning times when eruption clouds left the location of the volcano in GMS images.

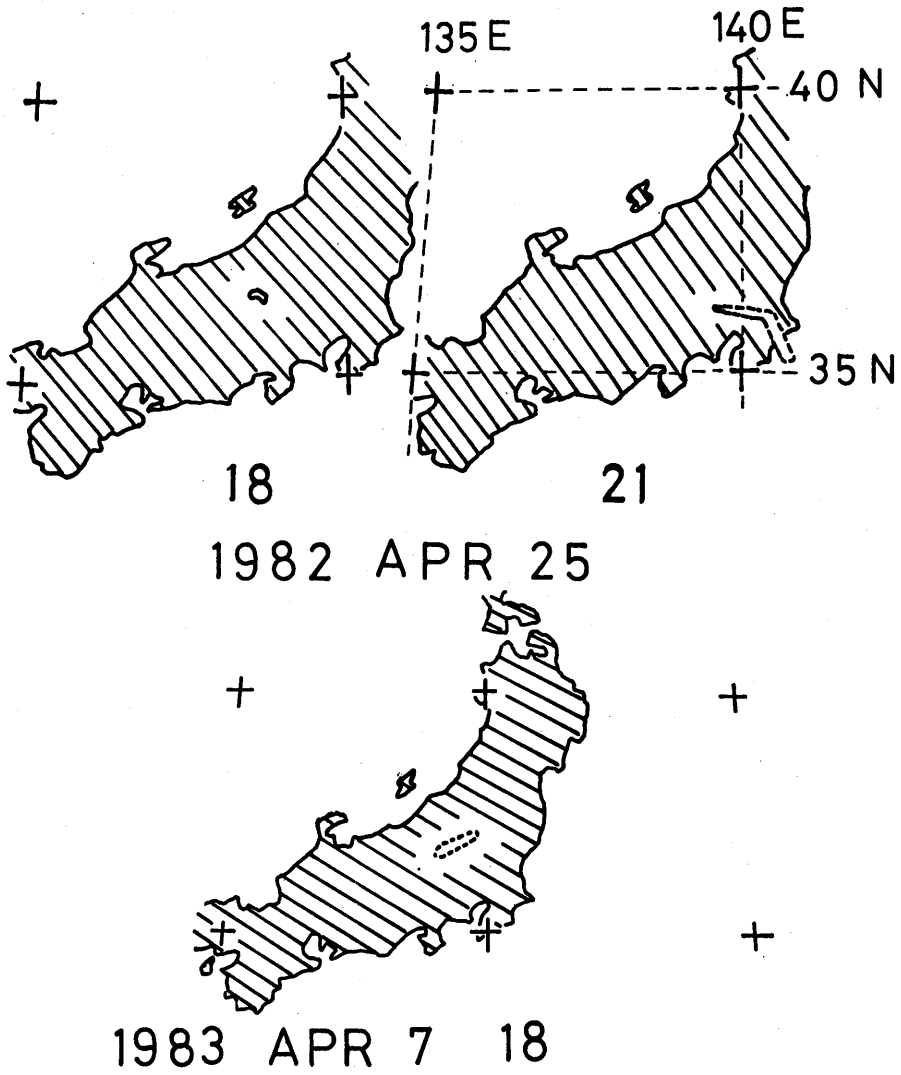

Fig. 3-9 Approximate extent of Asama eruption clouds detected at 18 and 21 GMT on April 25, 1982 (upper two figures) and at 18 GMT on April 7, 1983 (lower) shown with solid and dotted domains.

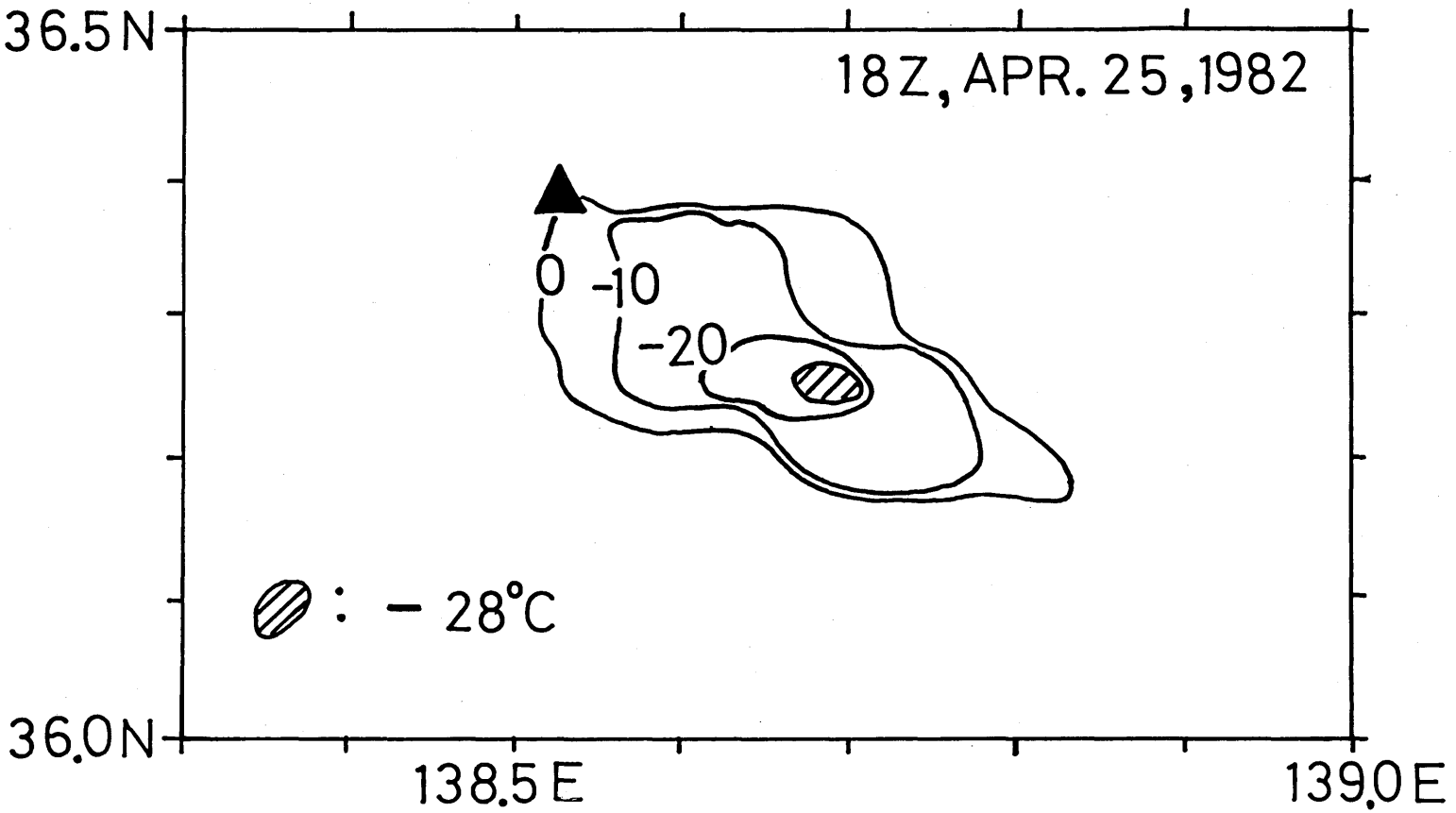

Fig. 3-10 Surface temperature distribution of the eruption cloud detected at 18 GMT on April 25, 1982. Triangle denotes the location of Asama volcano.

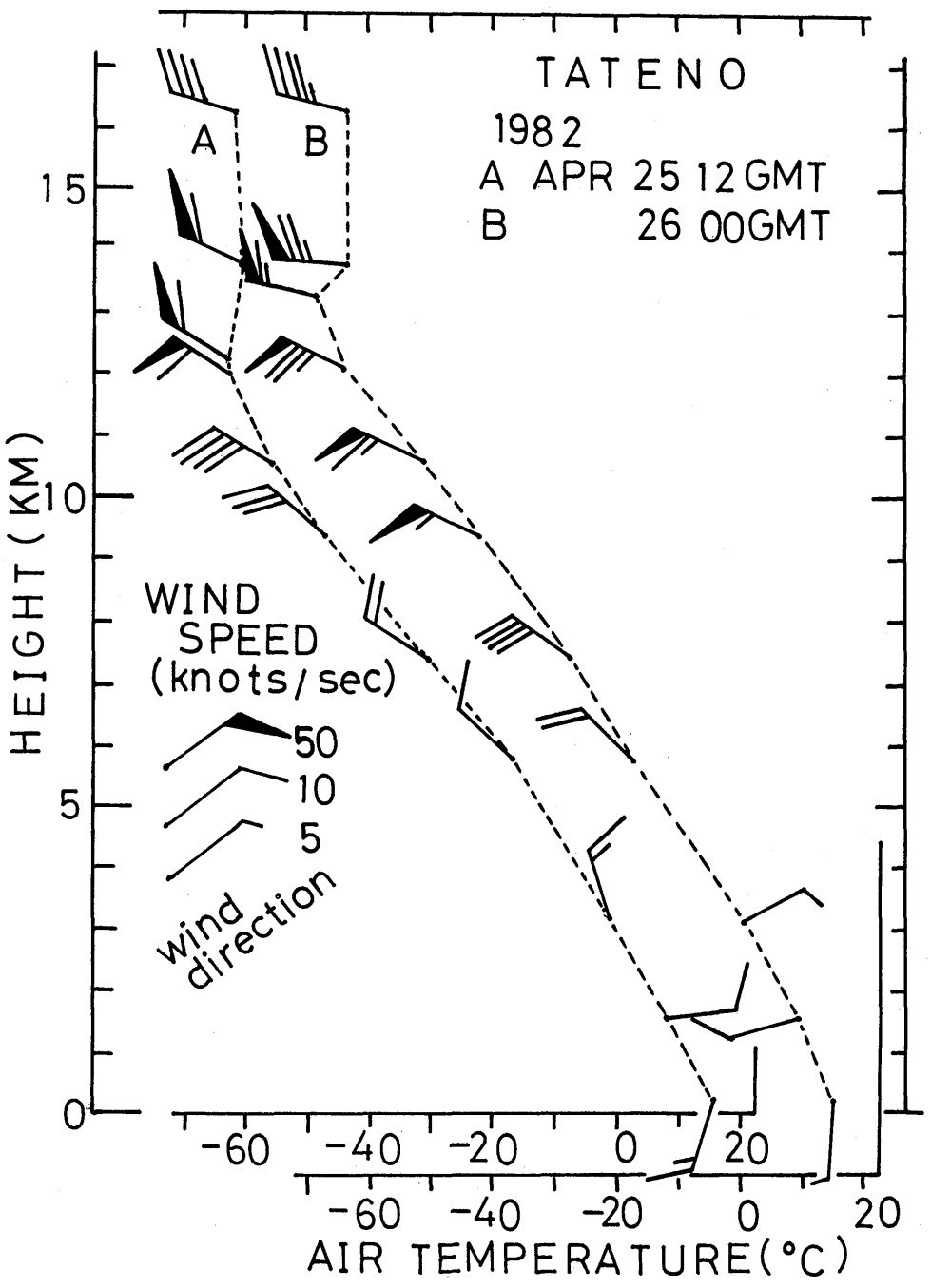

Fig. 3-11 Profiles of air-temperature, wind direction and wind speed expressed with international notations, based on radio-sounding observation data obtained at Tateno station at 12 GMT on April 25 and 00 GMT on April 26, 1982.

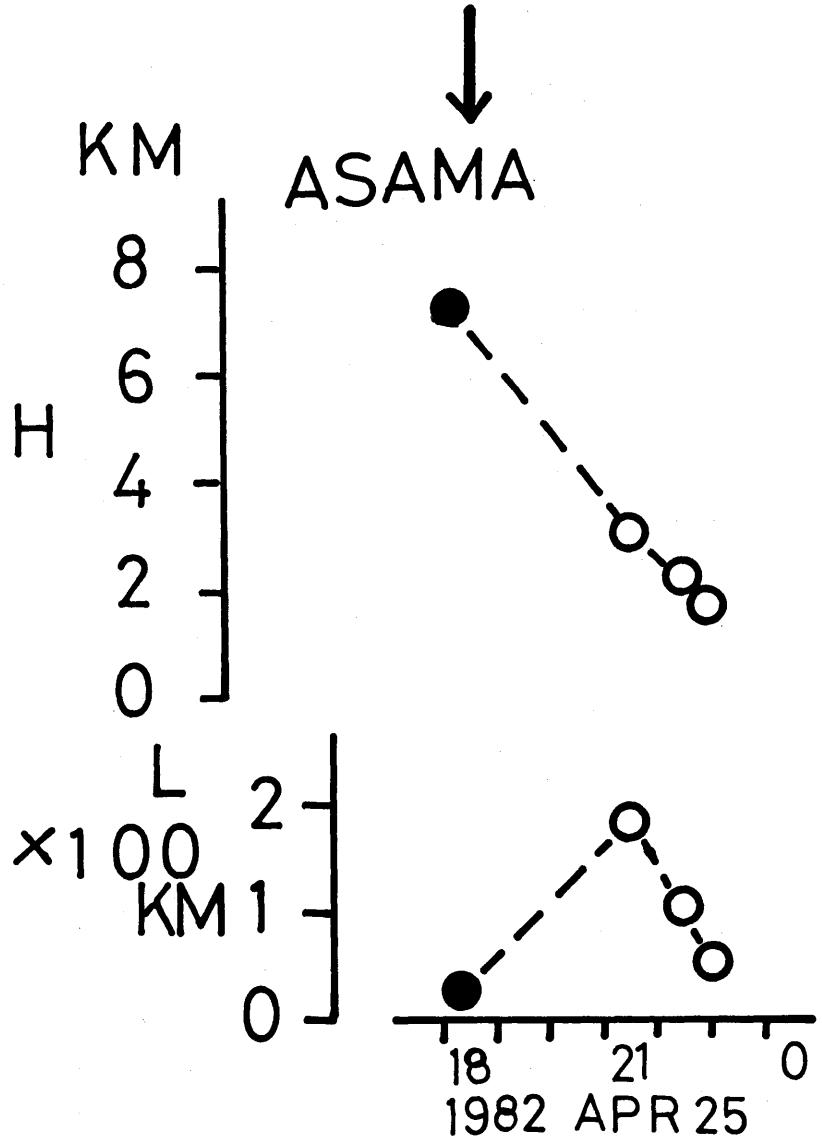

Fig. 3-12 Time variation of the estimated maximum altitude of detected eruption cloud (upper) and the horizontal length (lower) of the 1982 April 25 Asama Eruption. Solid circle and open one denote, respectively, that the eruption cloud was continuous from the location of Asama volcano and that it had left this volcano. Black arrows denote the time when the eruption almost ceased.

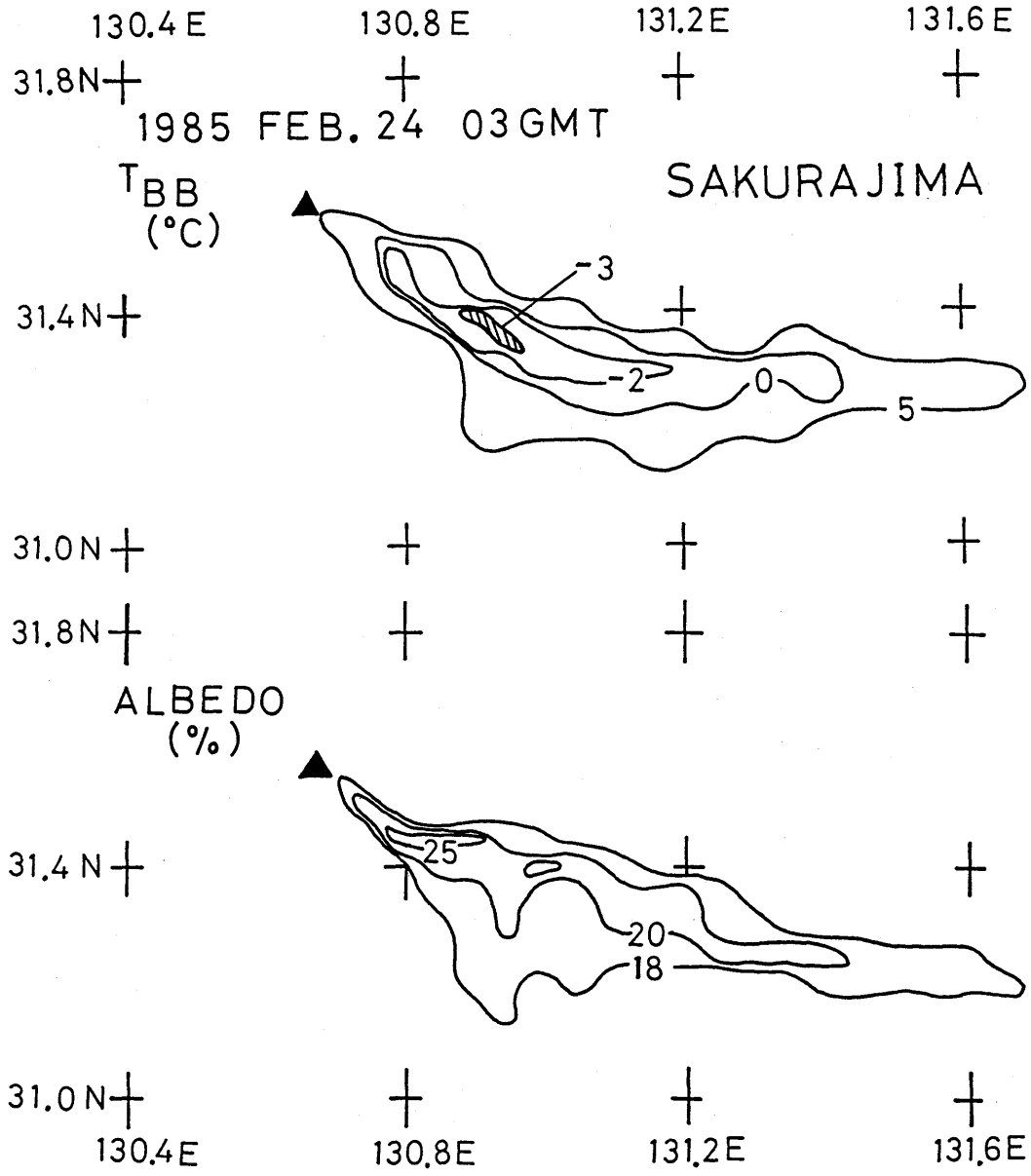

Fig. 3-13 Surface temperature distribution lower than +5°C (upper) and albedo distribution (lower) greater than 18% of the Sakurajima eruption cloud domain taken at 03 GMT on February 24, 1985.

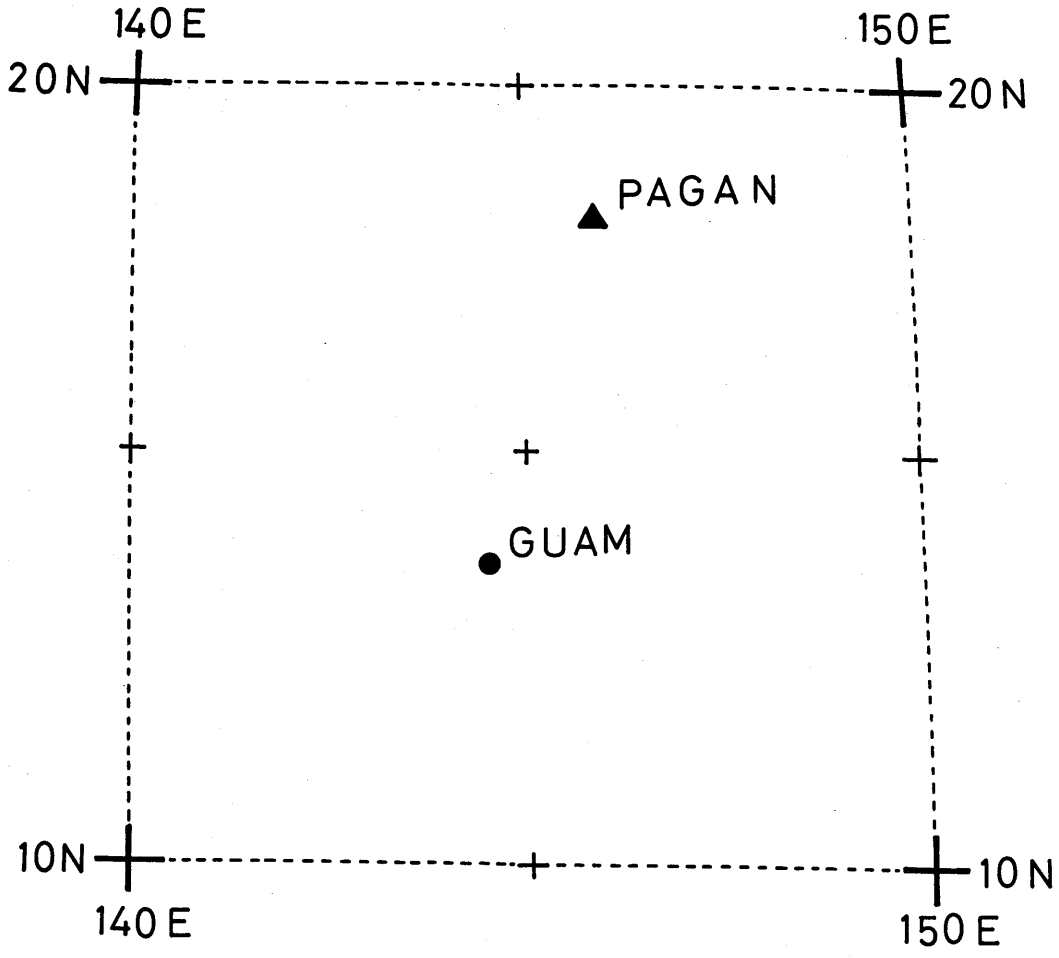

Fig. 3-14 Locations of Pagan volcano (solid triangle) and Guam station (solid circle), which provided radio-sounding observation materials used for estimation of altitude of detected eruption cloud.

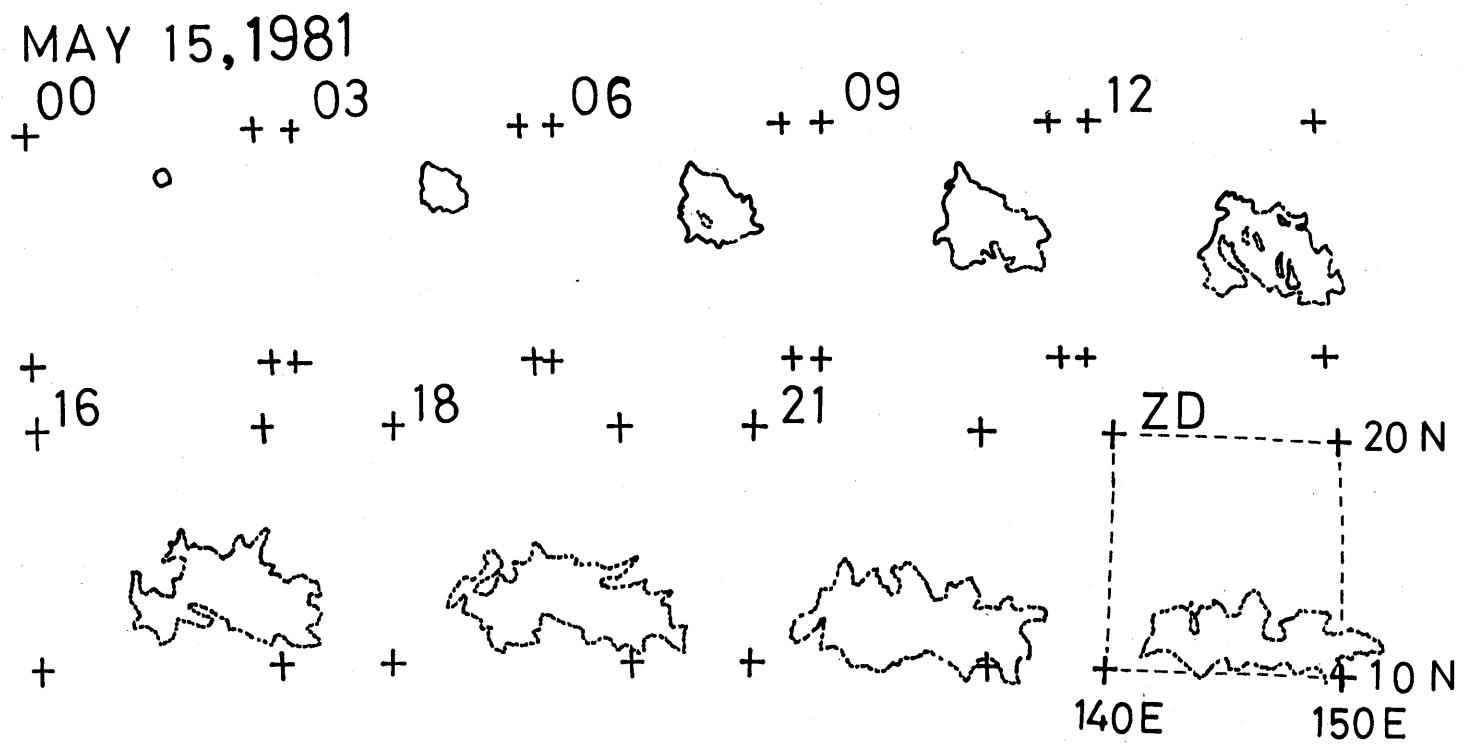

Fig. 3-15 Distinguished extent of detected eruption clouds of the May 1981 Pagan Eruption. Solid line and dotted one mean a clear extent and relatively indistinct one, respectively.

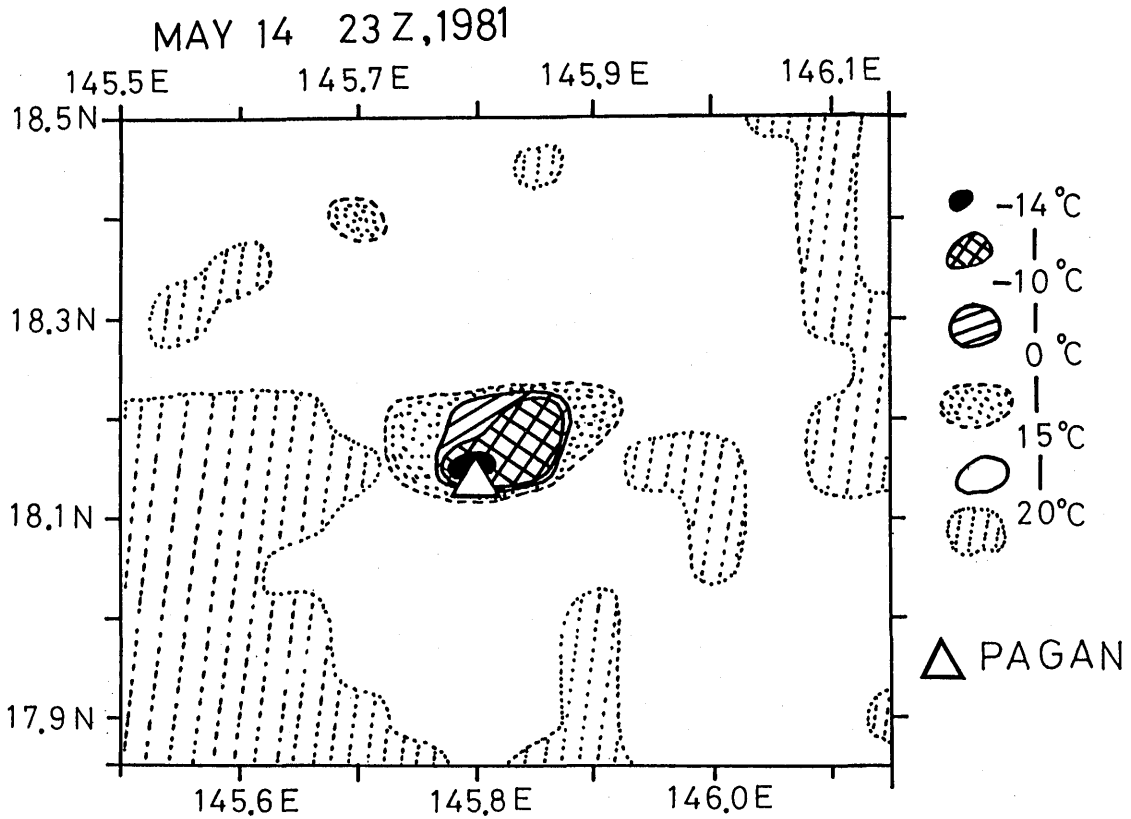

Fig. 3-16 Surface temperature distribution of the first eruption cloud from Pagan volcano, detected at 23 GMT on May 14, 1981. An open triangle indicates the location of this volcano. The domain lower than 15°C around Pagan volcano is possibly eruption cloud, and the one lower than 0°C is eruption cloud.

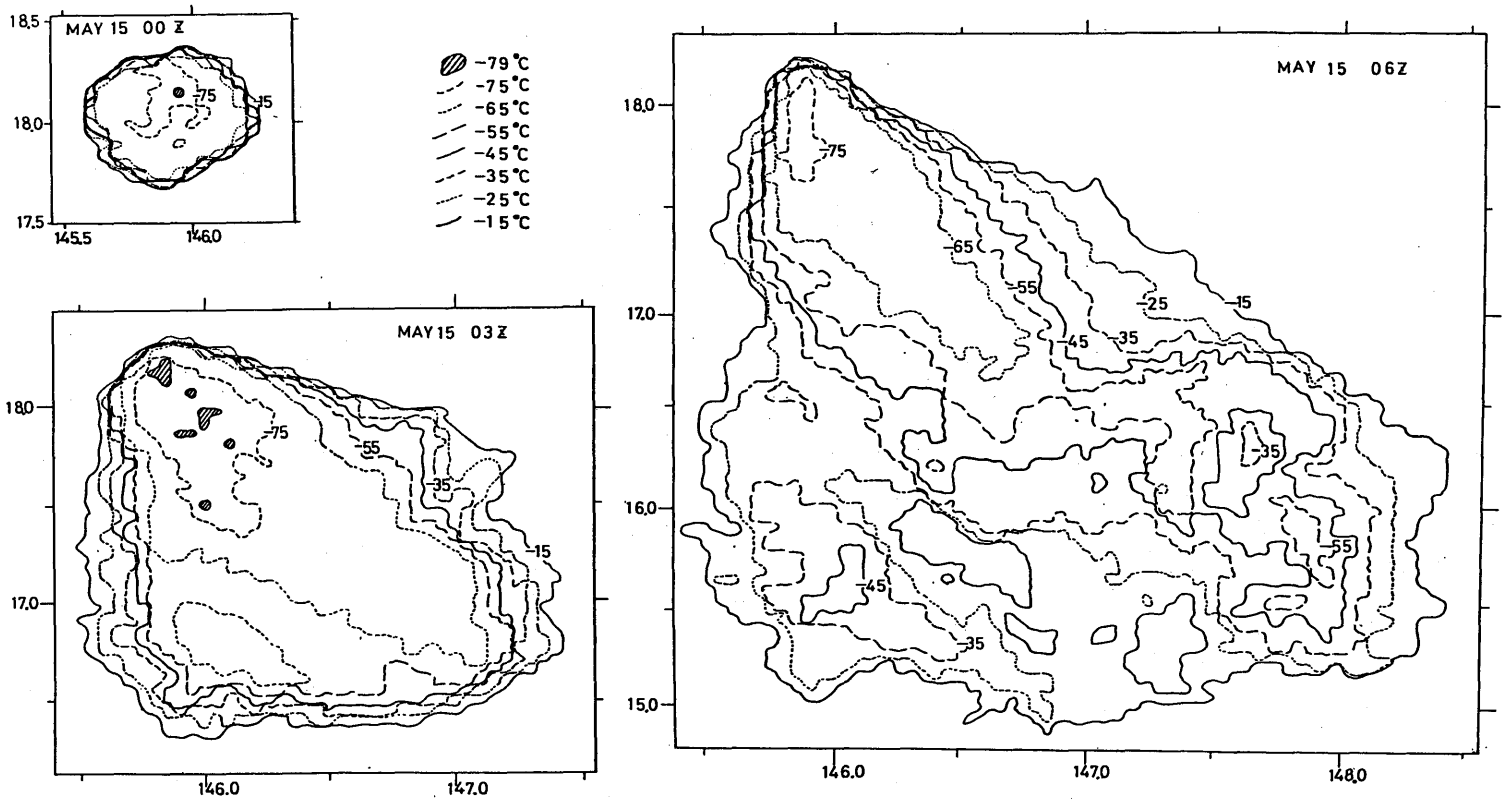

Fig. 3-17 Surface temperature contours of eruption clouds from Pagan volcano taken at 00, 03 and 06 GMT on May 15, 1981.

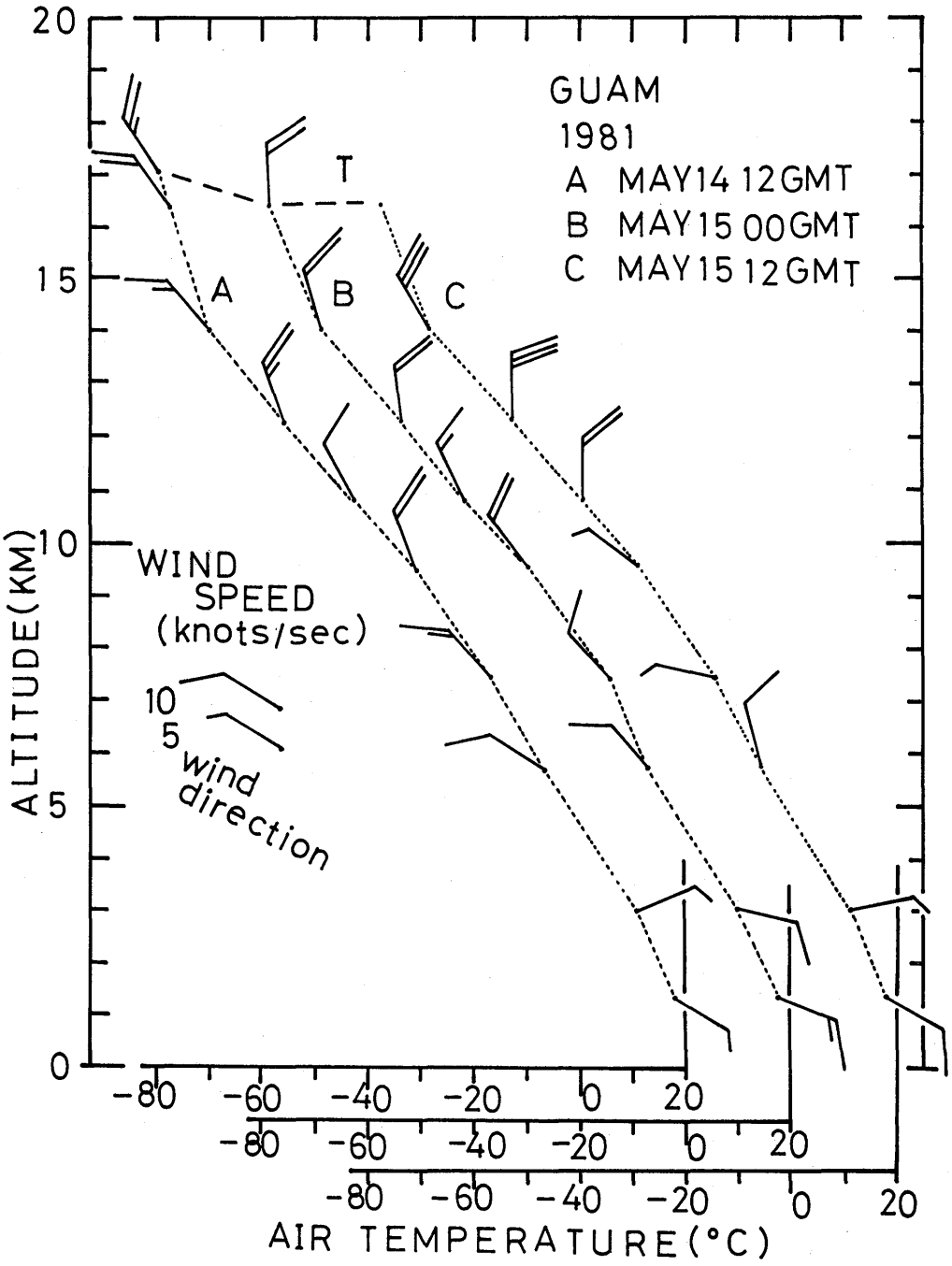

Fig. 3-18 Profiles of air-temperature, wind direction and wind speed expressed by international notation, based on observation data at Guam radio-sounding station at 12 GMT on May 14 and 00 and 12 GMT on May 15, 1981.

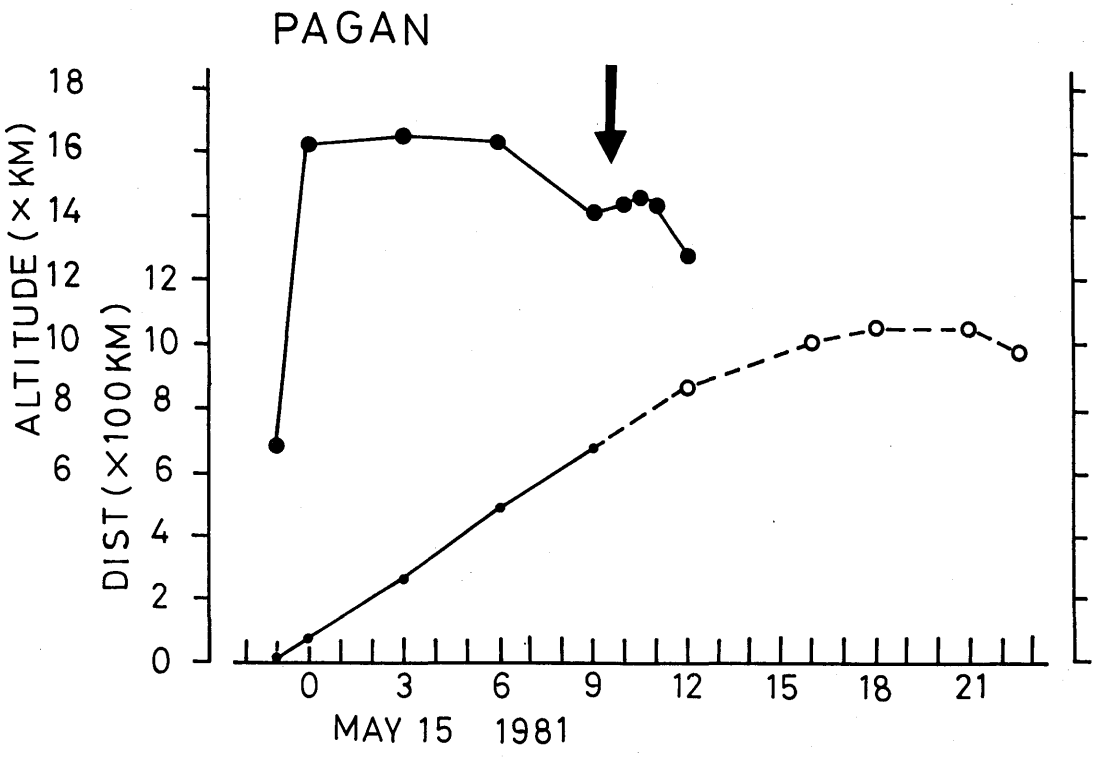

Fig. 3-19 Time variations of the estimated maximum altitude (upper) and the maximum horizontal length (under) of detected eruption clouds of the May 1981 Pagan Eruption. Arrow denotes the time when eruptive activity almost decayed. Smaller solid circles and open ones in the maximum horizontal length mean, respectively, that the eruption clouds were cotinuous from the location of Pagan volcano and that they had already left the volcano in GMS images.

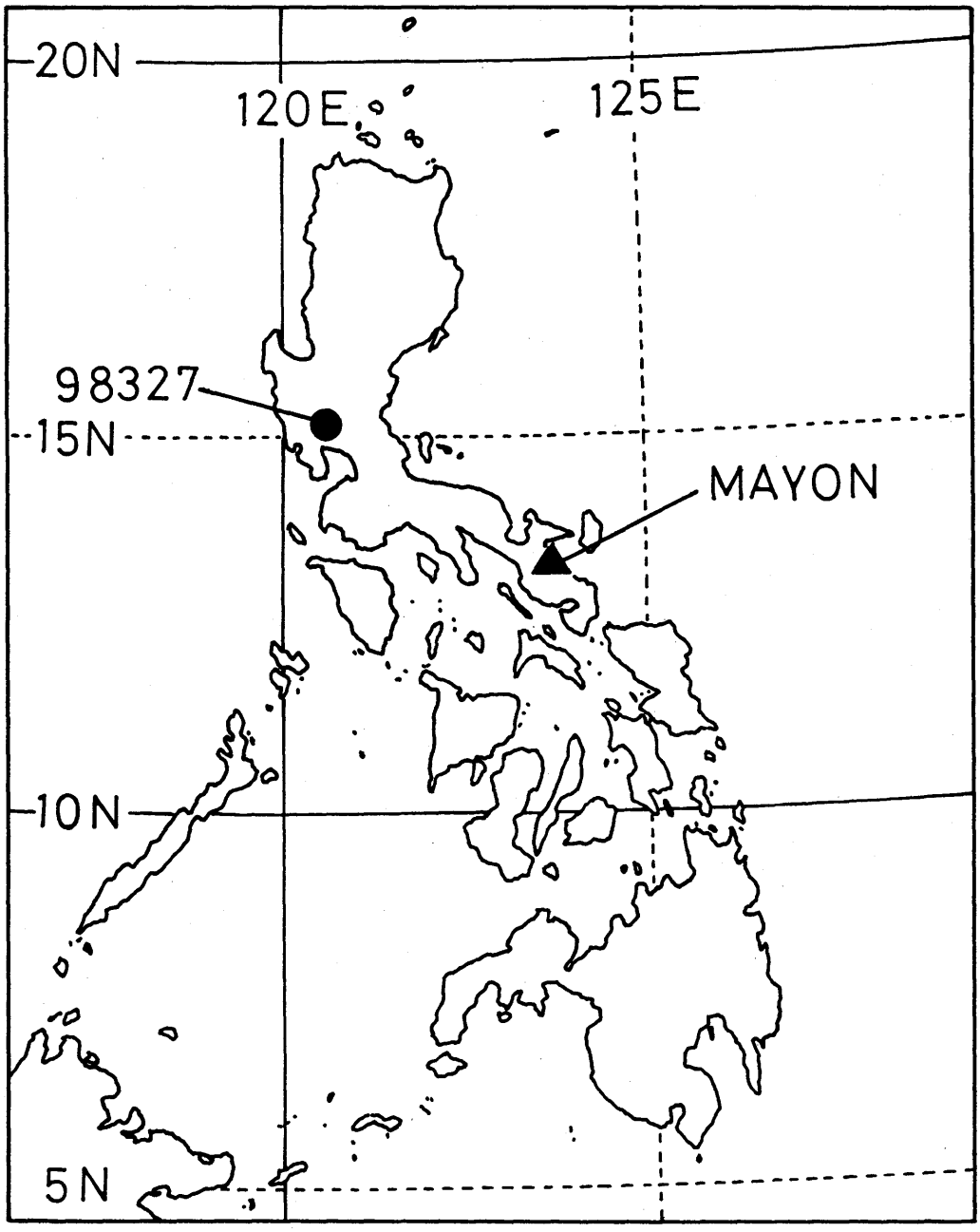

Fig. 3-20 Locations of Mayon volcano (solid triangle) and CAB station (No. 98327, solid circle) which afforded radio-sounding observation data used for estimation of altitudes of eruption clouds.

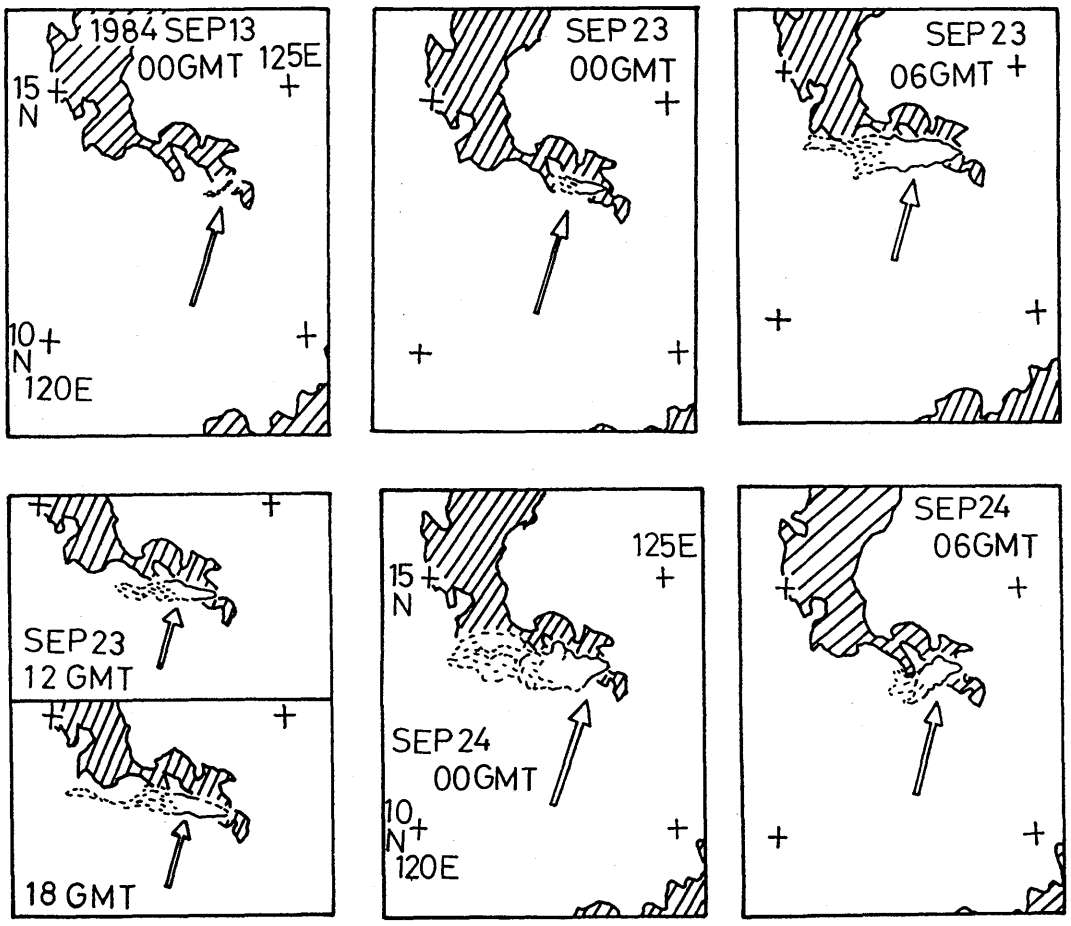

Fig. 3-21 Approximate extent of eruption clouds from Mayon volcano detected in GMS images. It is pointed out by white arrows, while the dotted portion means indistinct domain owing to surrounding atmospheric clouds.

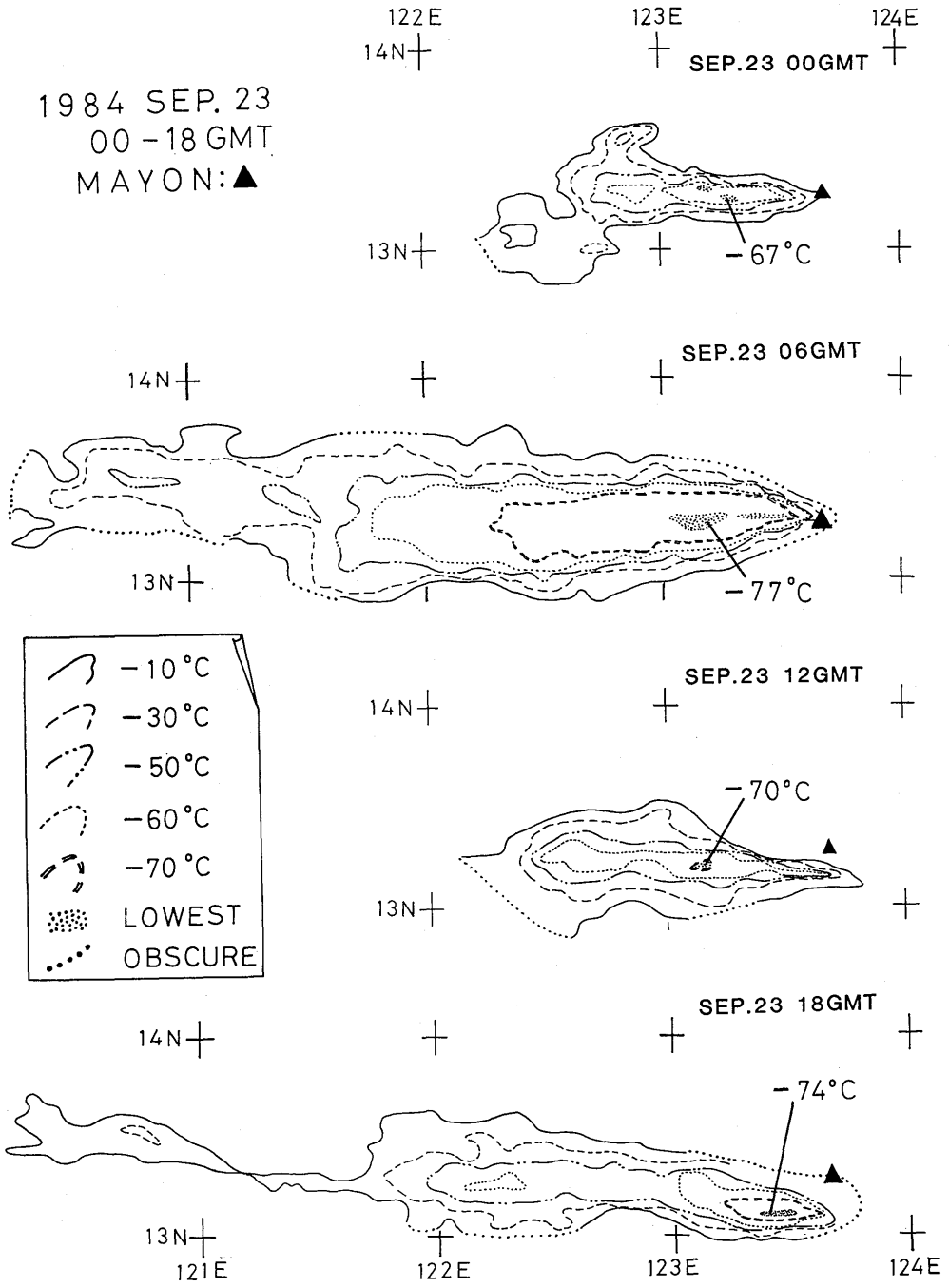

(a)

Fig.3-22 (a)-(b)

Surface temperature contours of detected eruption clouds based on IR digital image data. The portion of the lowest temperature is expressed by dotted area with numerals denoting temperature in °C. Solid triangle indicates the location of Mayon volcano.

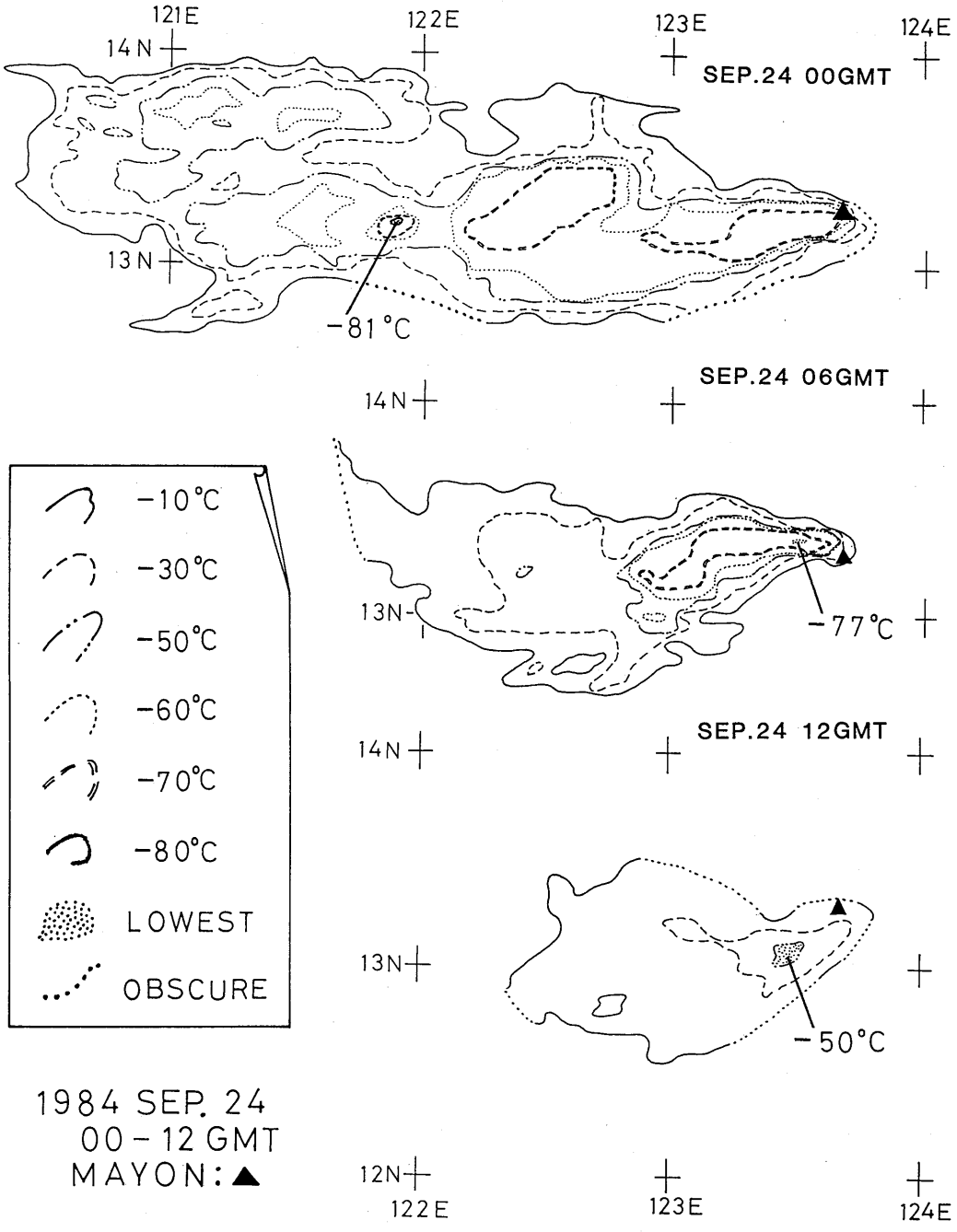
121E
122E
123E
124E
14N
13N
SEP.24 00GMT
-81°C
SEP.24 06GMT
-77°C
SEP.24 12GMT
-50°C
-10°C
-30°C
-50°C
-60°C
-70°C
-80°C
LOWEST
OBSCURE
1984 SEP. 24
00-12 GMT
MAYON: ▲
12N

(b)

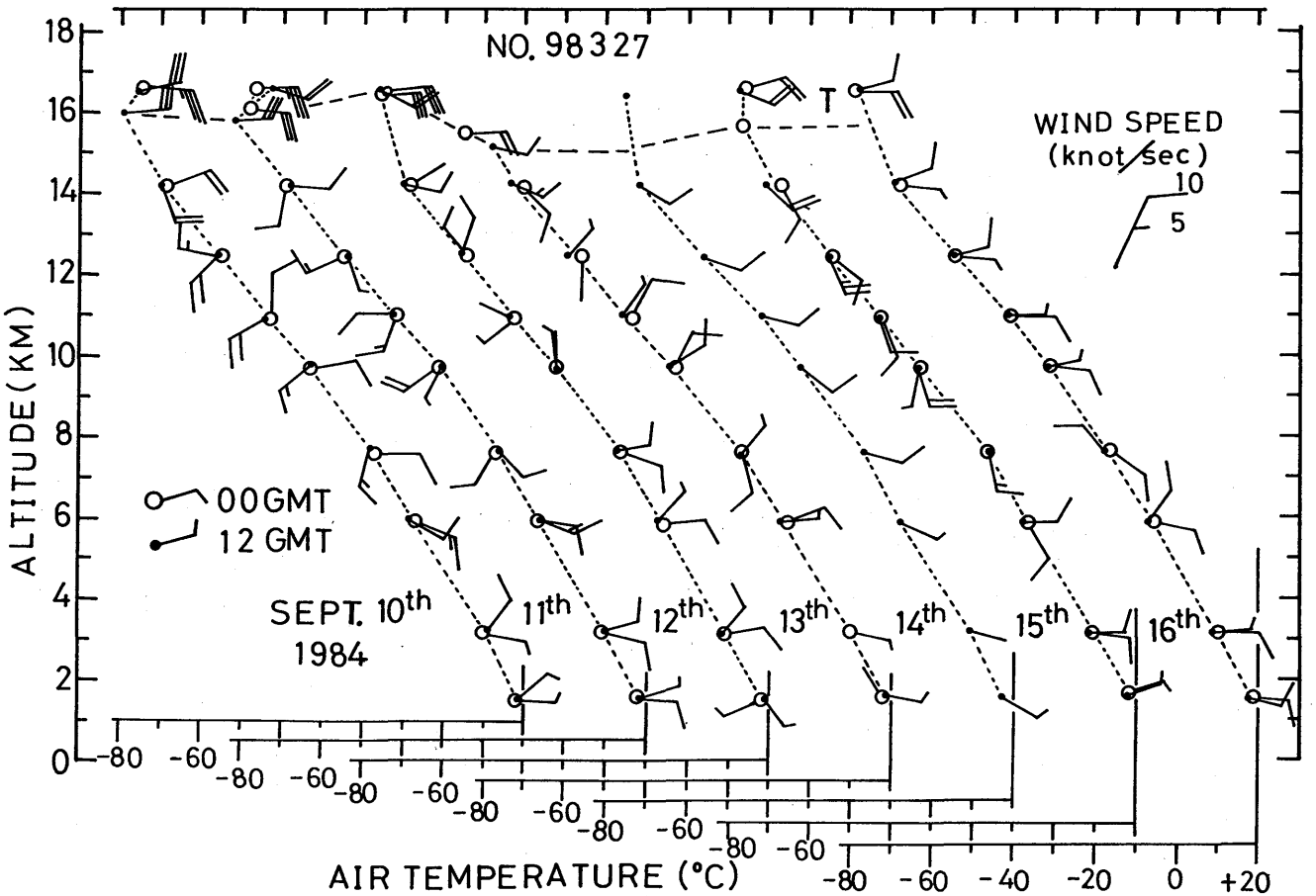

(a)

Fig. 3-23(a)-(c) Profiles of air-temperature, wind direction and wind speed expressed with international notation, based on radio-sounding observation data at CAB station.

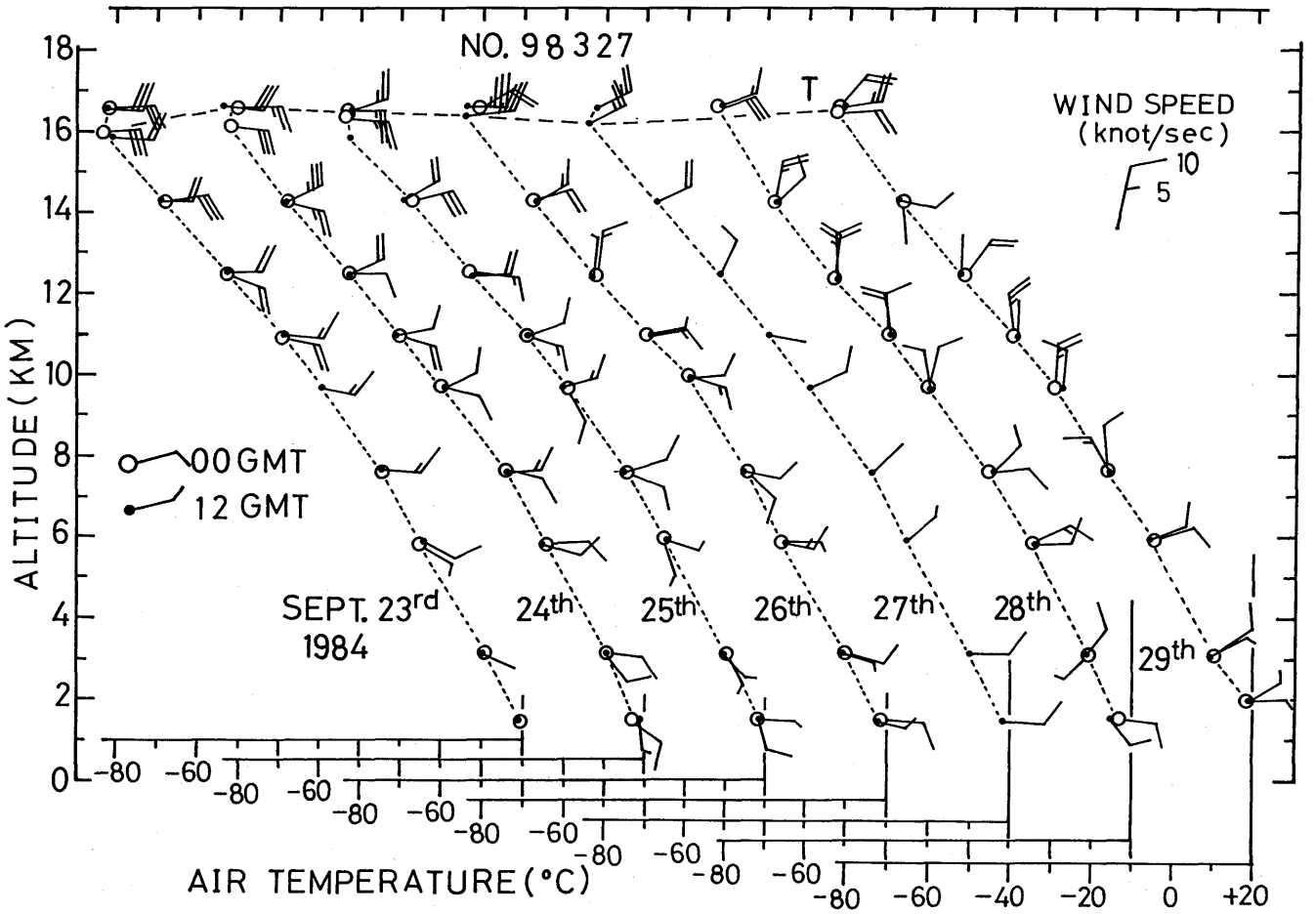
NO. 98327
T
WIND SPEED
(knot/sec)
10
5
00 GMT
12 GMT
SEPT. 23rd
1984
24th
25th
26th
27th
28th
29th
ALTITUDE (KM)
AIR TEMPERATURE (°C)
18
16
14
12
10
8
6
4
2
0
-80
-60
-40
-20
0
+20

(b)

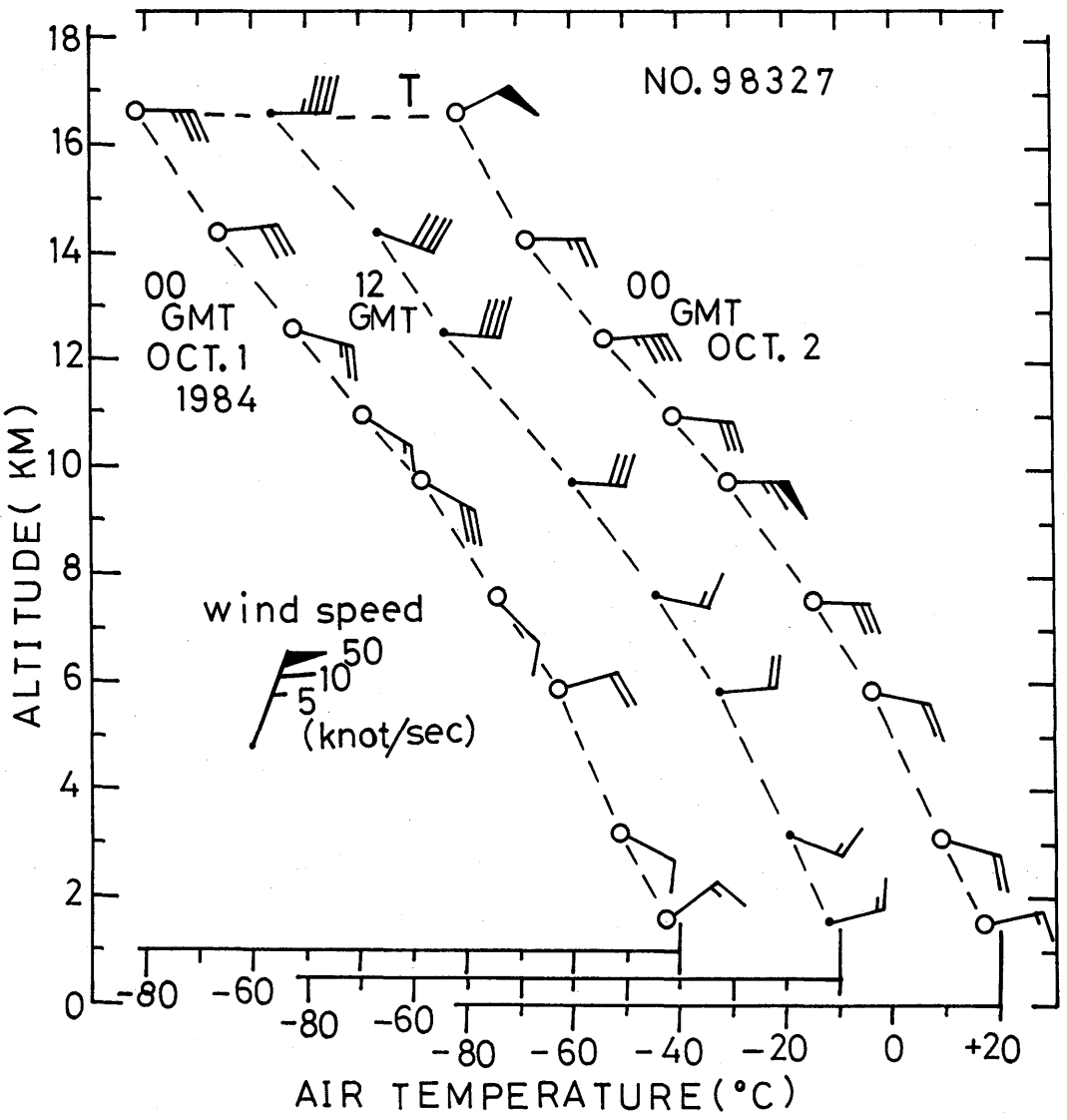
NO. 98327
T
00 GMT OCT. 1 1984
12 GMT
00 GMT OCT. 2
wind speed
50
10
5
(knot/sec)
ALTITUDE(KM)
AIR TEMPERATURE(°C)
18
16
14
12
10
8
6
4
2
0
-80 -60 -80 -60 -80 -60 -40 -20 0 +20

(c)

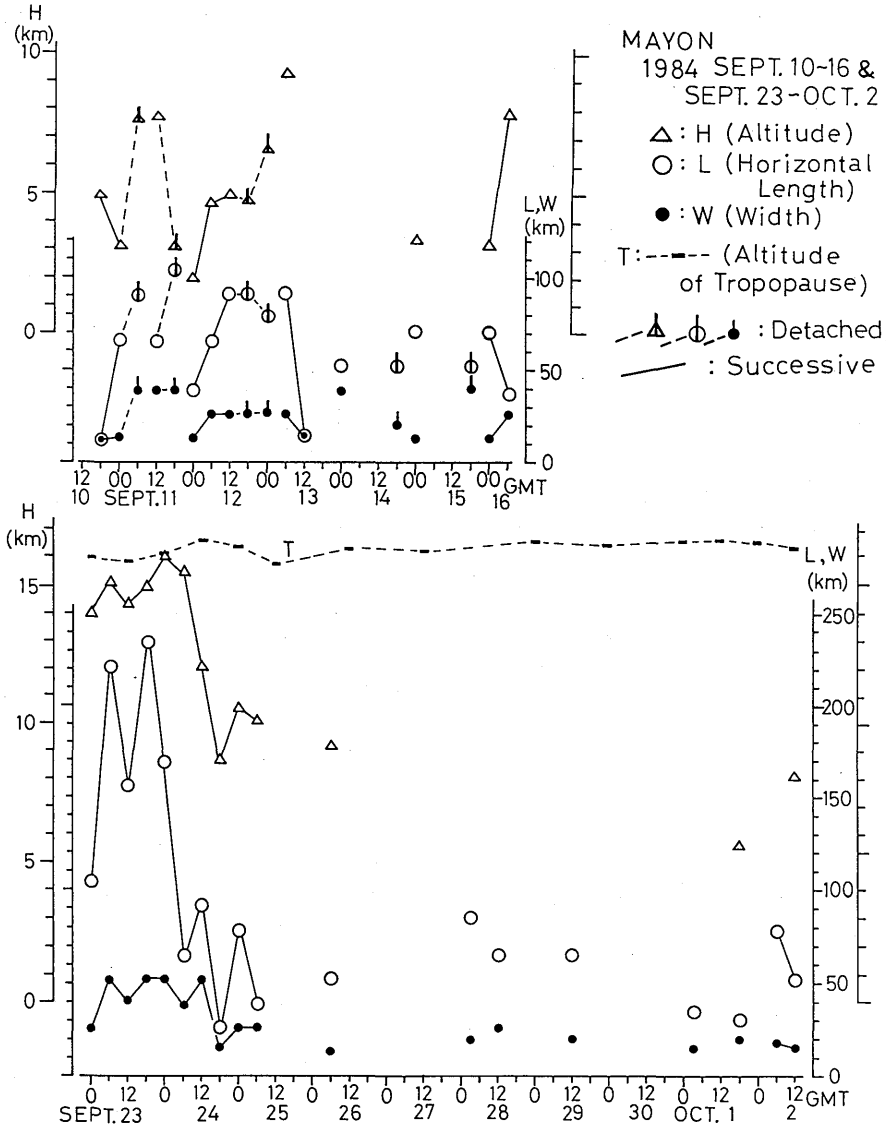

Fig. 3-24 Time variations of the estimated highest altitude (open triangle), the maximum horizontal length (open circle) and the maximum width (solid circle) of detected eruption clouds. Solid line between respective symbols means that the eruption cloud was continuous from the location of Mayon volcano and dotted line bound to symbols with vertical bars denotes that the eruption cloud was detached from the volcano. The individual vertical axes in km are shown with letters H, L and W for altitude, length and width, respectively. T means the altitude of the tropopause.

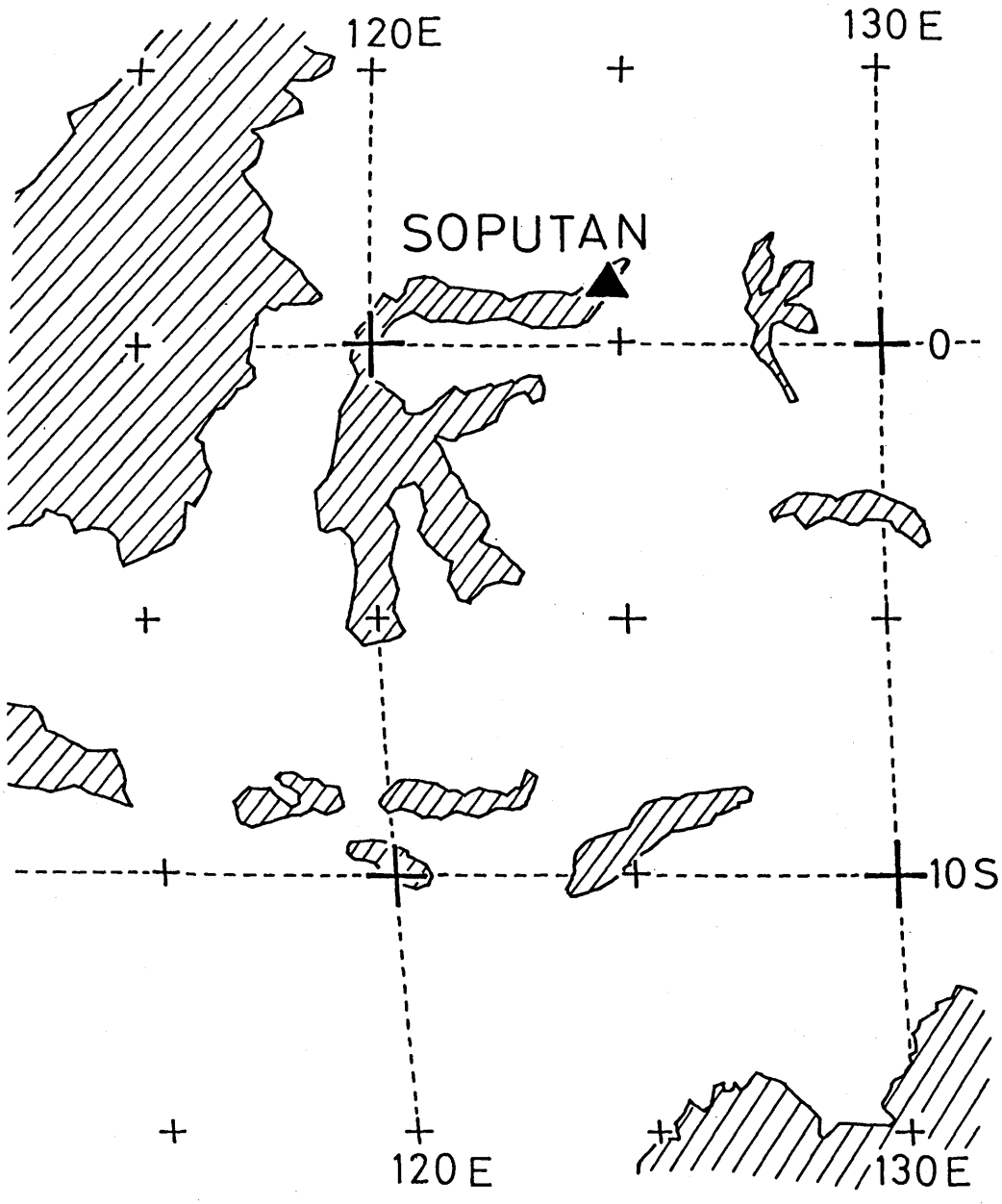

Fig. 3-25 Location of Soputan volcano (solid triangle).

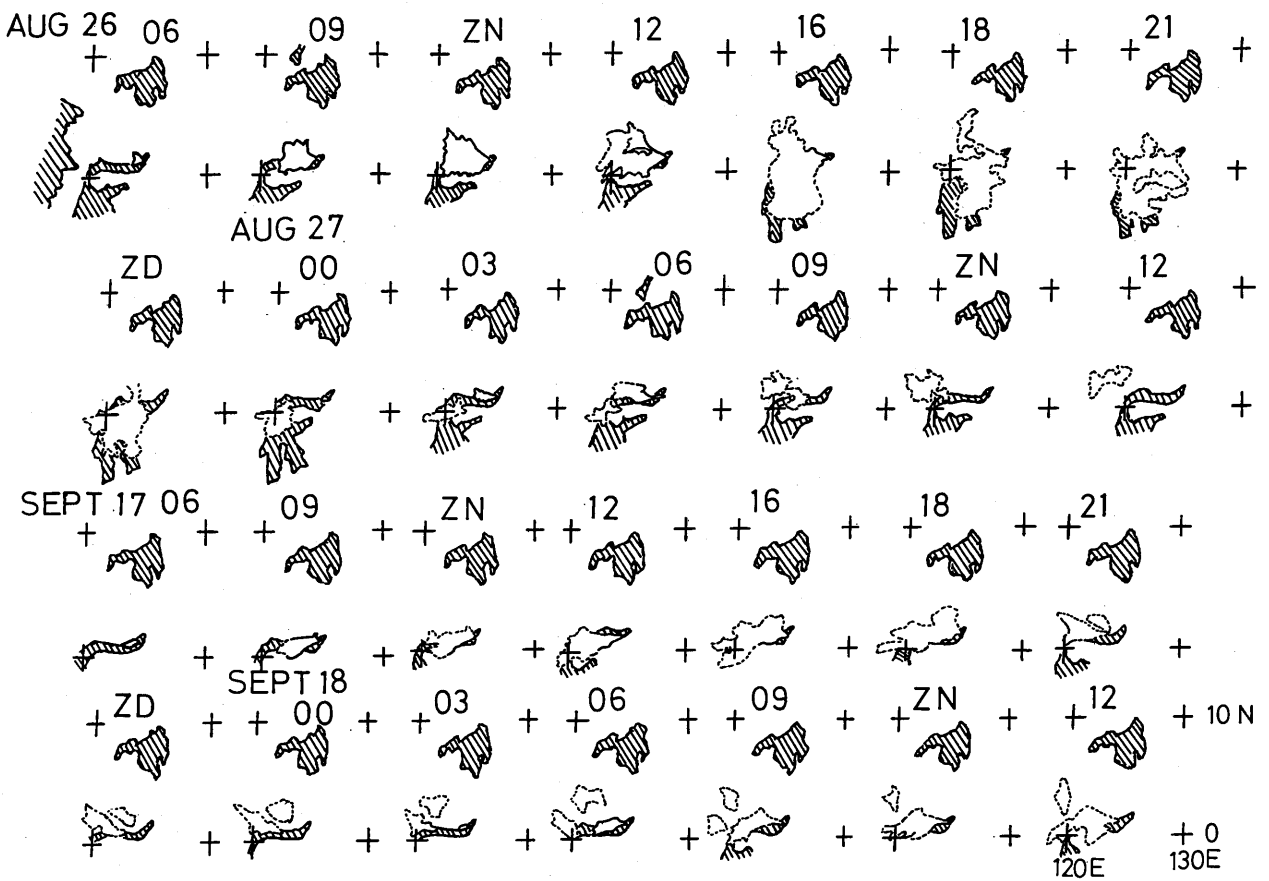

Fig. 3-26 Spreading eruption clouds outlined with solid line in case of a distinct domain and dotted line for a relatively indistinct one, from Soputan volcano during the 1982 August and September Eruptions.

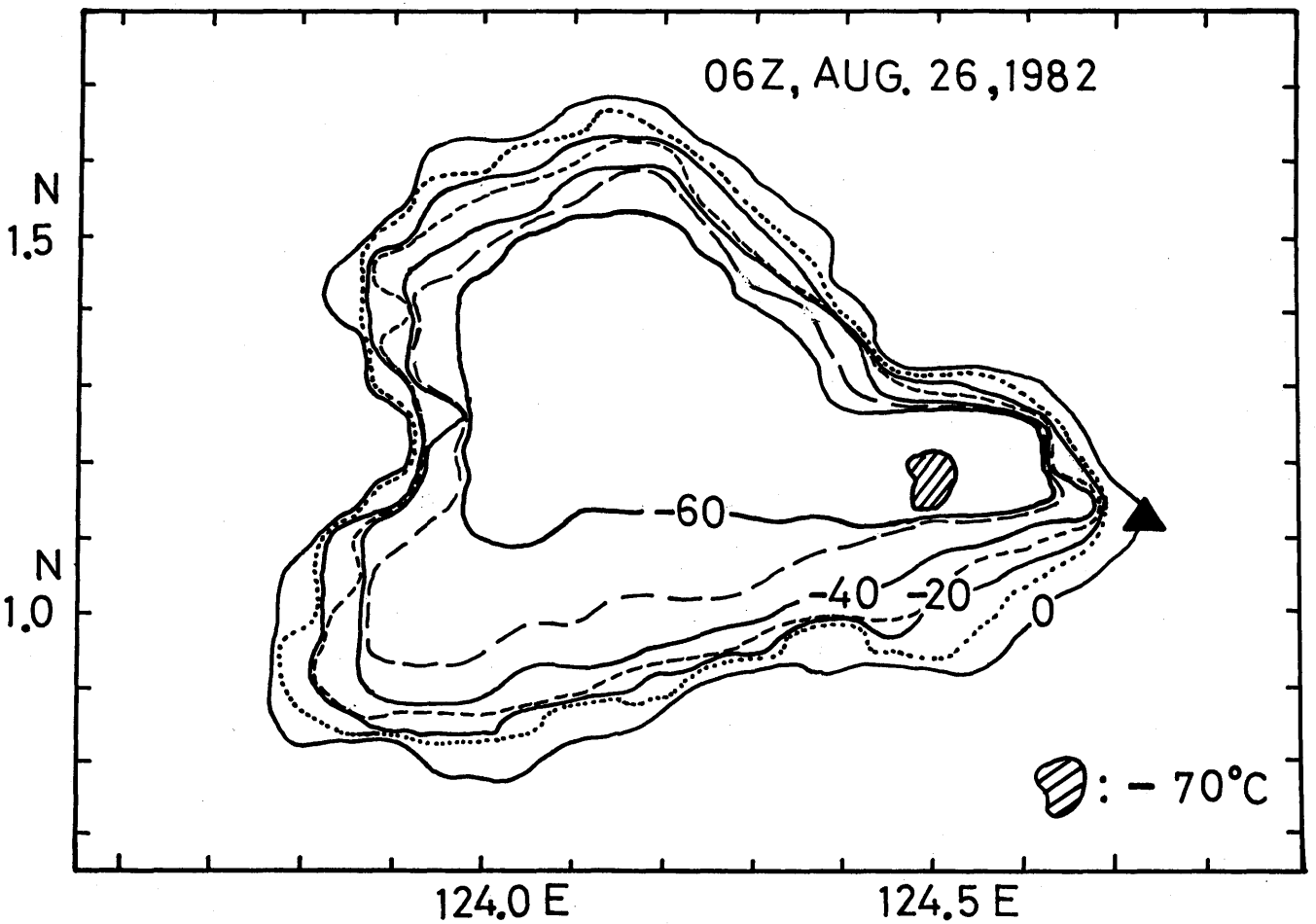

(a)

Fig. 3-27 (a)-(c)

Surface temperature contours of eruption clouds from Soputan volcano taken at 06, 09 and 11 GMT on August 26, 1982. The coldest portions were shown with hatched areas. Solid triangle means the location of this volcano.

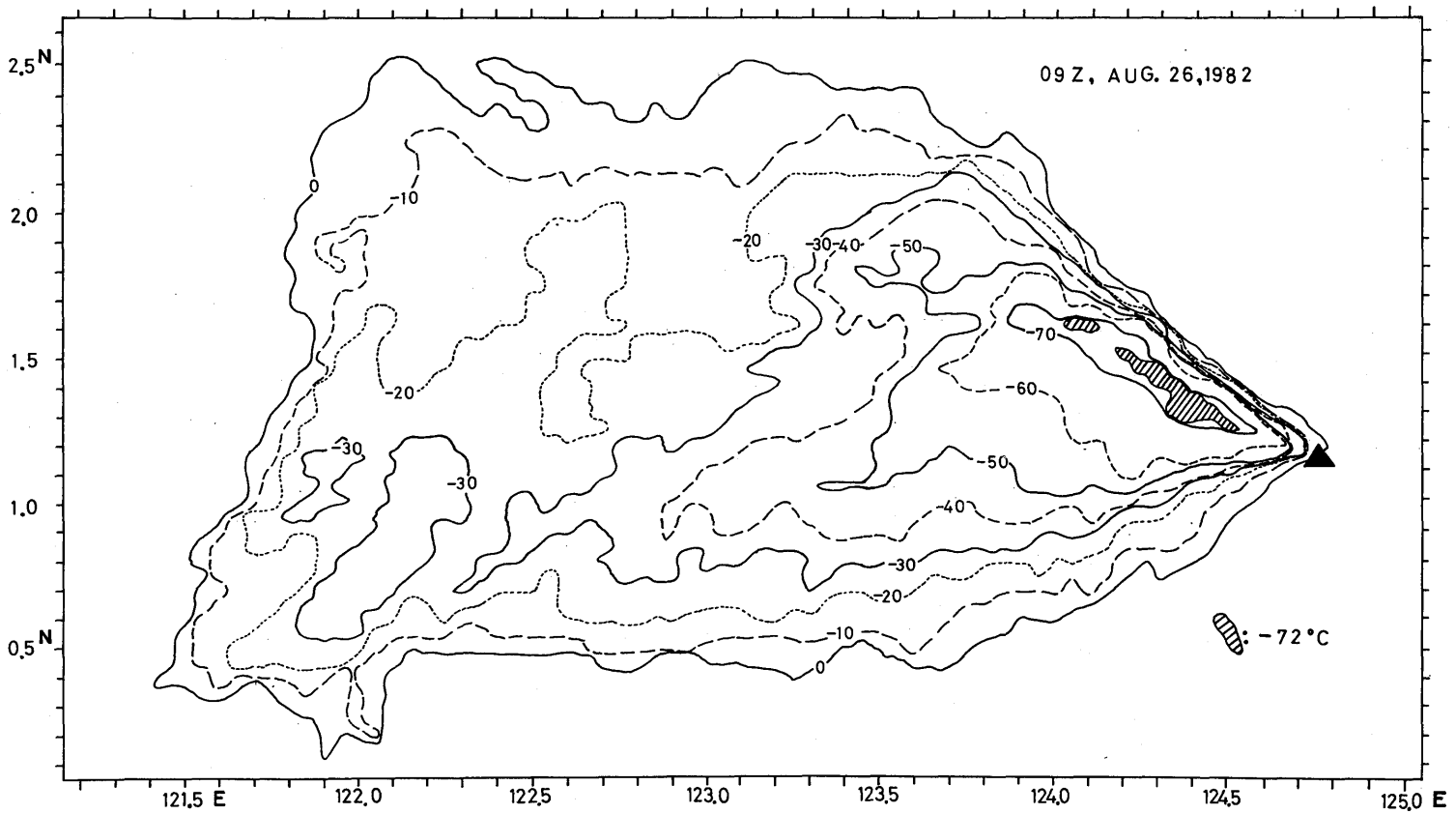
09 Z, AUG. 26, 1982
2.5 N
2.0
1.5
1.0
0.5 N
121.5 E
122.0
122.5
123.0
123.5
124.0
124.5
125.0 E
0
-10
-20
-30
-40
-50
-70
-60
: -72 °C

(b)

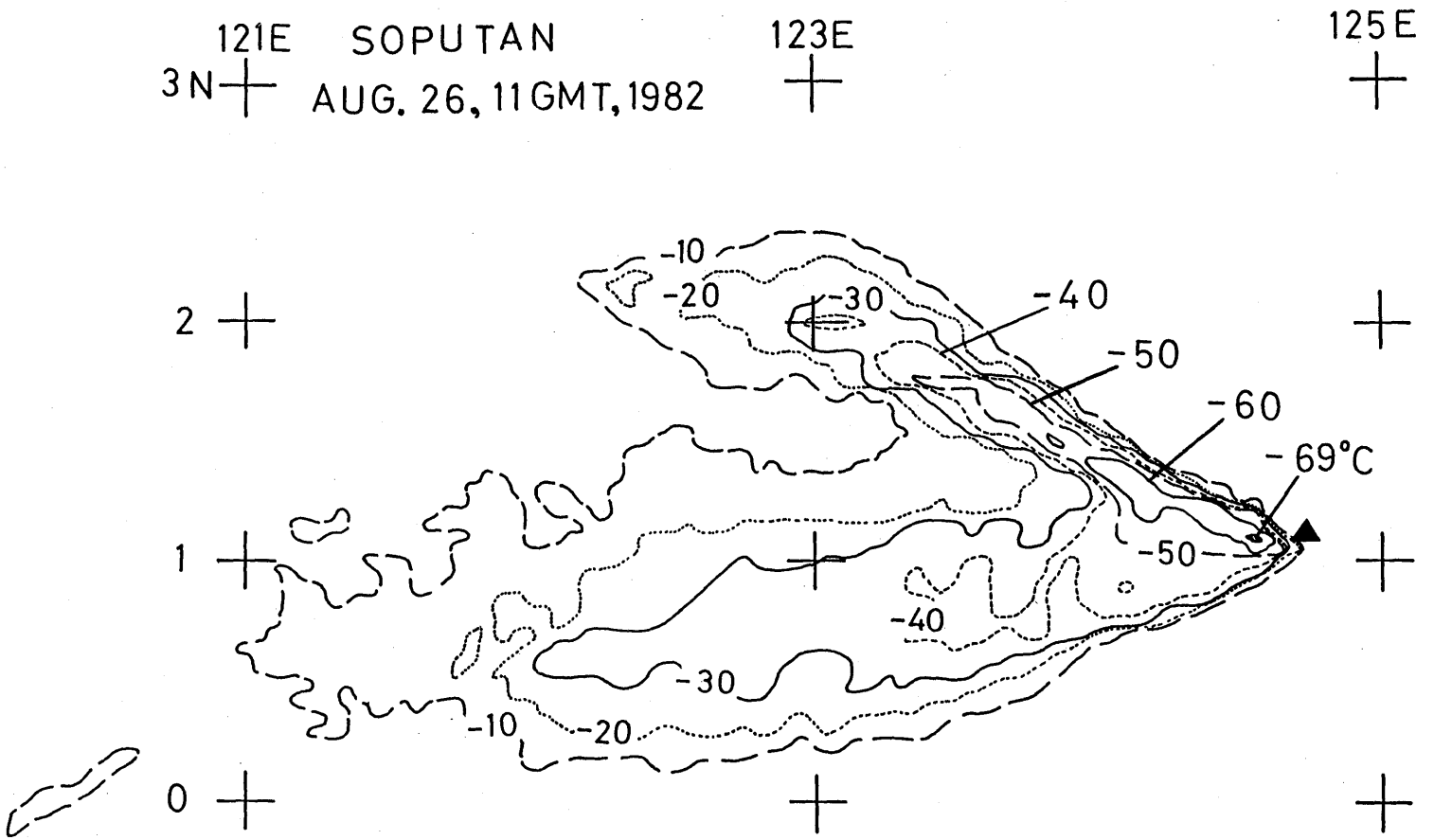
121E
SOPUTAN
AUG. 26, 11GMT, 1982
123E
125E
3N
2
1
0
-10
-20
-30
-40
-50
-60
-69°C
-50
-40
-30
-10
-20

(c)

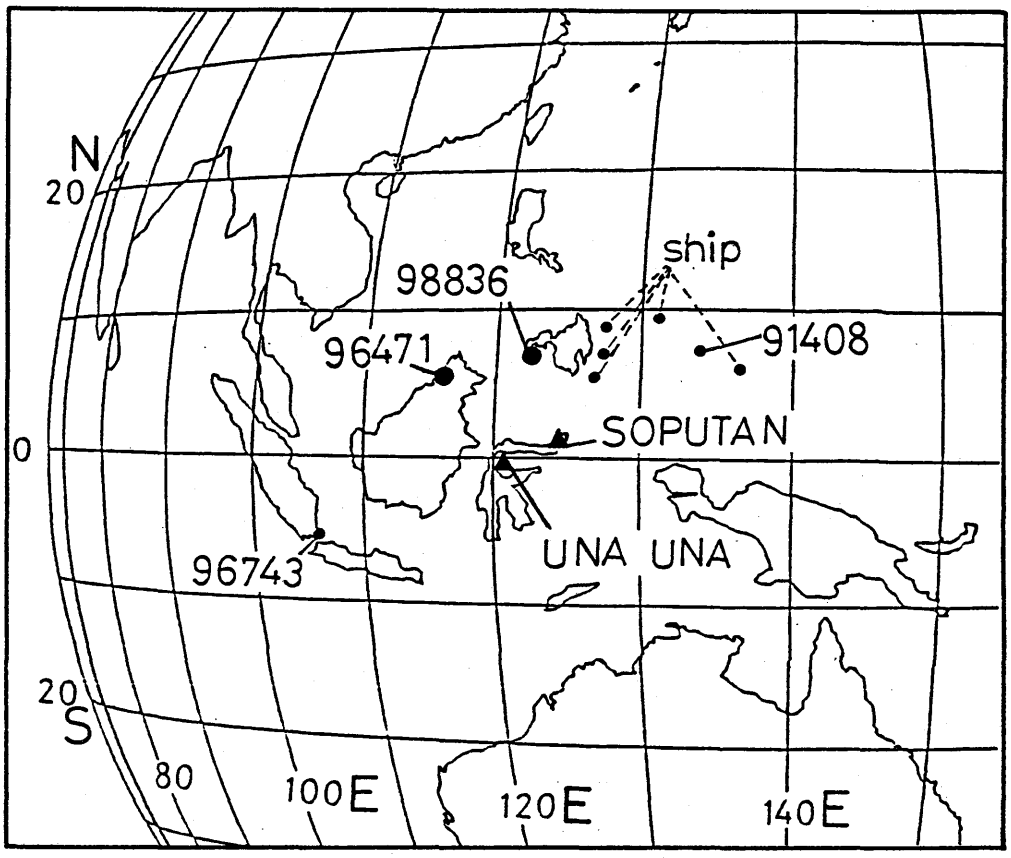

Fig. 3-28 Locations of radio-sounding stations (solid circles) which provided observation data used for altitude-estimations of detected eruption clouds from Soputan and from Una Una volcanoes (solid triangles)

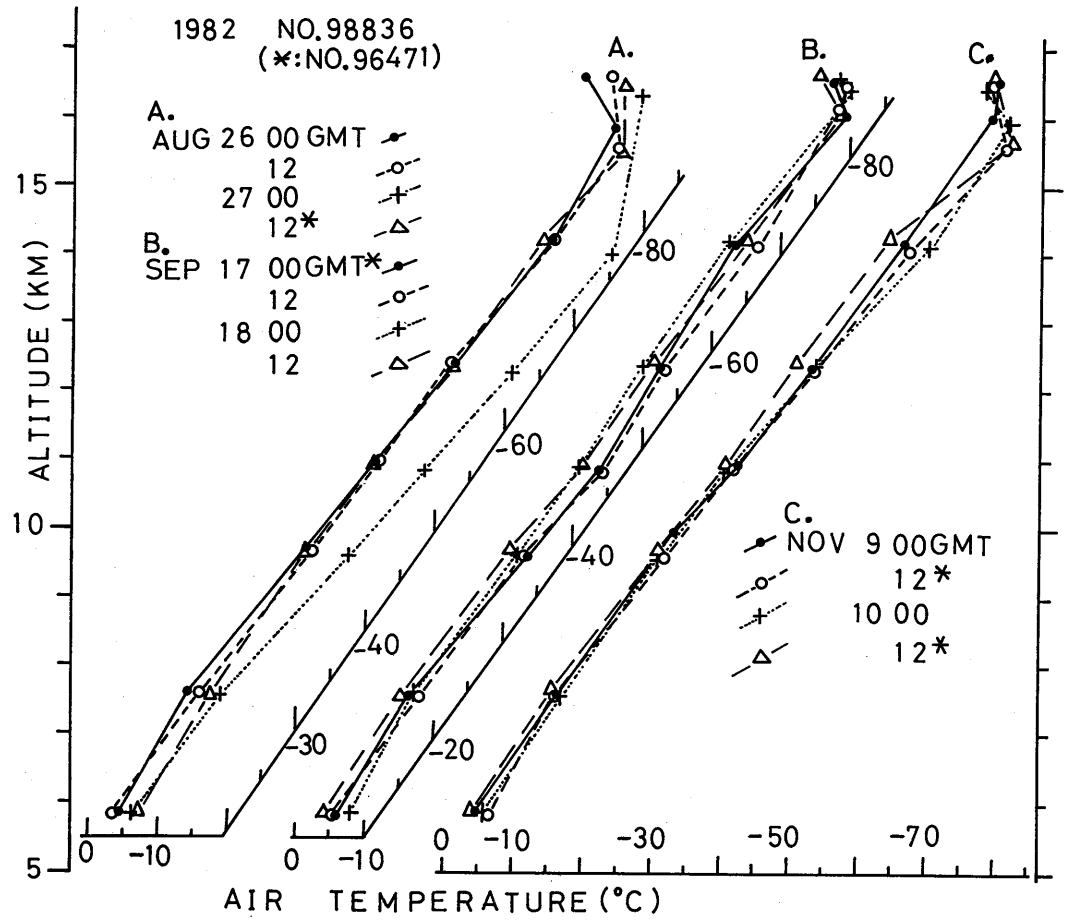

Fig. 3-29 Air-temperature profiles based on radio-sounding observation materials at No. 98836 and No. 96471 (see Fig. 3-28) in August 26-27, September 17-18 and November 9-10, 1982.

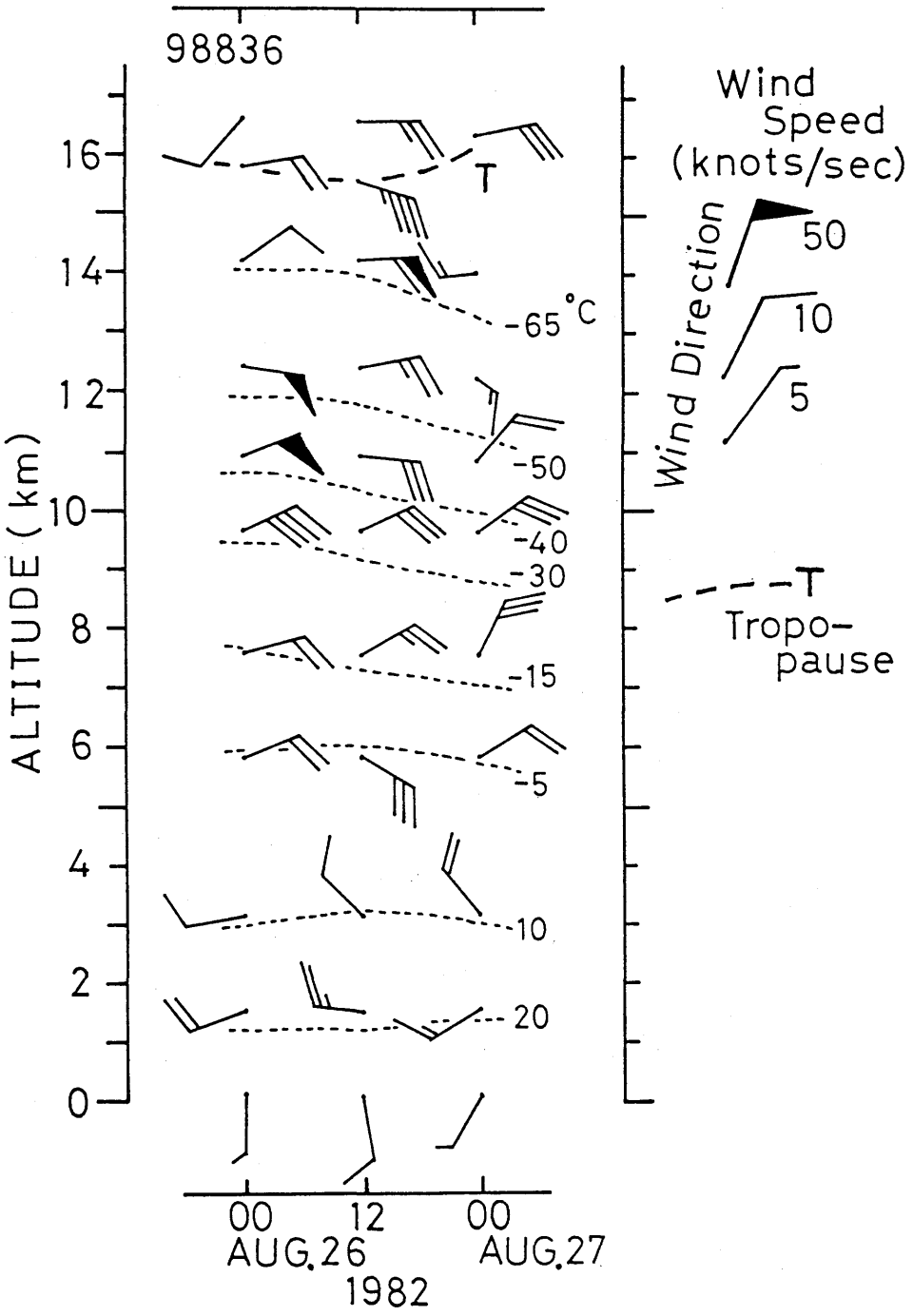

Fig. 3-30 Profiles of wind directions and wind speeds expressed by international notations, based on observations at No. 98836 on August 26-27, 1982.

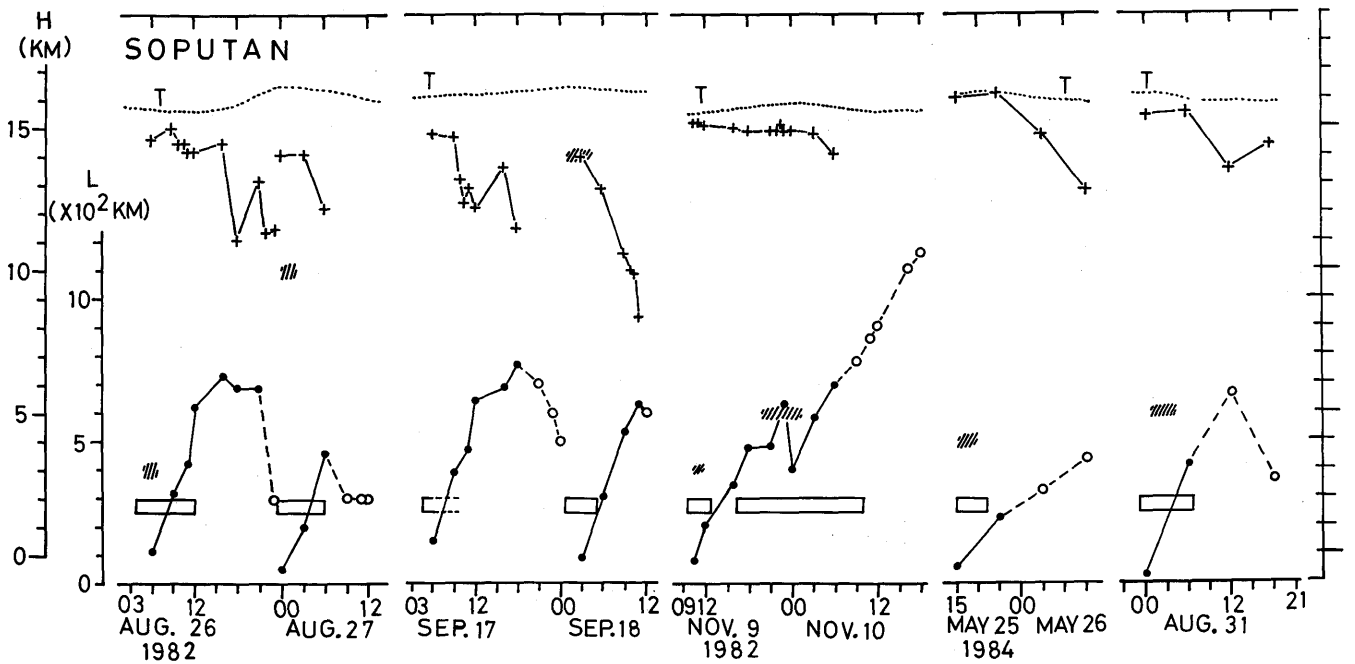

Fig. 3-31 Time variations of the estimated highest altitude (cross marks by H axis) and the longest length (solid and open circles by L axis) of the eruption clouds detected during August, September and November, 1982, and May and August, 1984. T means the altitude of the tropopause. Solid circles and dotted ones with solid and dotted lines denote that the cloud was continuous from the location of Soputan volcano and that it was detached from the volcano, respectively. Hatched portion and rectangle mean the top of eruption clouds and the duration period of individual eruptions observed by the ground observations, respectively.

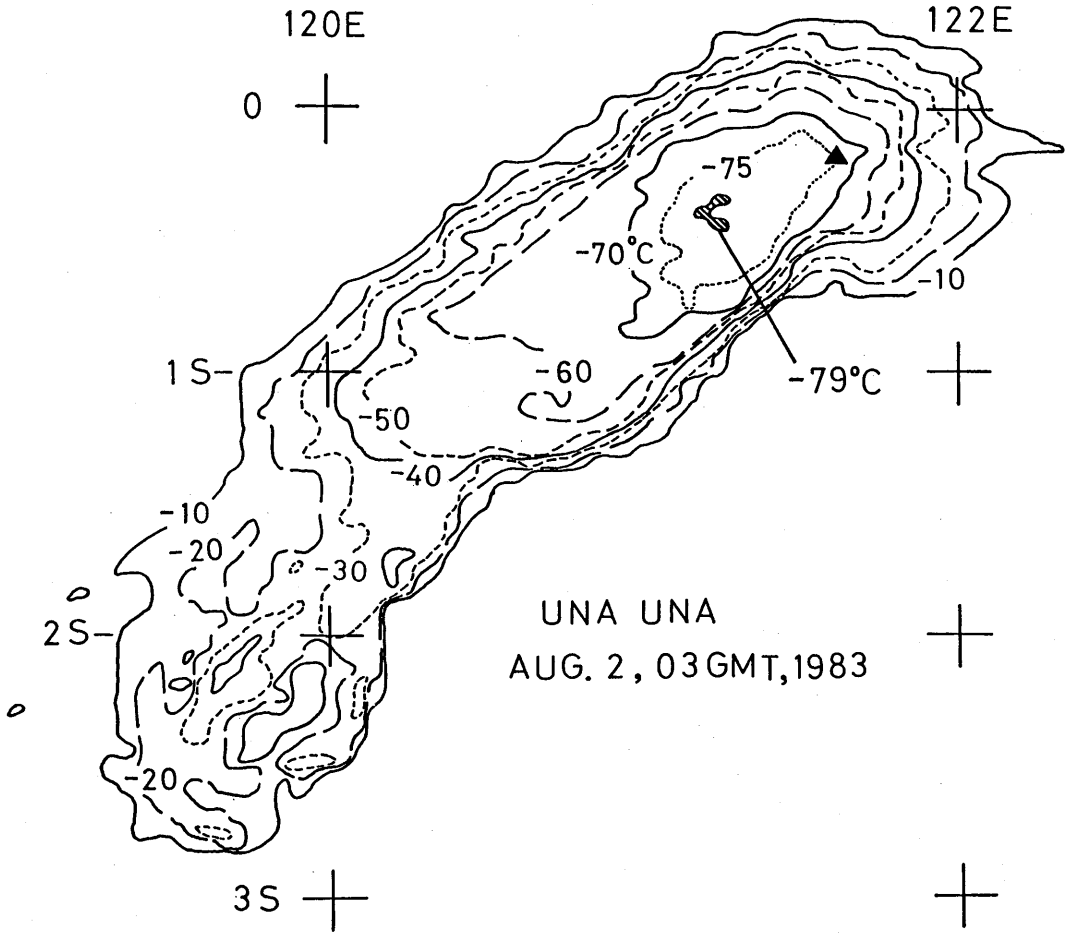

Fig. 3-32 Surface temperature contours in °C of the eruption cloud of Una Una volcano taken at 03 GMT on August 2, 1983. The lowest temperature was -79°C. Triangle means the location of this volcano.

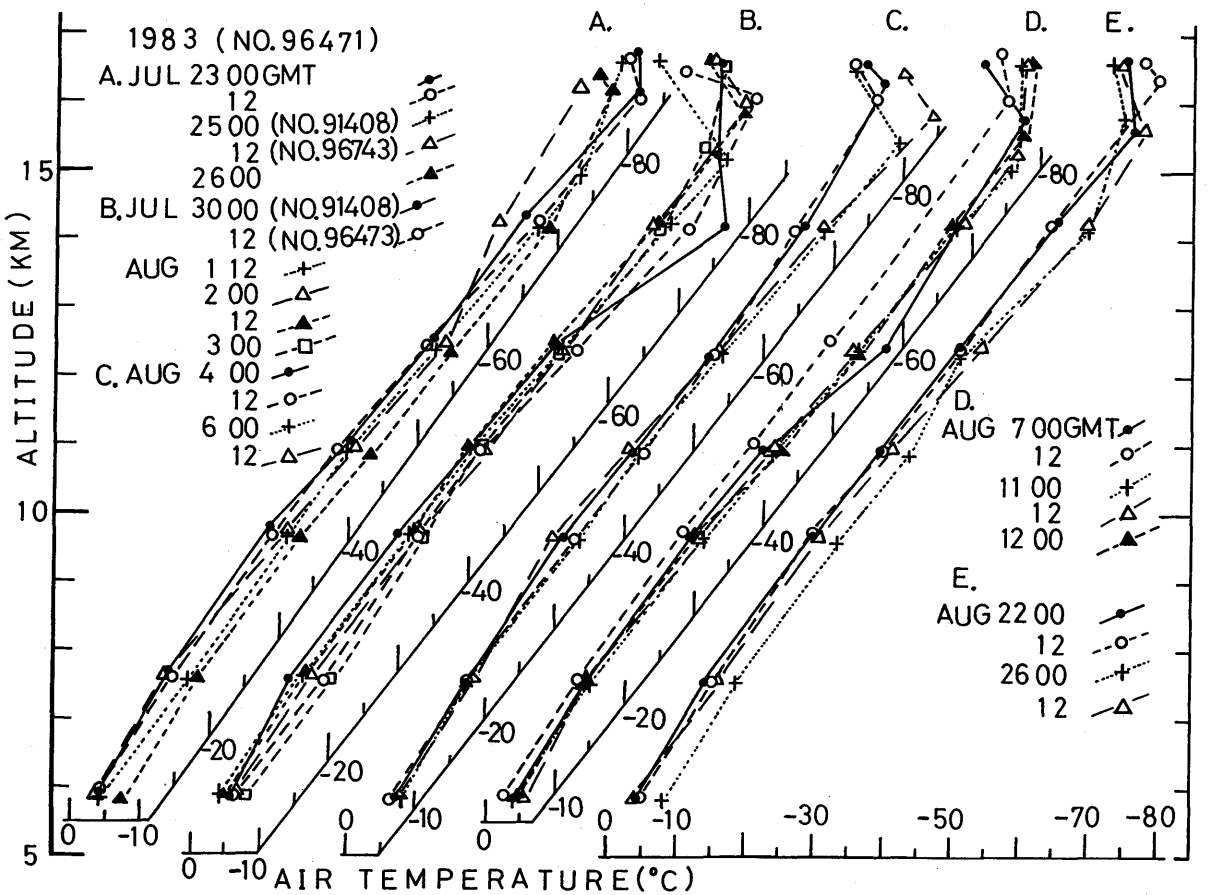

Fig. 3-33 Air-temperature profiles at 00 GMT and 12 GMT on July 23, 25-26 and 30 and August 1-4, 6-7, 11-12, 22 and 26, 1983, used for estimation of altitude of Una Una eruption clouds (see Fig. 3-28 for the location of radio-sounding stations).

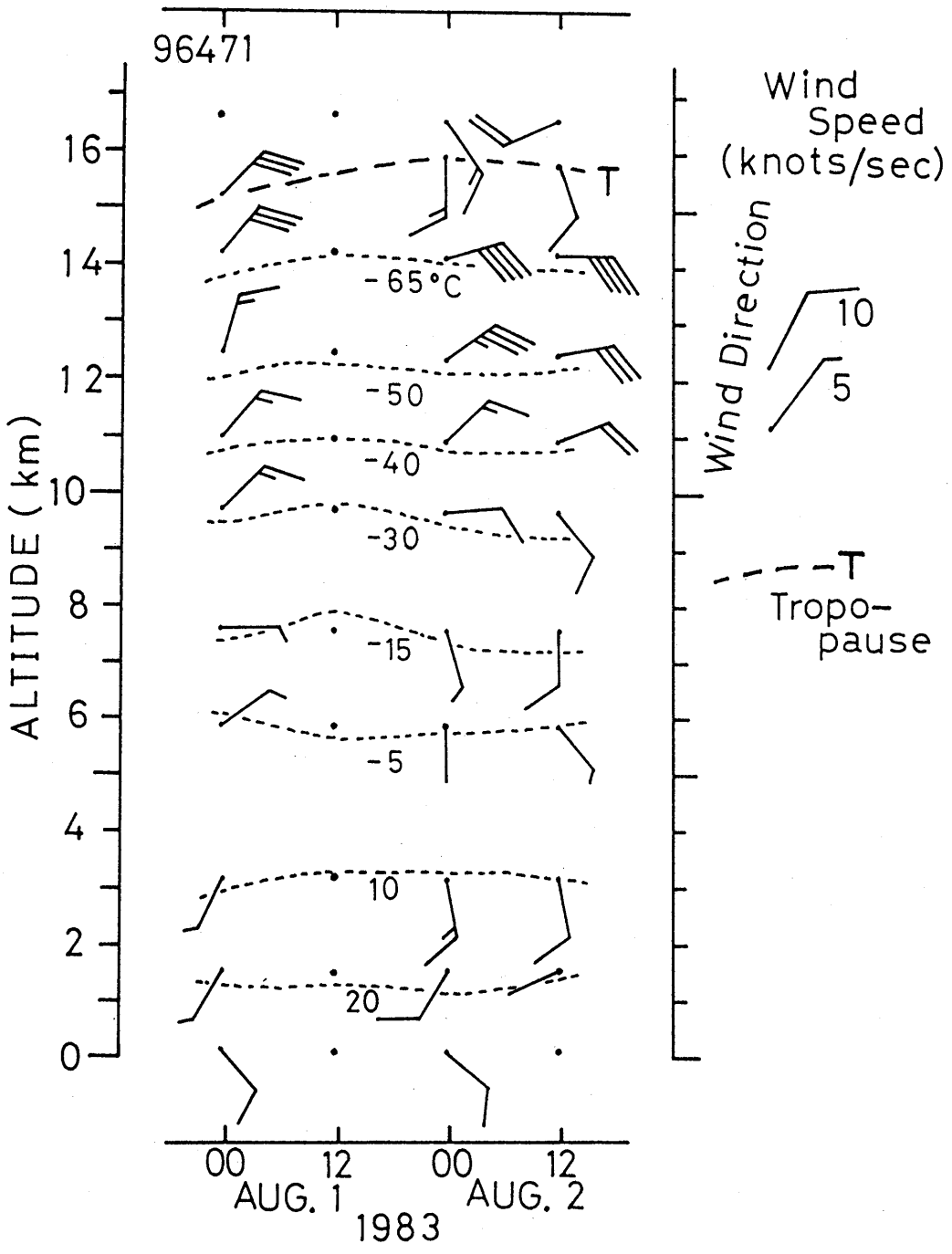

Fig. 3-34 Profiles of air-temperature, wind direction and wind speed expressed by the international notation based on radio-sounding observations at No. 96471 station (see the location of radio-sounding stations in Fig. 3-28).

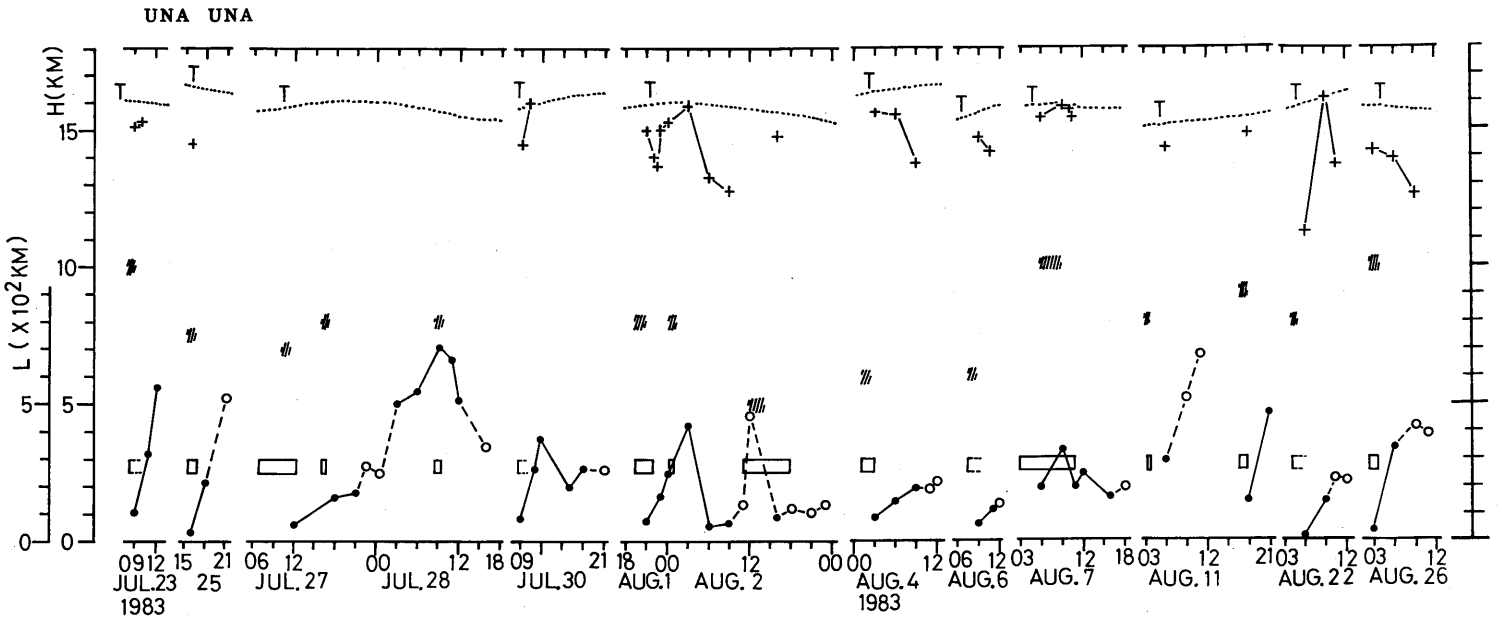

Fig. 3-35 Time variations of estimated highest altitude (cross marks with H axis) and maximum horizontal length (solid circle and open one with L axis) of detected eruption clouds from Una Una volcano during the period of July-August, 1983 Eruptions. T means altitude of the tropopause. Solid circles and open ones denote that the eruption clouds were continuous from the location of Una Una volcano and that they were detached from the volcano in GMS images, respectively. Hatched portion and rectangle mean the highest altitude of eruption clouds and the duration time of eruptions by ground observations, respectively.

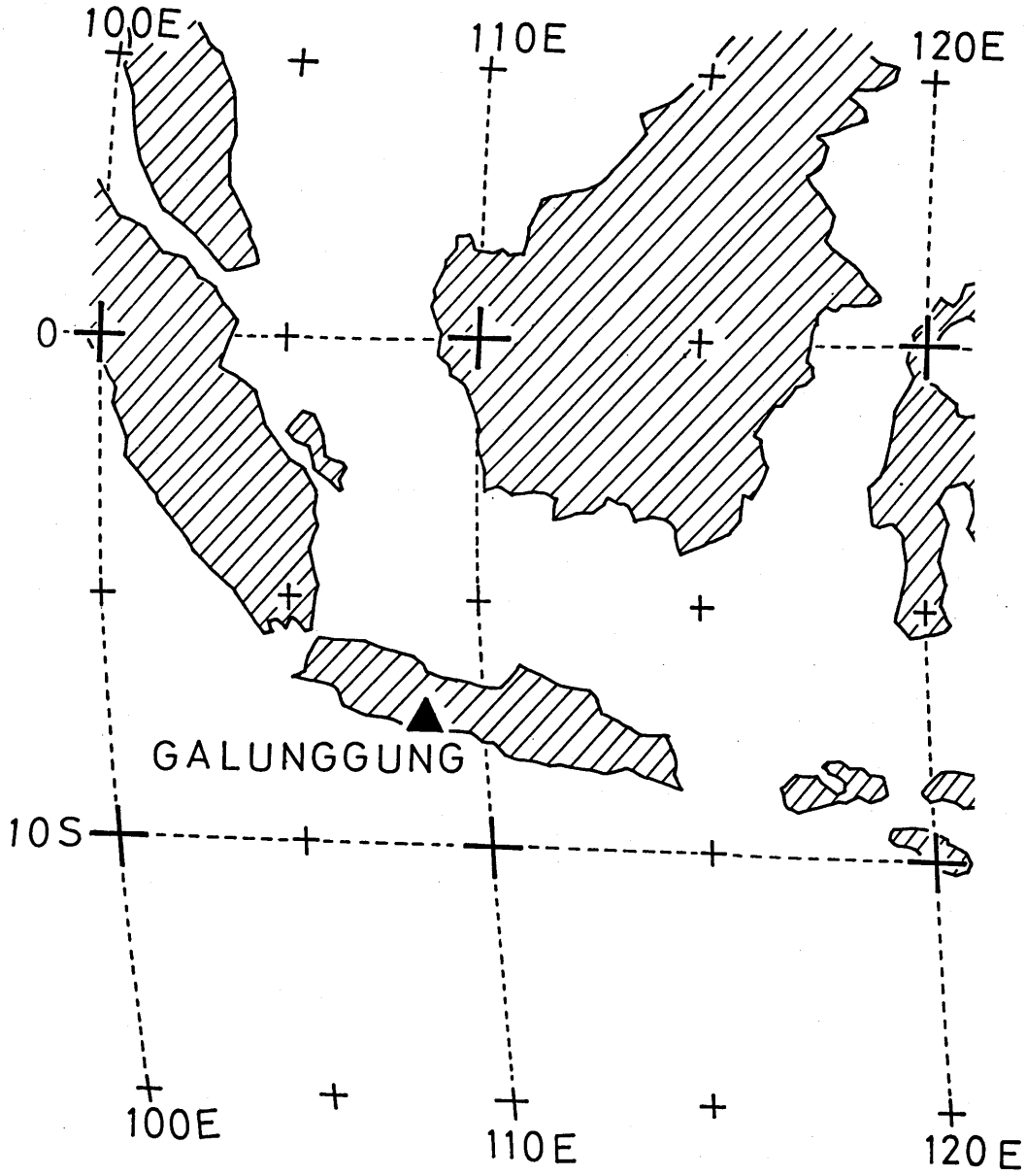

Fig. 3-36 Location of Galunggung volcano (solid triangle).

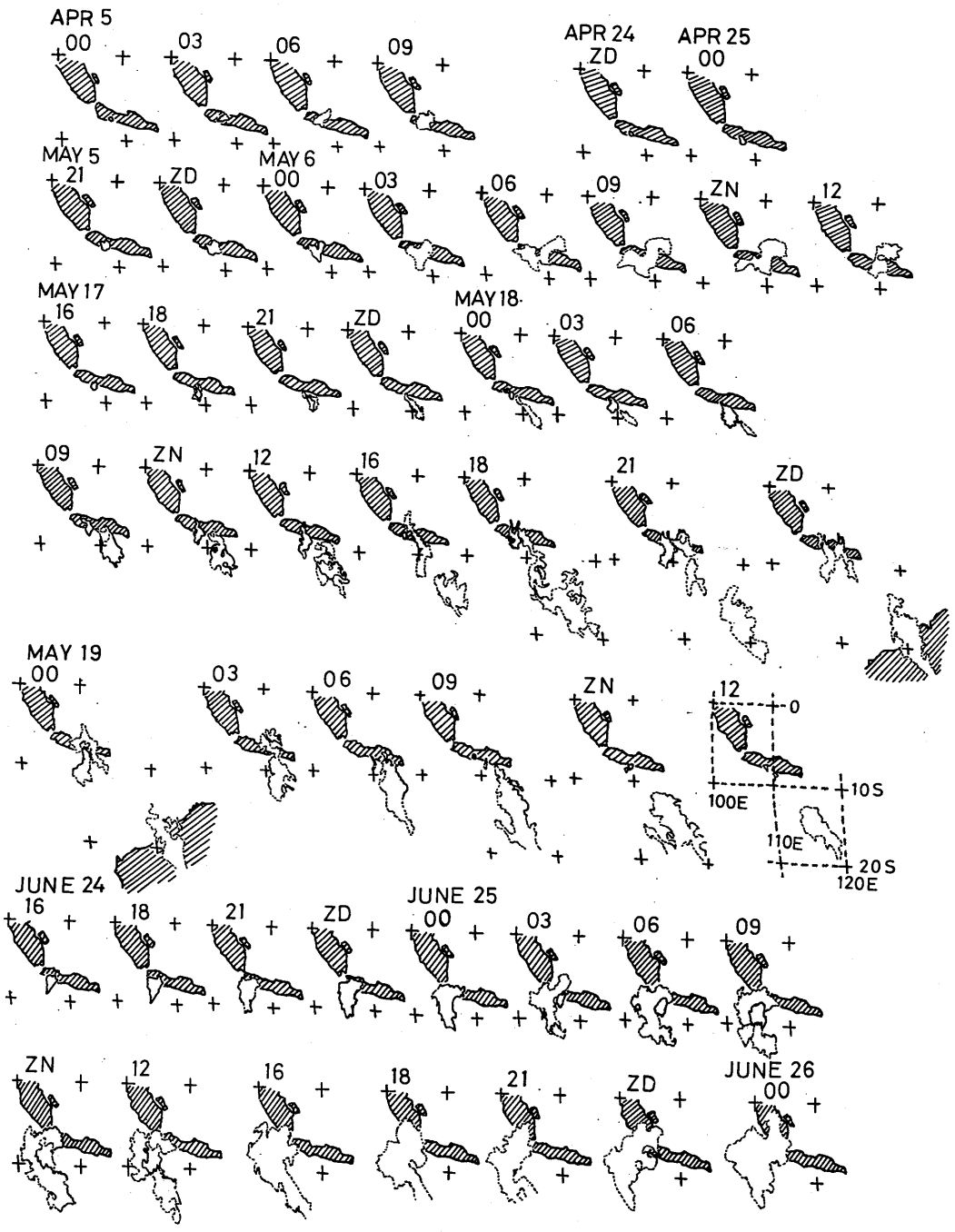

(a)

Fig. 3-37 (a)-(d)

Extent of eruption clouds from Galunggung volcano detected in GMS images during the eruptions in April-October, 1982. They are outlined by solid lines for distinct domains and dotted lines for indistinct ones.

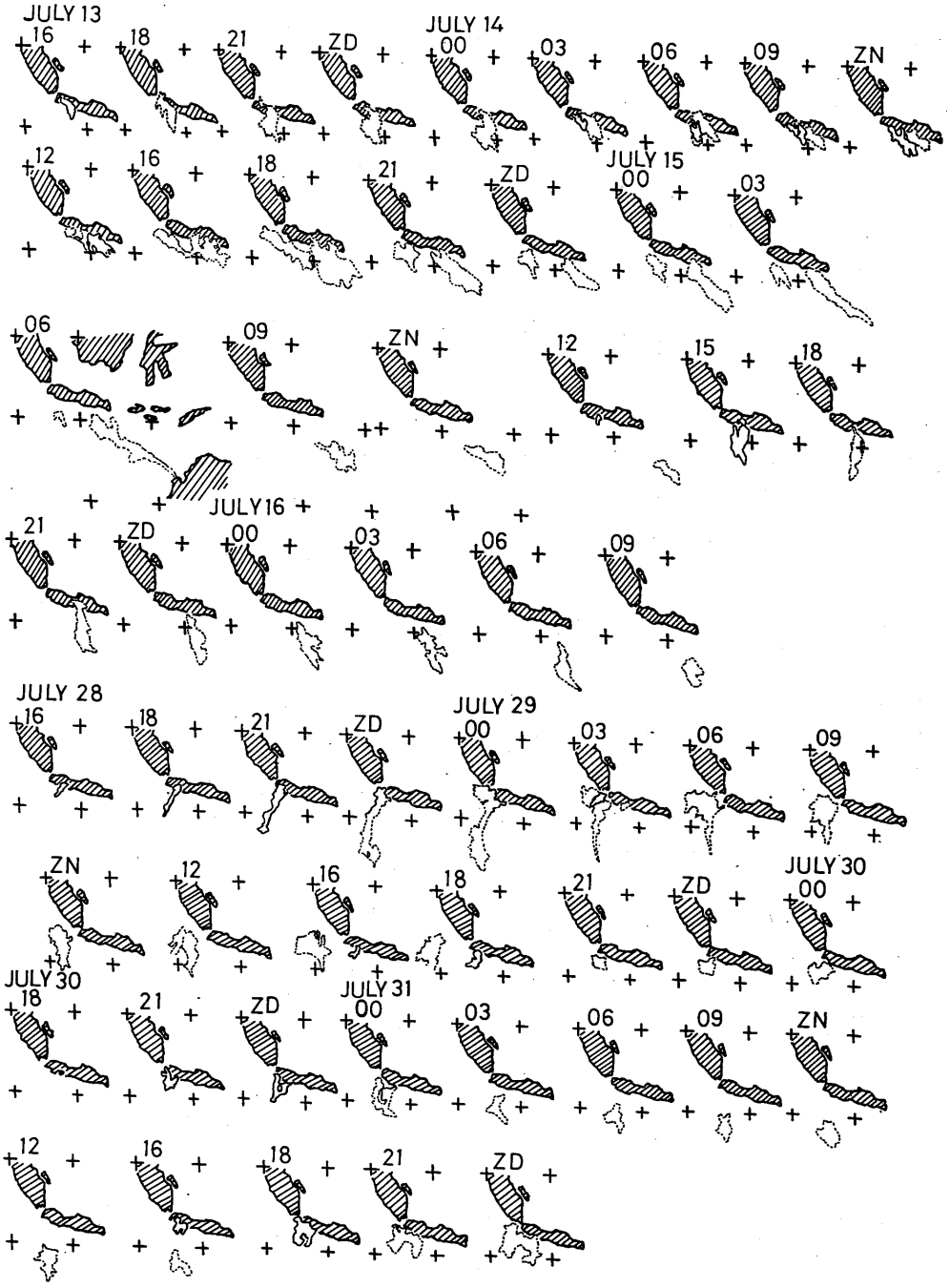
JULY 13
16
18
21
ZD
JULY 14
00
03
06
09
ZN
12
16
18
21
ZD
JULY 15
00
03
06
09
ZN
12
15
18
JULY16
21
ZD
00
03
06
09
JULY 28
16
18
21
ZD
JULY 29
00
03
06
09
ZN
12
16
18
21
ZD
JULY 30
00
JULY 30
18
21
ZD
JULY 31
00
03
06
09
ZN
12
16
18
21
ZD

(b)

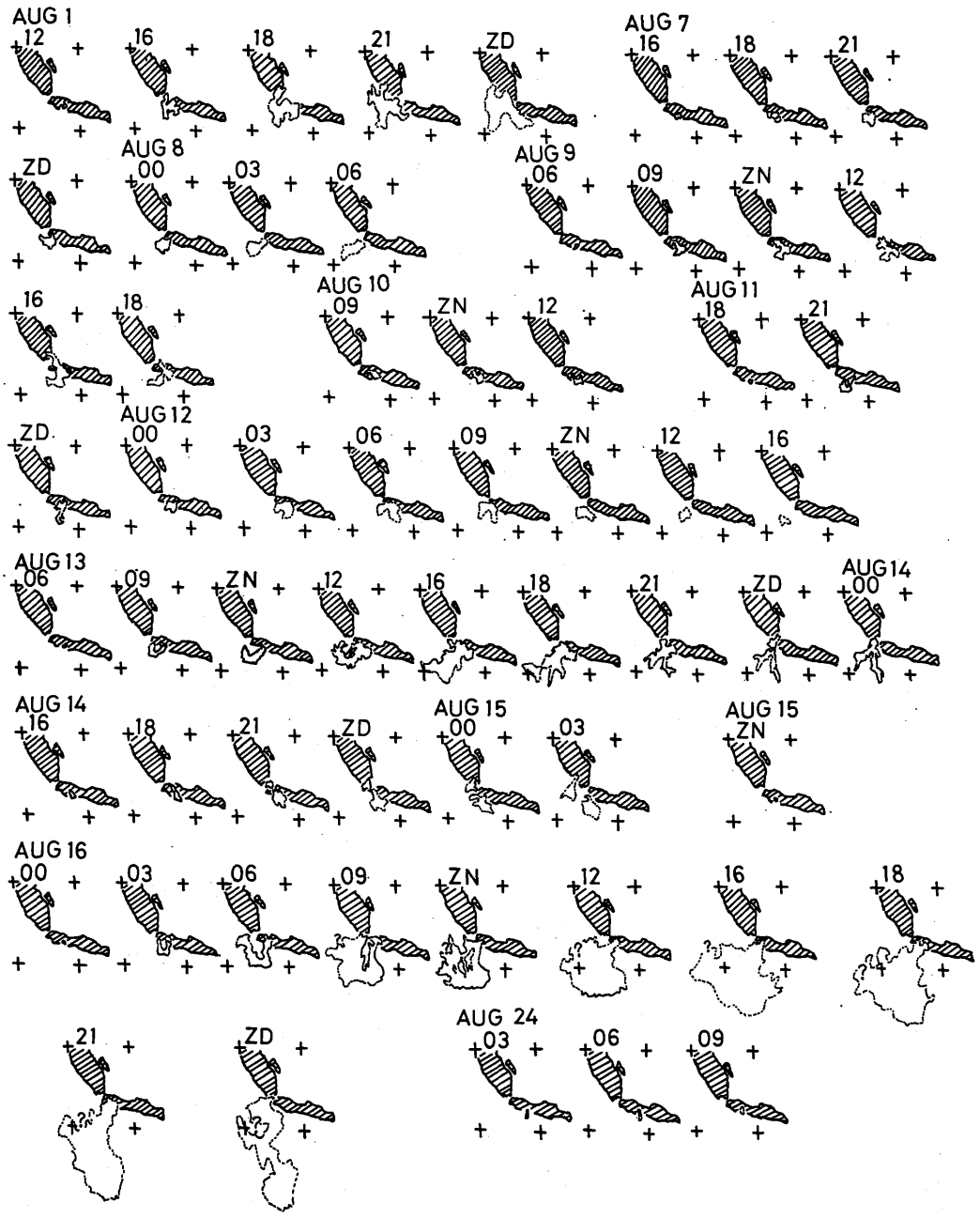
AUG 1
12
16
18
21
ZD
AUG 7
16
18
21
ZD
AUG 8
00
03
06
AUG 9
06
09
ZN
12
16
18
AUG 10
09
ZN
12
AUG 11
18
21
AUG 12
ZD
00
03
06
09
ZN
12
16
AUG 13
06
09
ZN
12
16
18
21
ZD
AUG 14
00
AUG 14
16
18
21
ZD
AUG 15
00
03
AUG 15
ZN
AUG 16
00
03
06
09
ZN
12
16
18
21
ZD
AUG 24
03
06
09

(c)

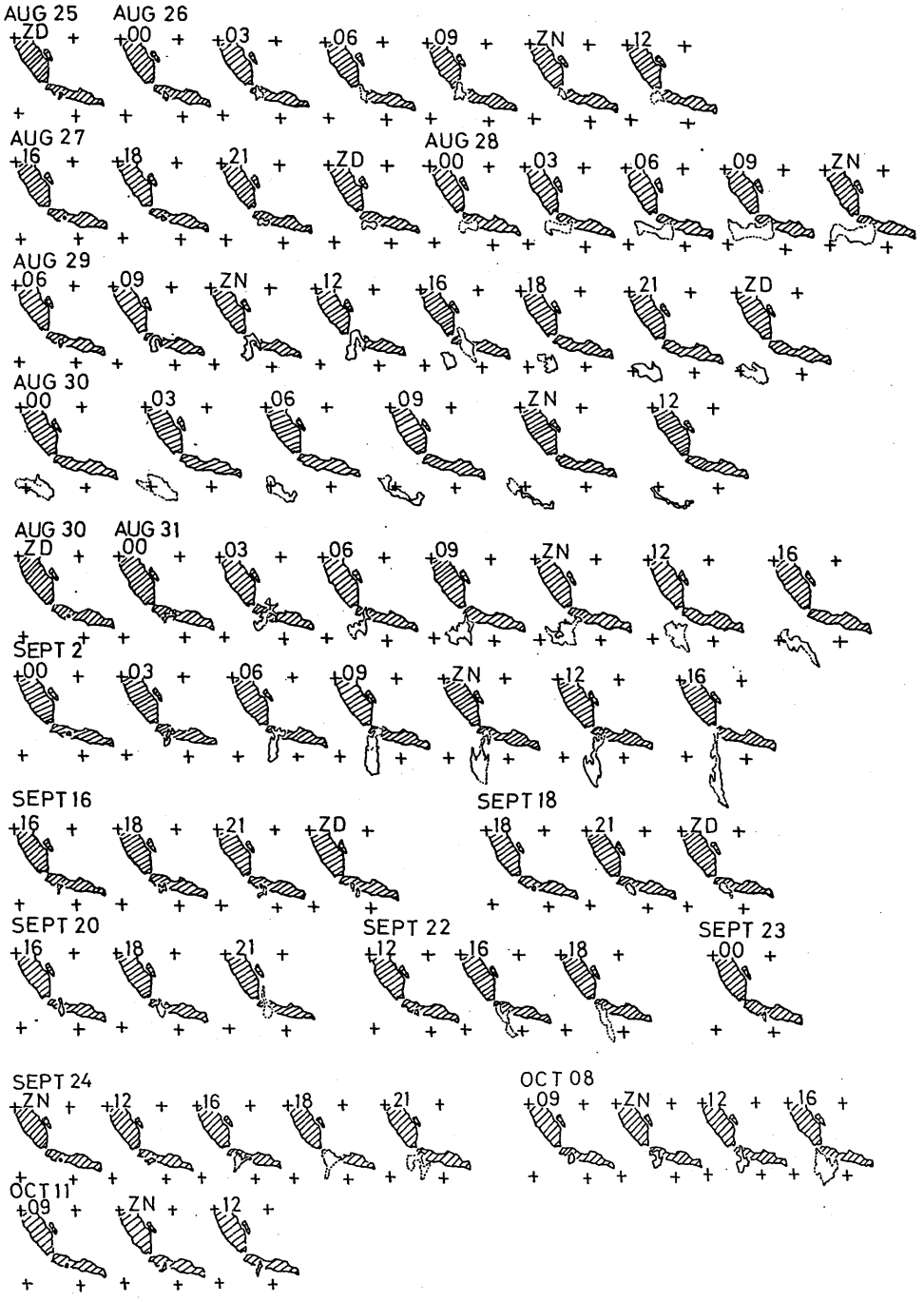
AUG 25
ZD
AUG 26
00
03
06
09
ZN
12
AUG 27
16
18
21
ZD
AUG 28
00
03
06
09
ZN
AUG 29
06
09
ZN
12
16
18
21
ZD
AUG 30
00
03
06
09
ZN
12
AUG 30
ZD
AUG 31
00
03
06
09
ZN
12
16
SEPT 2
00
03
06
09
ZN
12
16
SEPT 16
16
18
21
ZD
SEPT 18
18
21
ZD
SEPT 20
16
18
21
SEPT 22
12
16
18
SEPT 23
00
SEPT 24
ZN
12
16
18
21
OCT 08
09
ZN
12
16
OCT 11
09
ZN
12

(d)

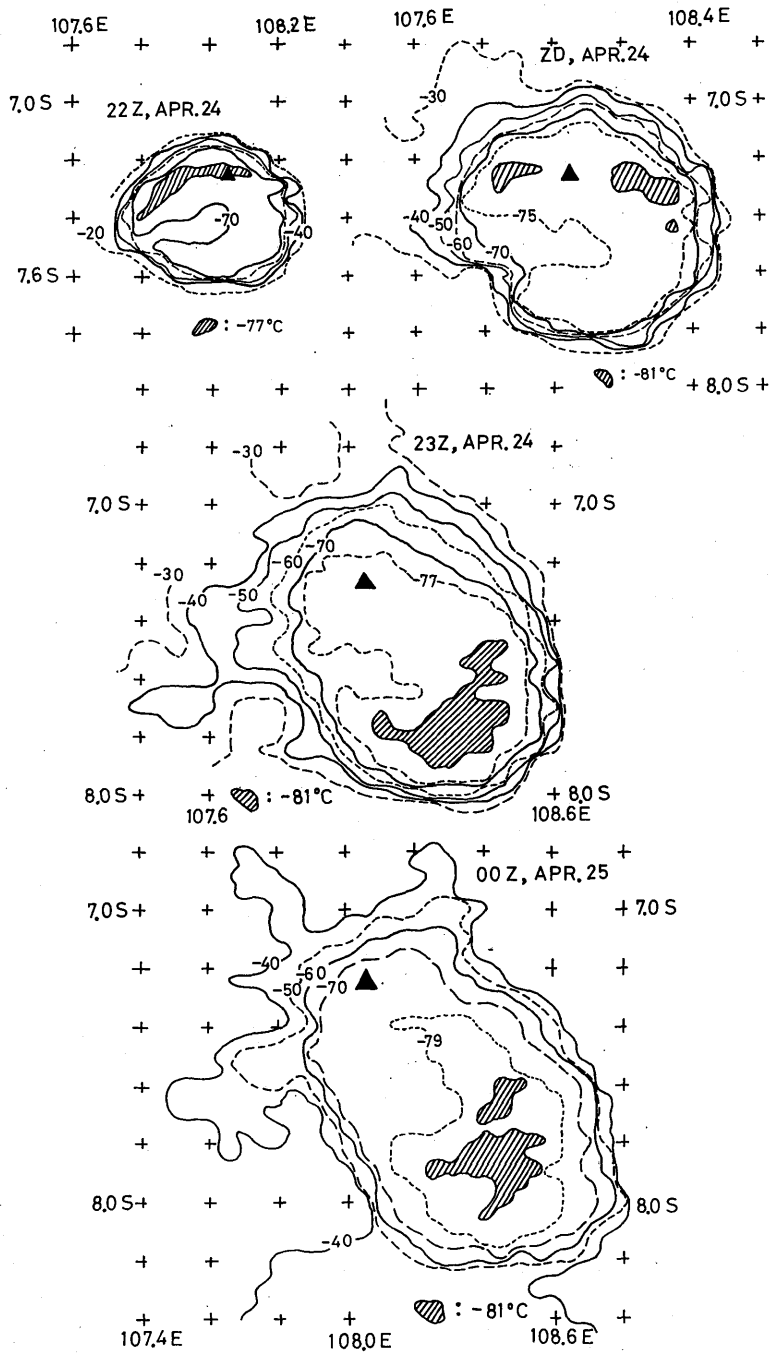

(a)

Fig. 3-38 (a)-(b)

Examples of surface temperature contours of eruption clouds by processing of GMS IR digital image data. The coldest portions of the eruption clouds are shown with hatched domains with individual numerals in °C. Triangle denotes the location of Galunggung volcano.

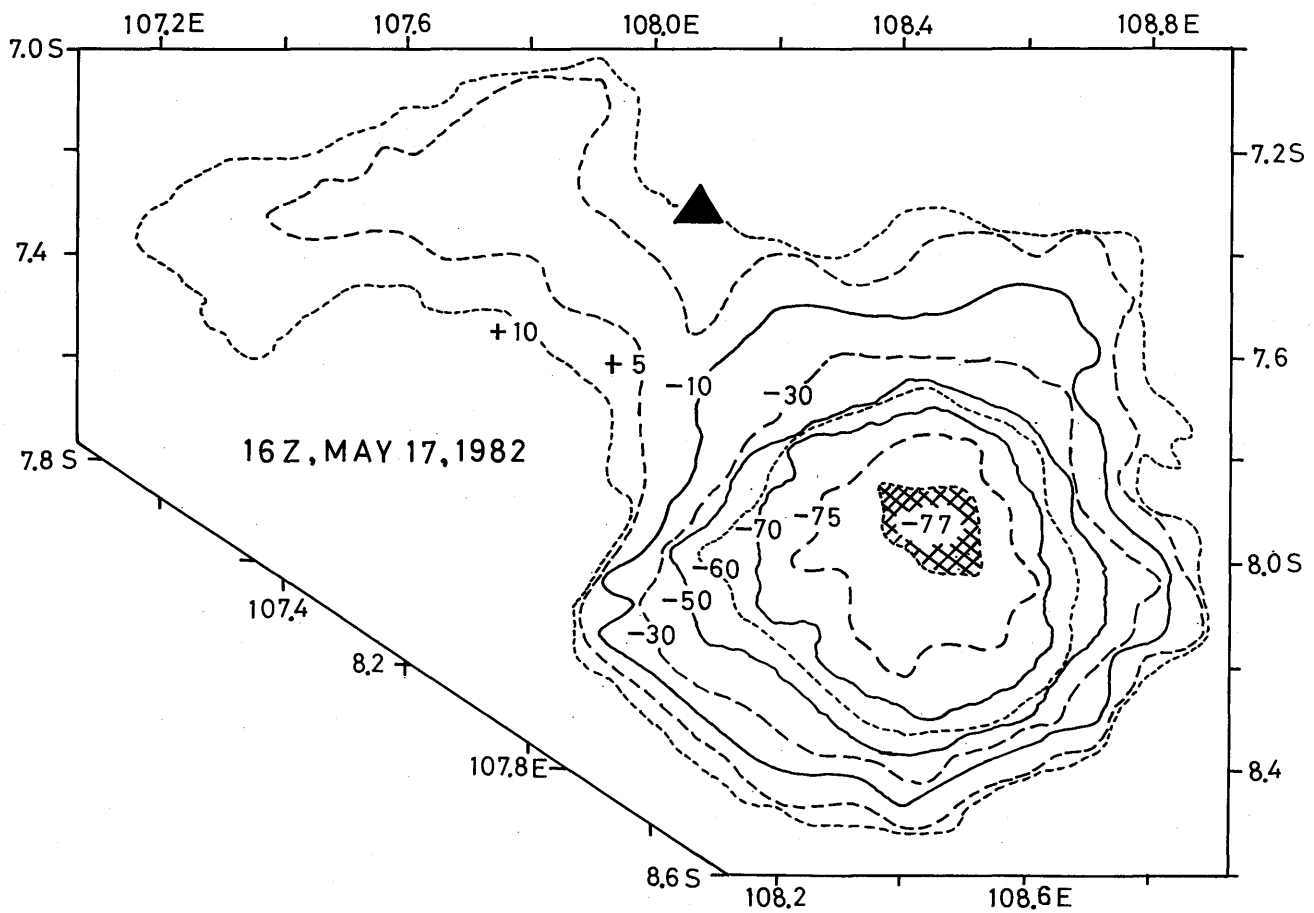
107.2E
107.6
108.0E
108.4
108.8E
7.0S
7.4
7.8S
7.2S
7.6
8.0S
8.4
8.6S
108.2
108.6E
107.4
8.2
107.8E
16Z, MAY 17, 1982
+10
+5
-10
-30
-70
-75
-77
-60
-50
-30

(b)

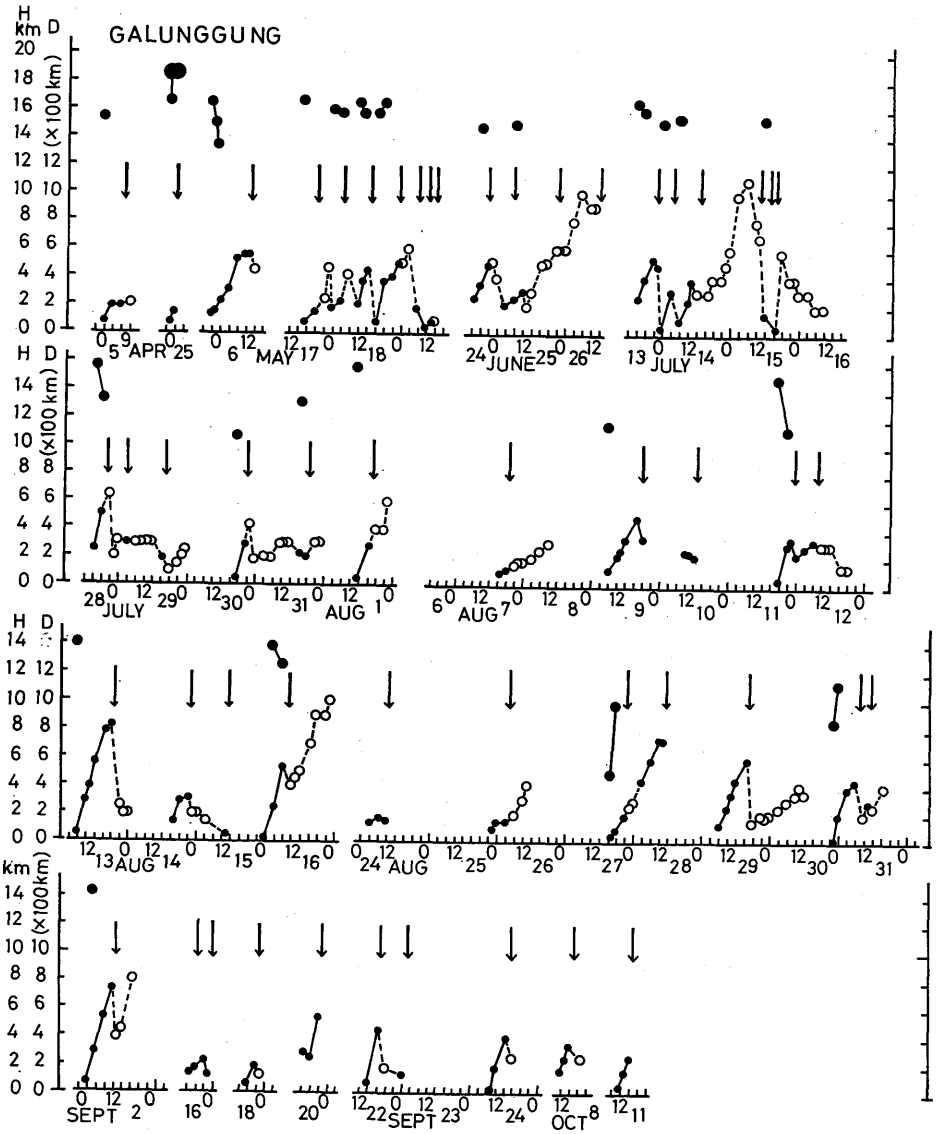

Fig. 3-39 Time variations of estimated highest altitudes (larger solid circles at upper side with H axis) and longest horizontal lengths (smaller solid circles and open ones with D axis) of detected eruption clouds from Galunggung volcano during the eruptions in April-October, 1982. Black and downward arrow denotes the estimated time of the end of an individual eruption based on the judgement of its detachment from the location of this volcano, as expressed in open circle, while smaller solid circle denotes that eruption cloud was coming from the location of this volcano.

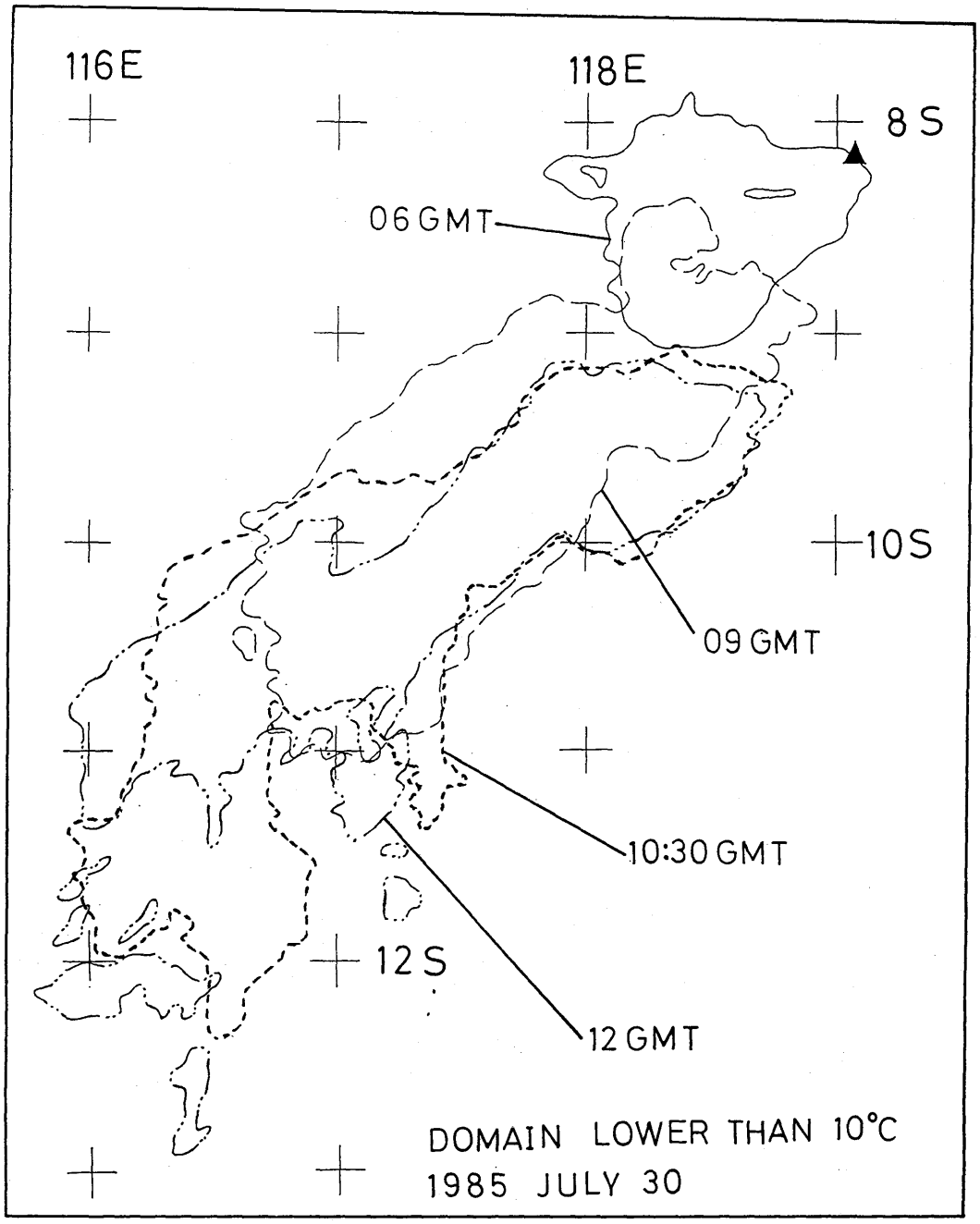

Fig. 3-40 Extent of eruption clouds colder than +10°C coming from Sangeang Api volcano. Solid triangle means the location of the volcano.

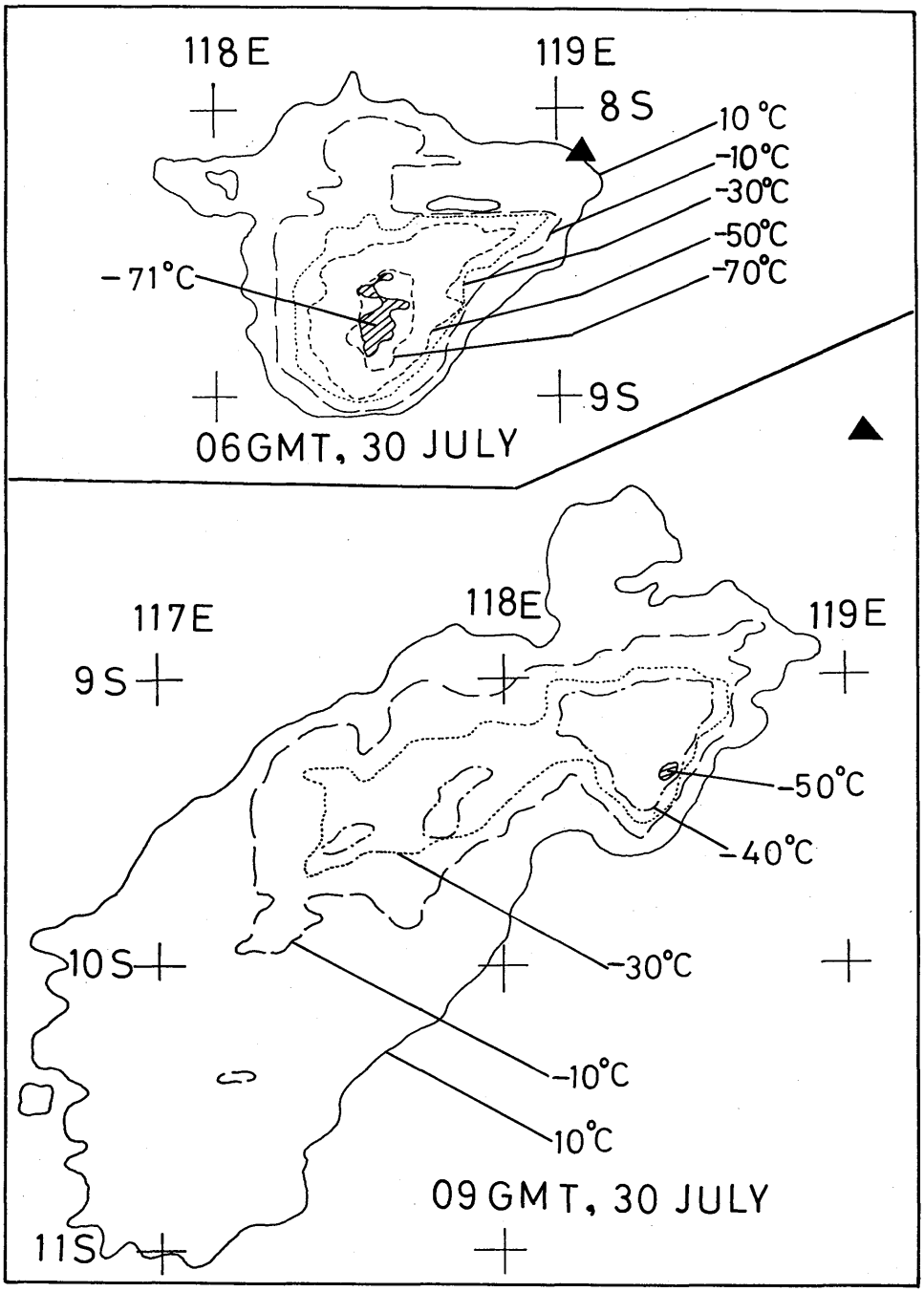

Fig. 3-41 Surface temperature contours colder than +10°C of the eruption clouds detected at 06 GMT and 09 GMT on July 30, 1985. The coldest portion was shown with hatched area with numerals showing temperature in °C.

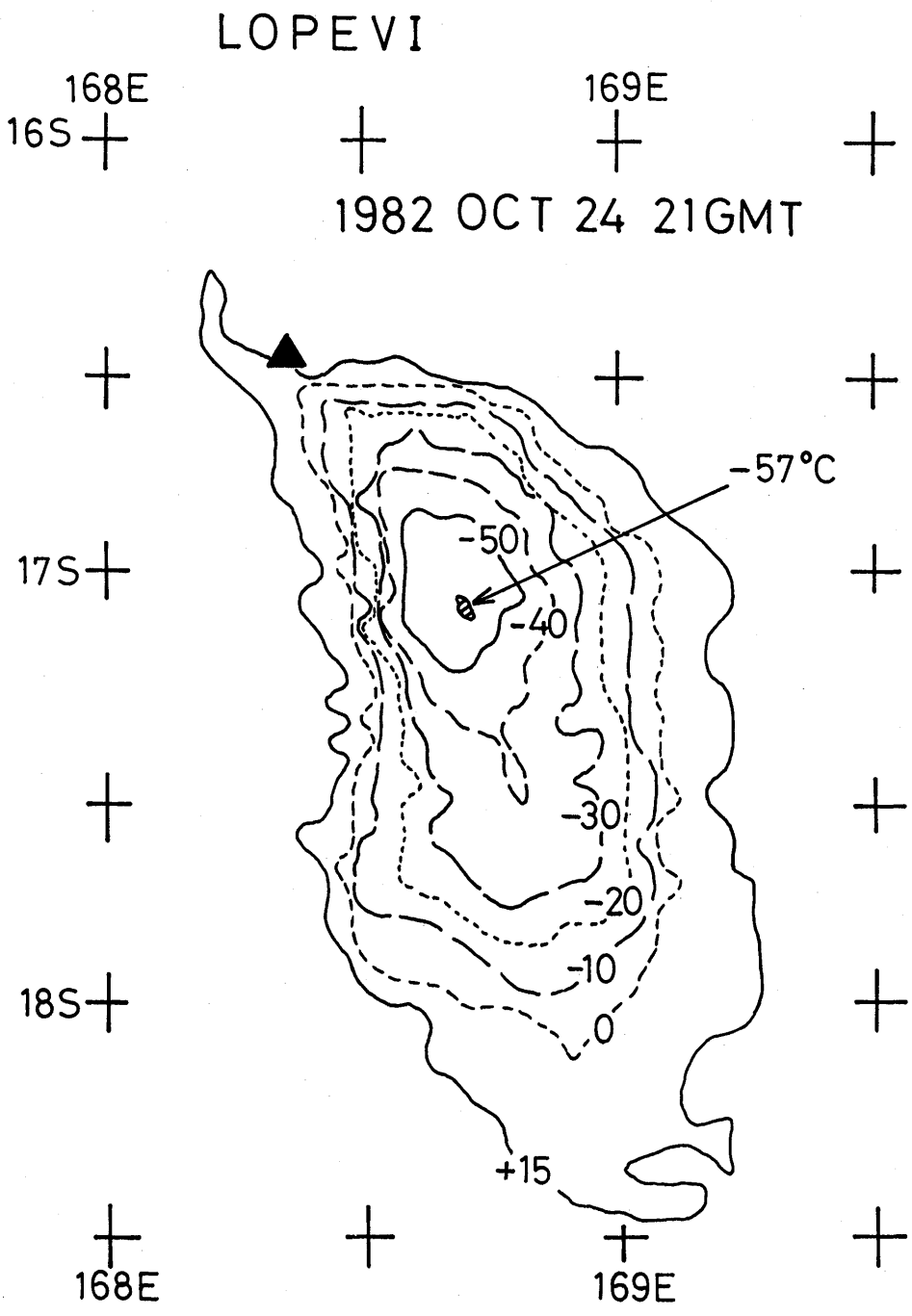

Fig. 3-42 Surface temperature contour in °C of the Lopevi eruption cloud taken at 21 GMT on October 24, 1982. The coldest portion was -57°C. Solid triangle means the location of Lopevi volcano.

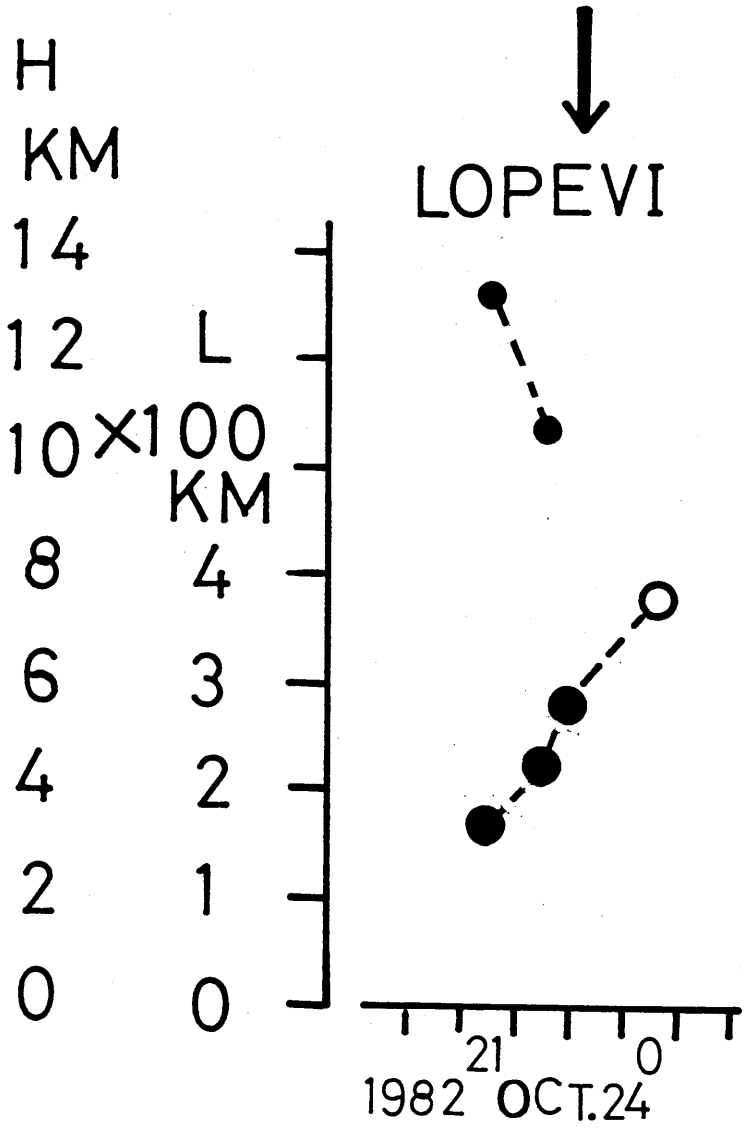

Fig. 3-43 Time variations of the highest altitude (upper solid circle with H axis) and the longest horizontal length (lower solid circle with L axis) of the detected eruption cloud from Lopevi volcano.

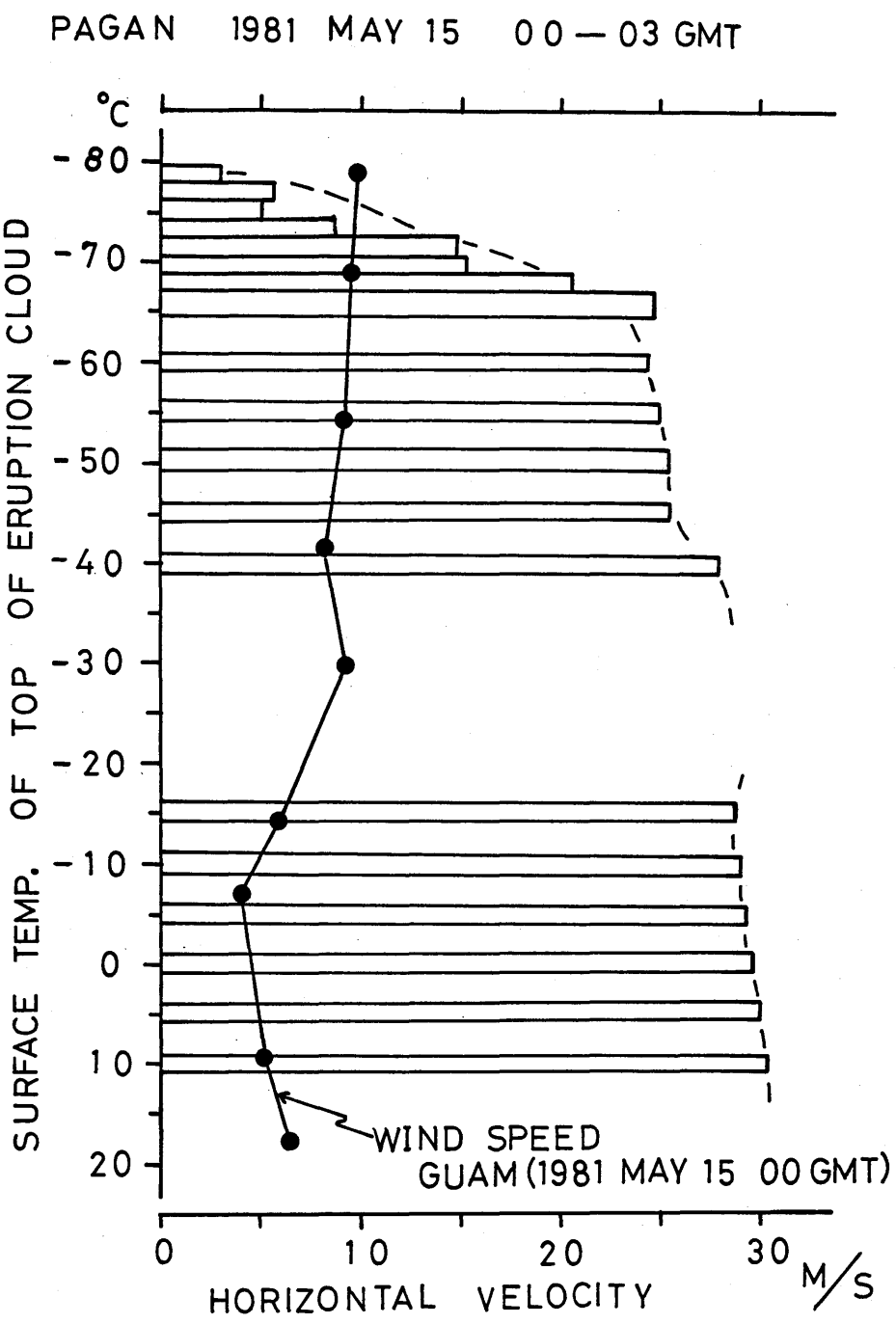

Fig. 4-1 Profiles of horizontal moving velocity of spreading eruption cloud by the May 15, 1981 Pagan Eruption (horizontal rectangles). Solid circles denote the wind speed profiles based on the radio-sounding data at Guam station.

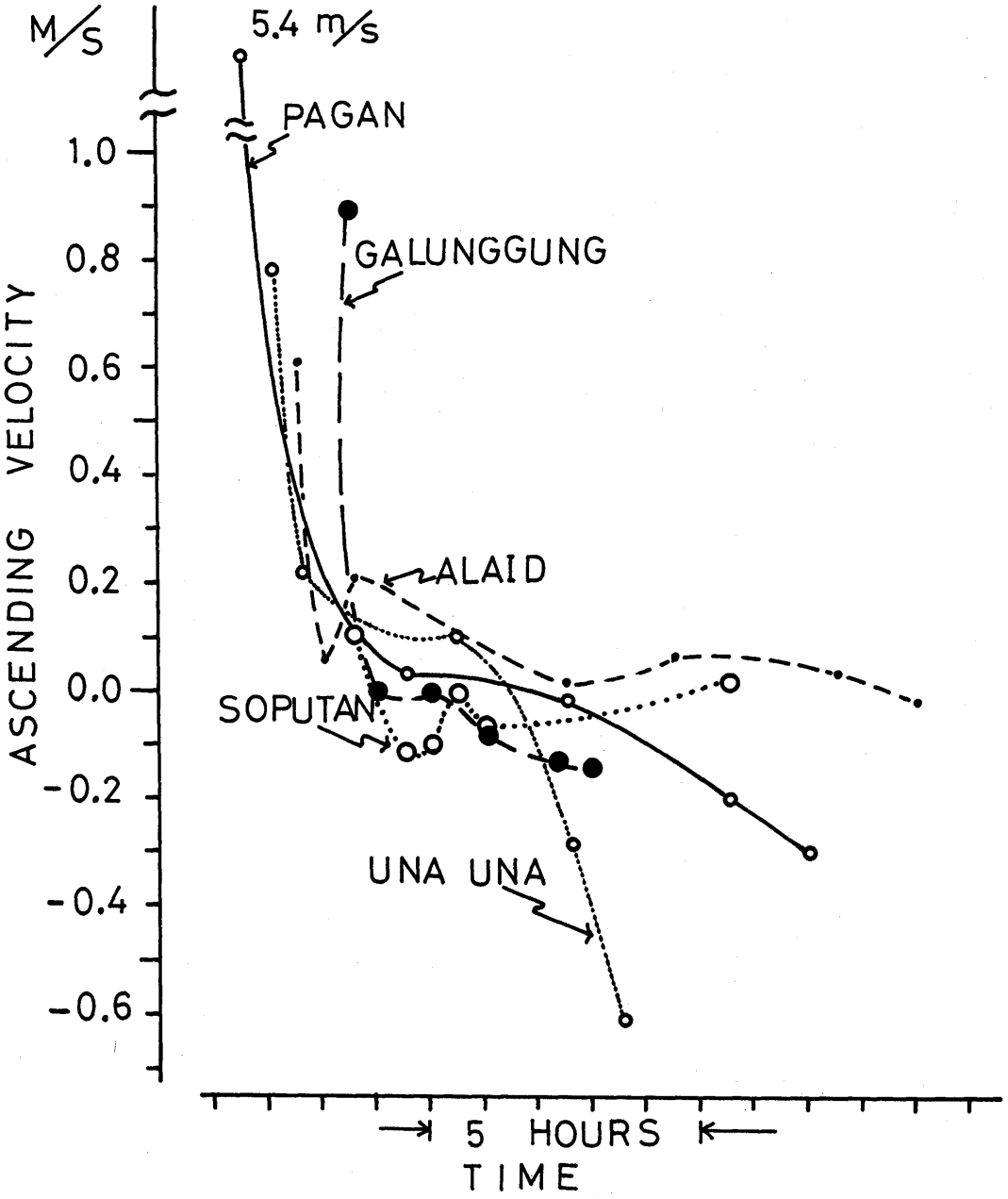

Fig. 4-2 Estimated ascending velocities obtained by analyses of eruption clouds at Alaid, Pagan, Soputan, Galunggung and Una Una volcanoes.

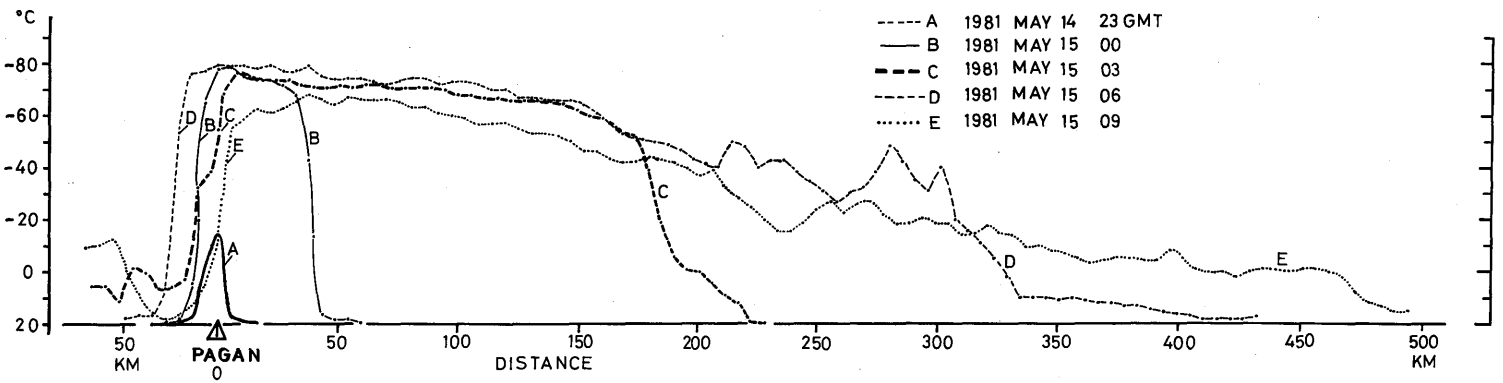

Fig. 4-3 Time variations of the profiles of eruption clouds.

(a) Pagan eruption clouds during the May 1981 Eruption.

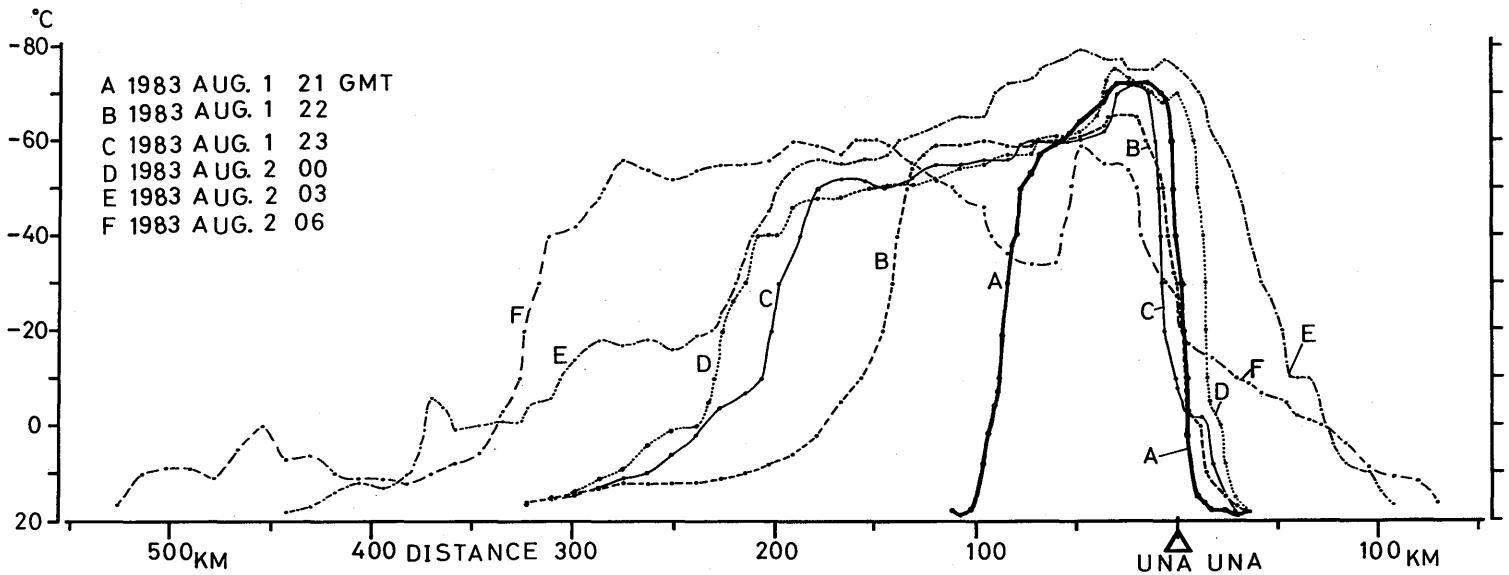

(b) Una Una eruption clouds during the August 1983 Eruption.

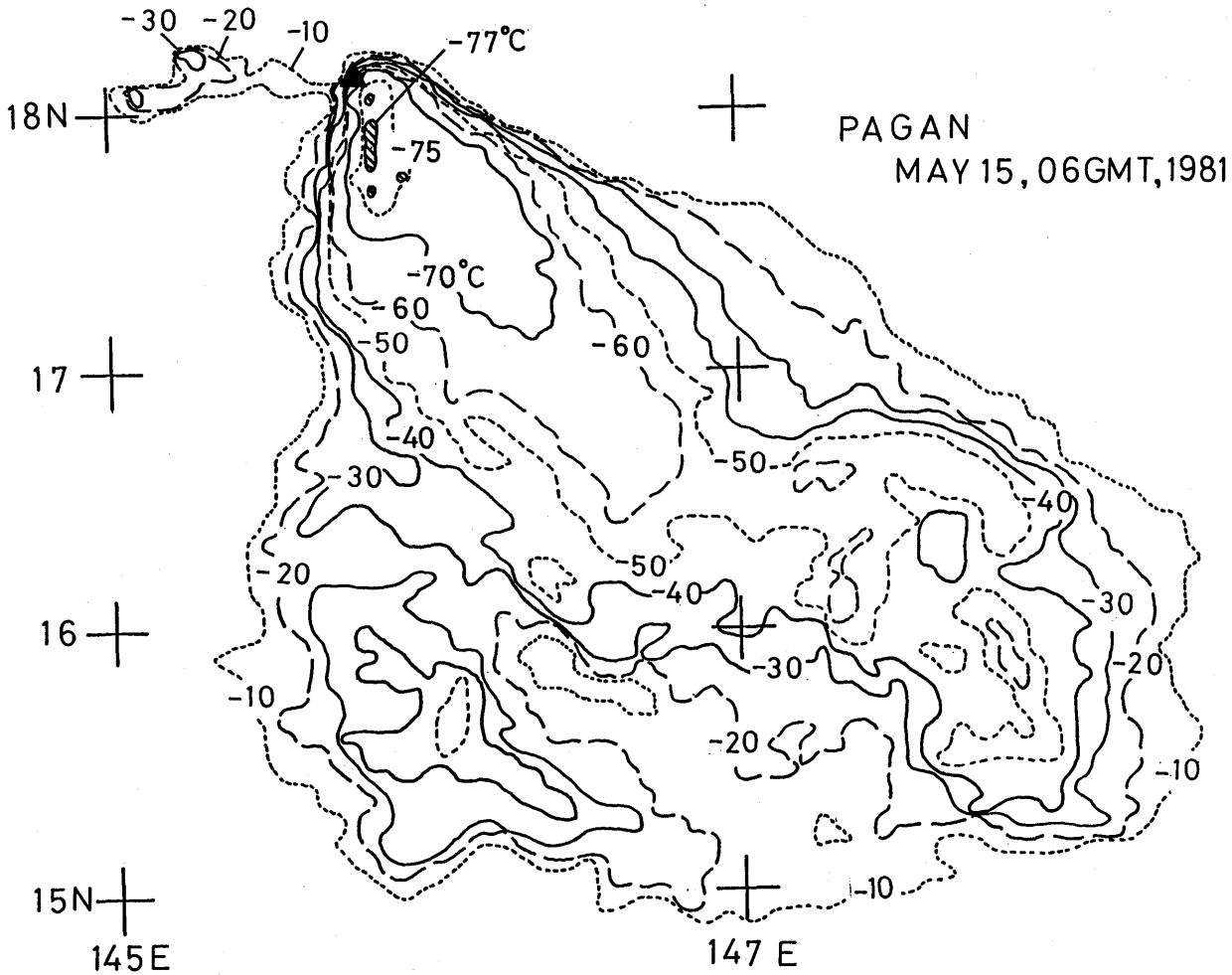

Fig. 4-4 Surface temperature contours in °C of Pagan eruption cloud taken at 06 GMT on May 15, 1981.

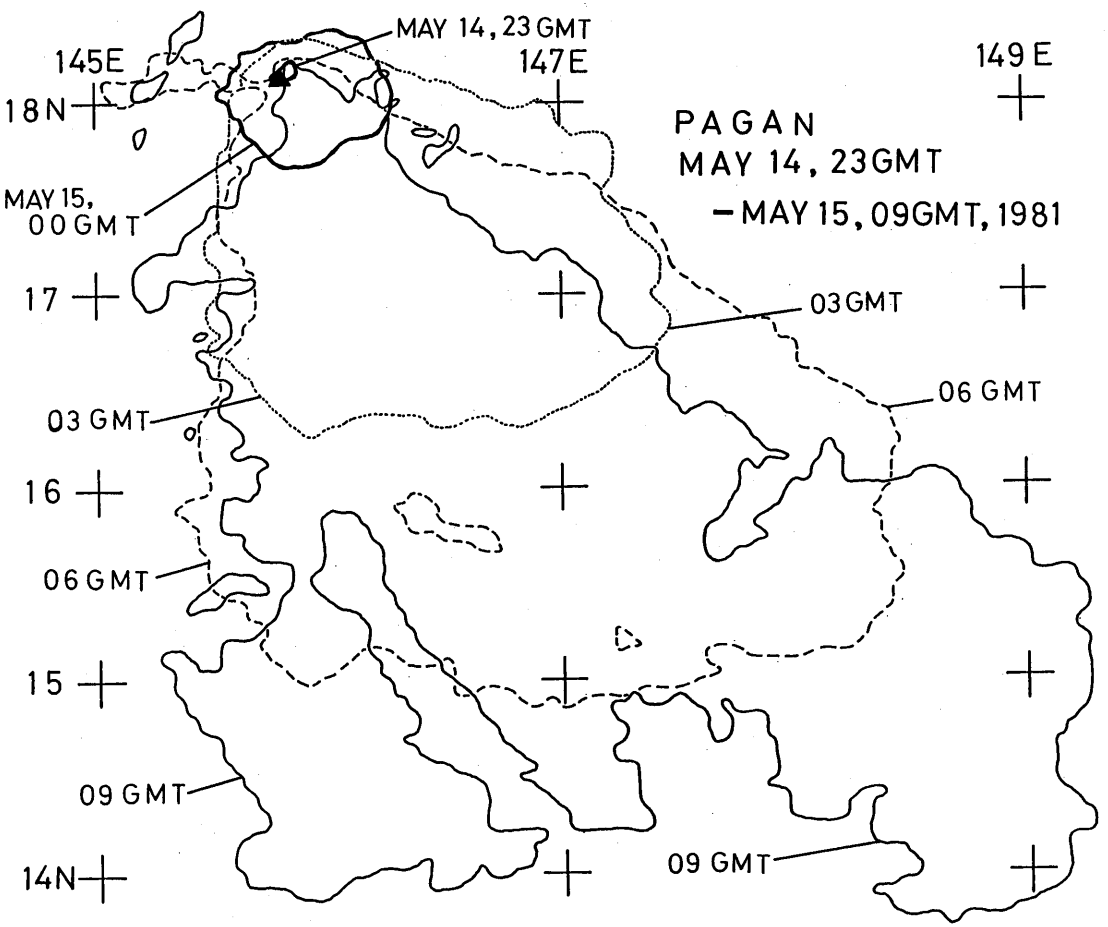

Fig. 4-5 Time variations of the extent colder than -10°C of Pagan eruption clouds.
(a) 23 GMT on May 14-09 GMT on May 15, 1981

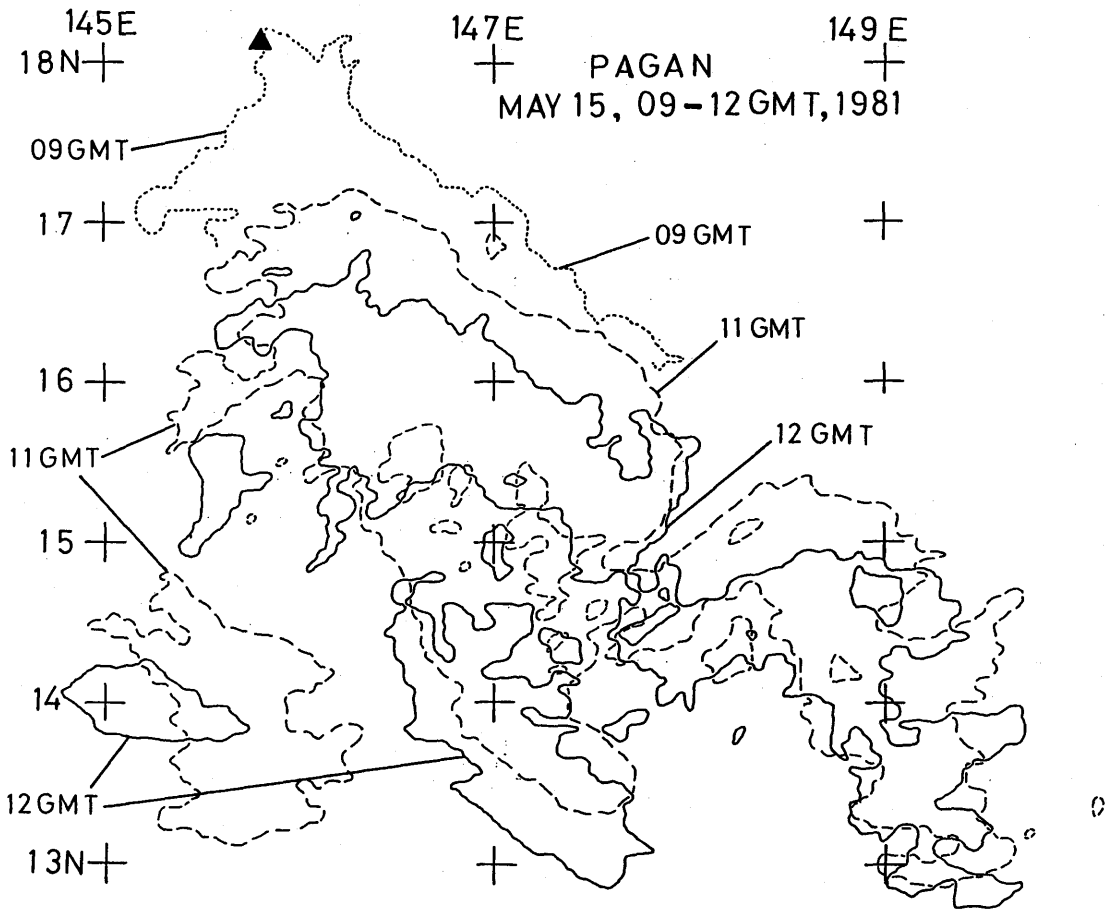

(b) 09 GMT-12 GMT on May 15, 1981

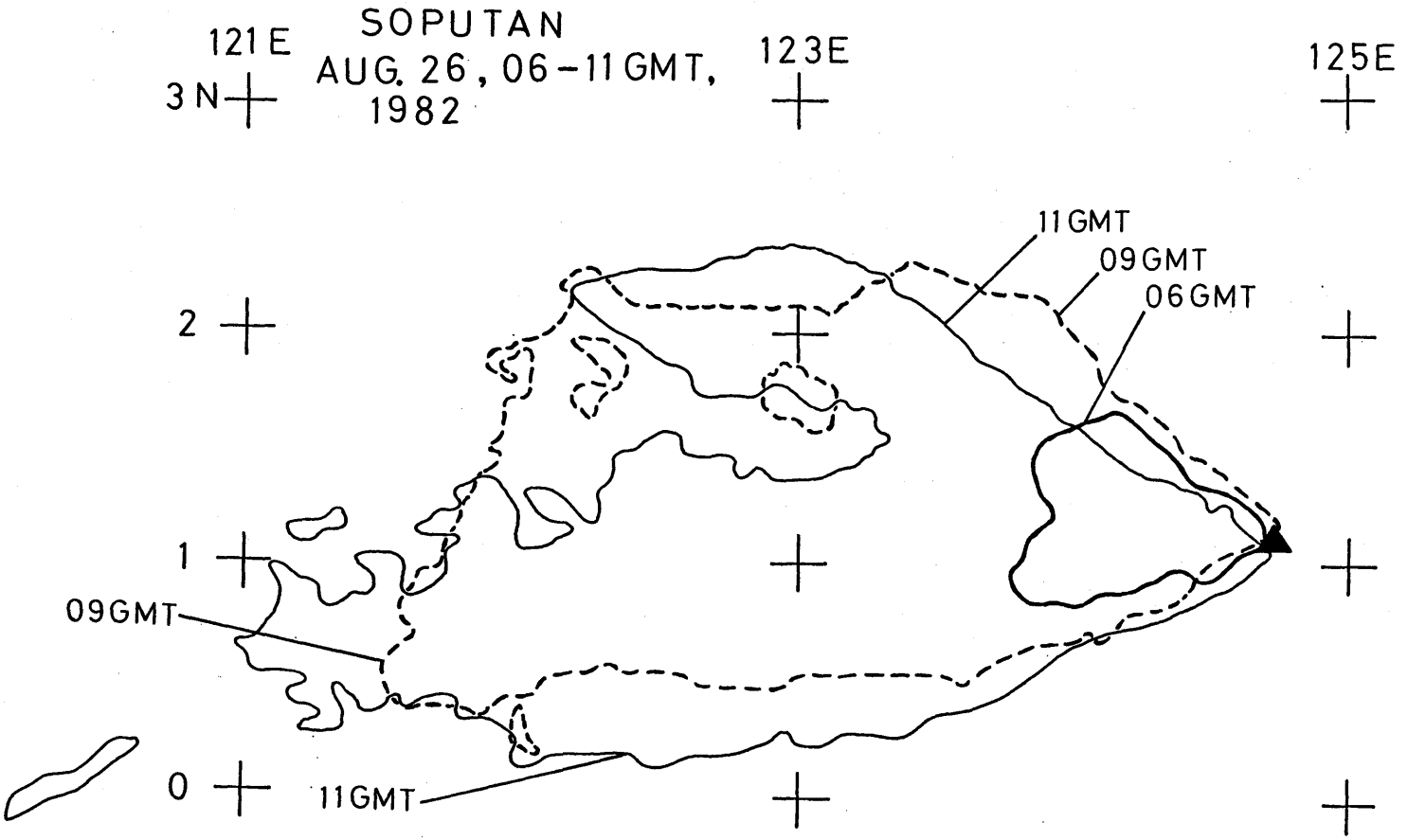

Fig. 4-6 Time variations of the extent colder than -10°C of Soputan eruption clouds.
(a) 06 GMT-11 GMT on August 26, 1982

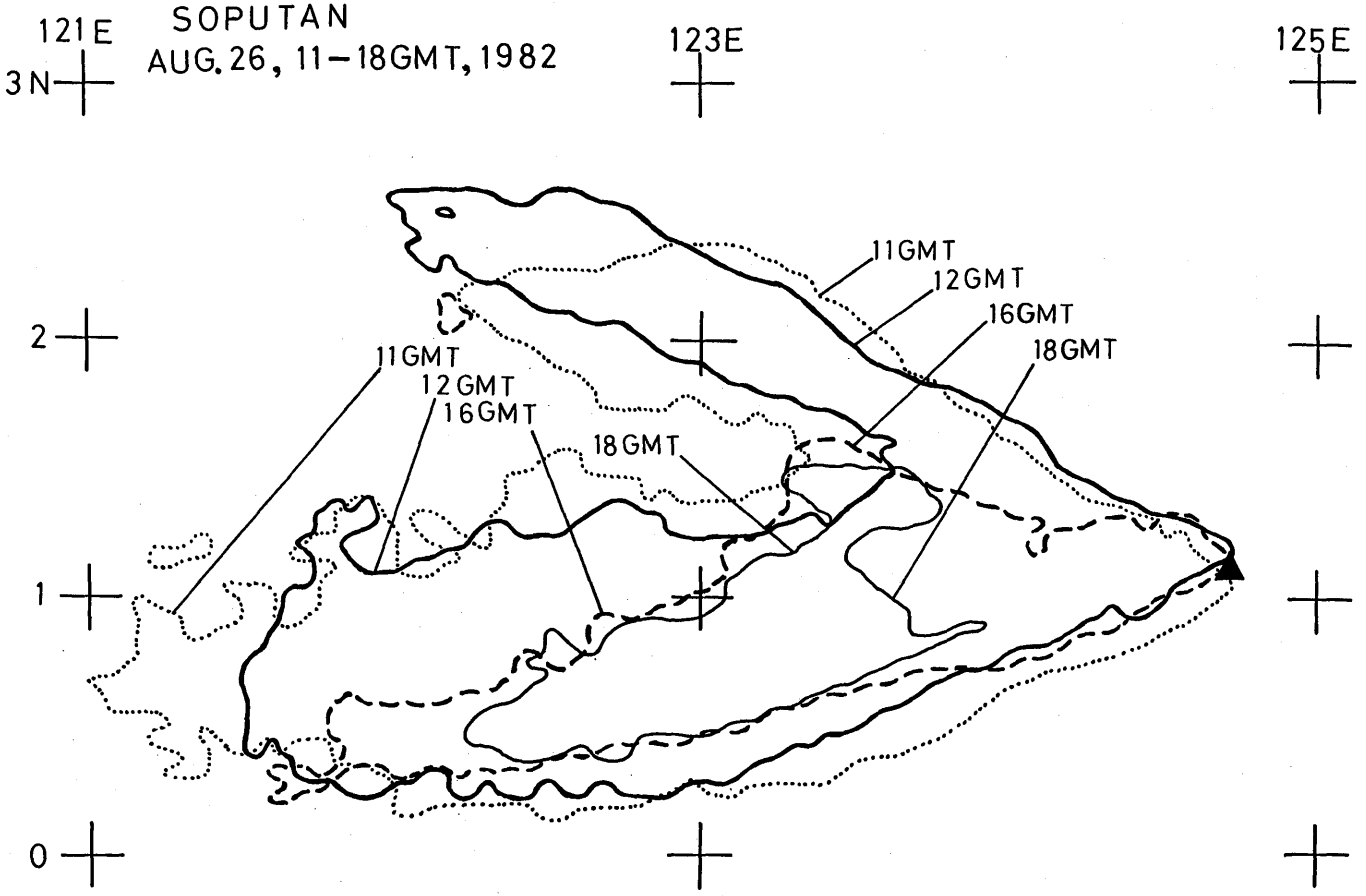

(b) 11 GMT-18 GMT on August 26, 1982

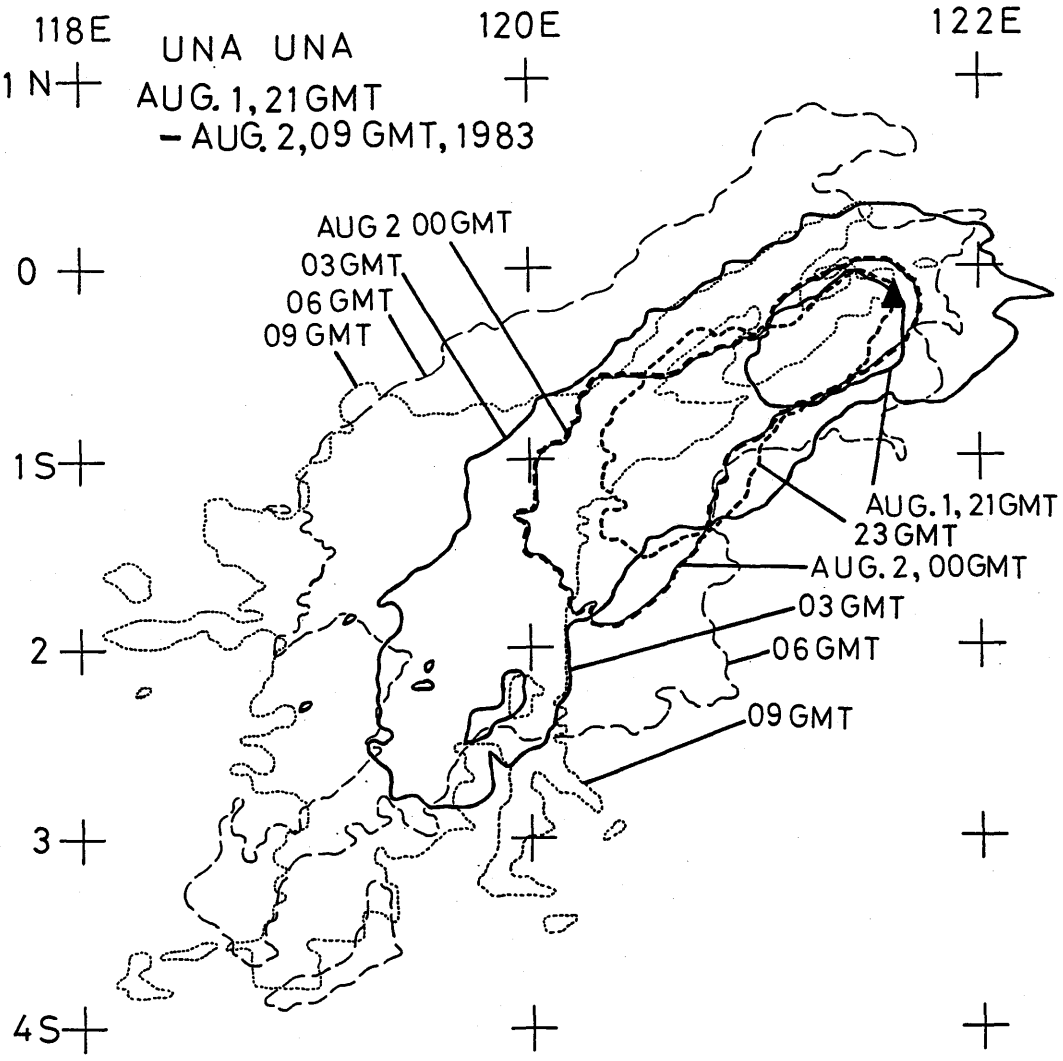

Fig. 4-7 Time variations of the extent colder than -10°C of Una Una eruption clouds during 21 GMT on August 1-09 GMT on August 2, 1983.

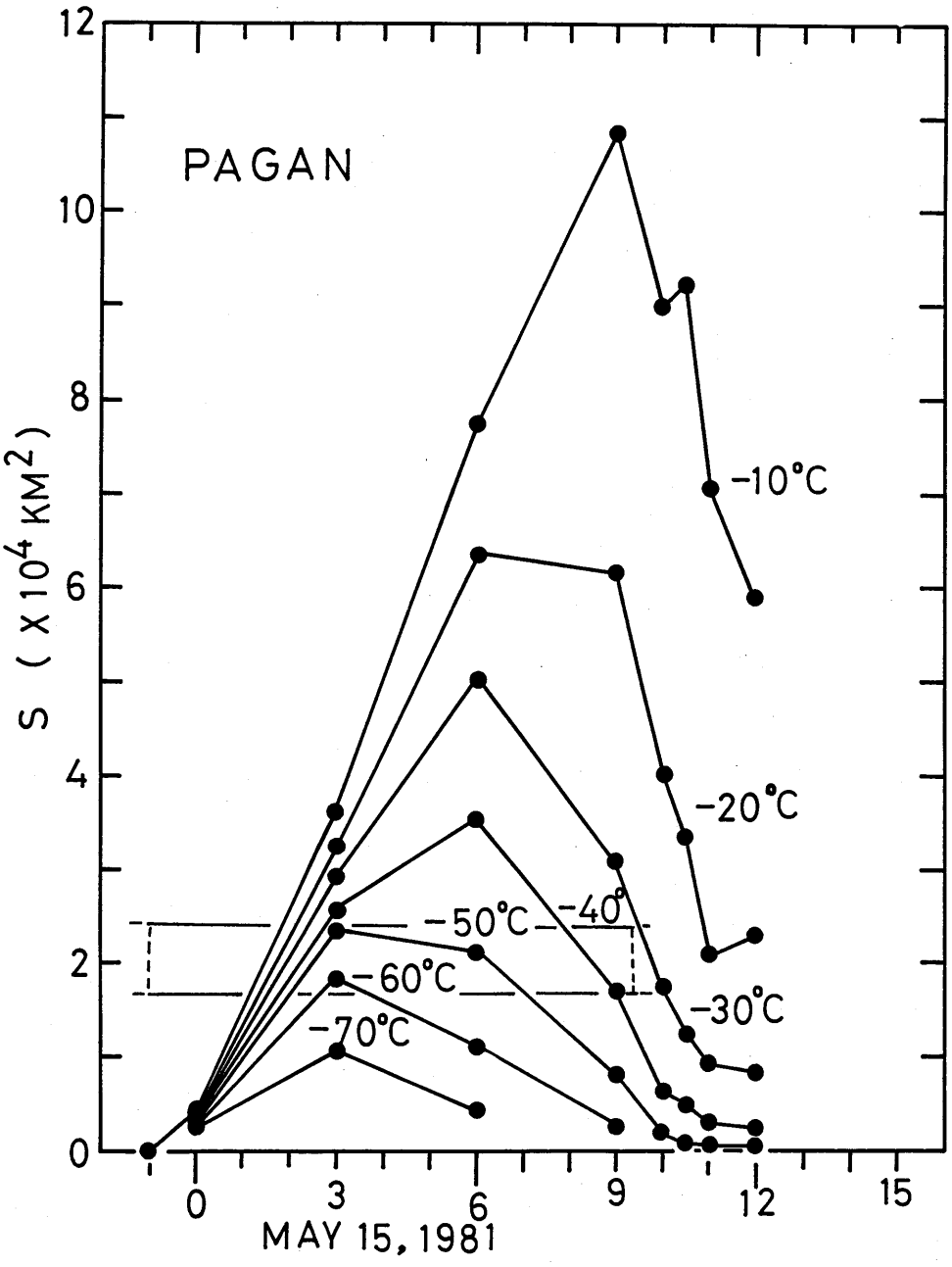

Fig. 4-8 Time variations of isothermal domains of the spreading eruption clouds. Rectangles denote duration periods of the individual eruptions.

(a) May 14-15, 1981, Pagan eruption cloud

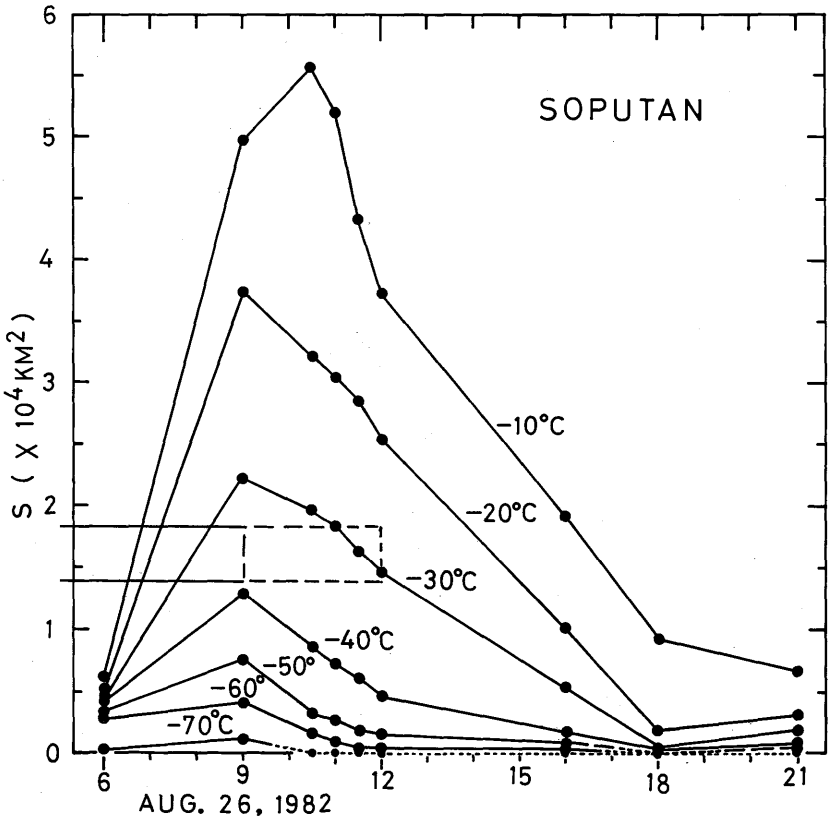

(b) August 26, 1982, Soputan eruption cloud

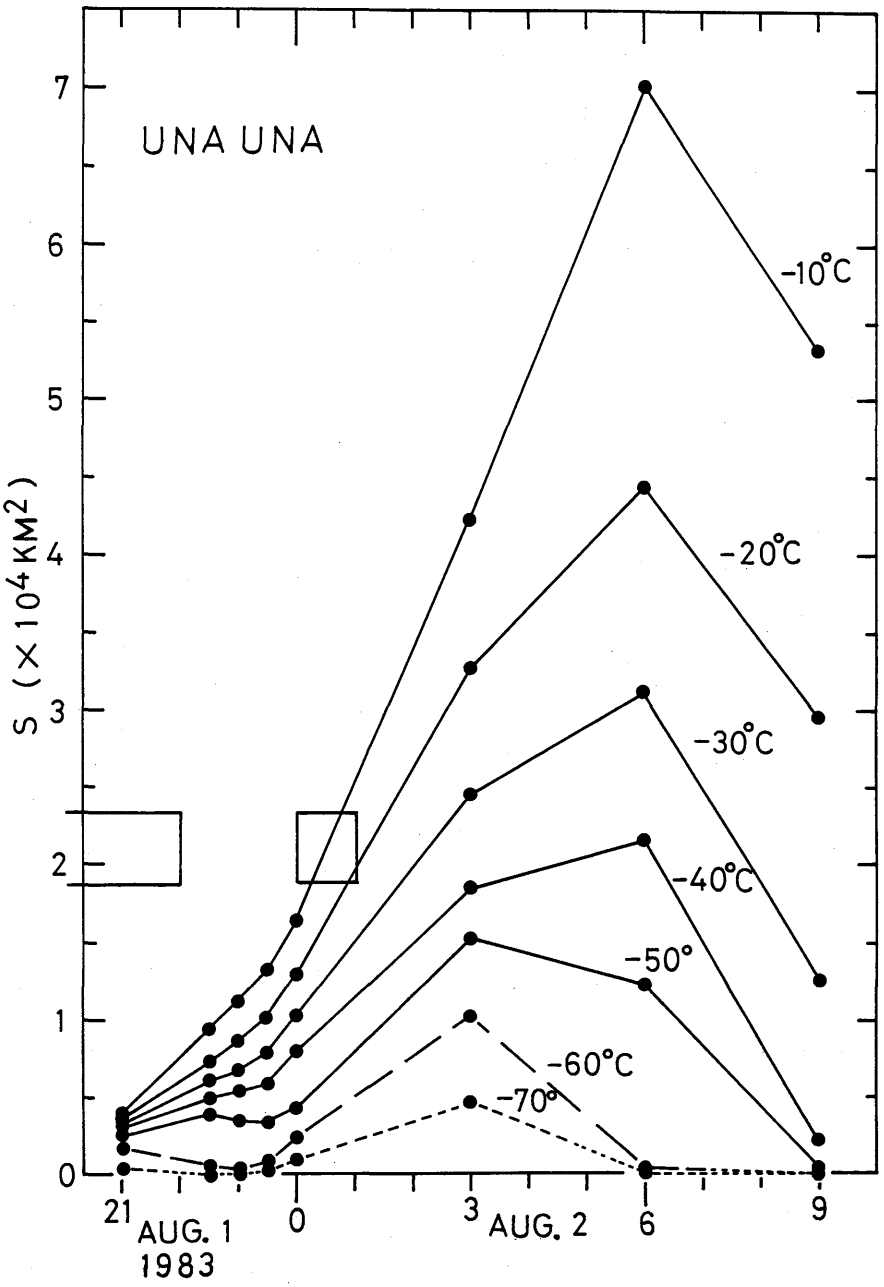

(c) August 1-2, 1983, Una Una eruption cloud

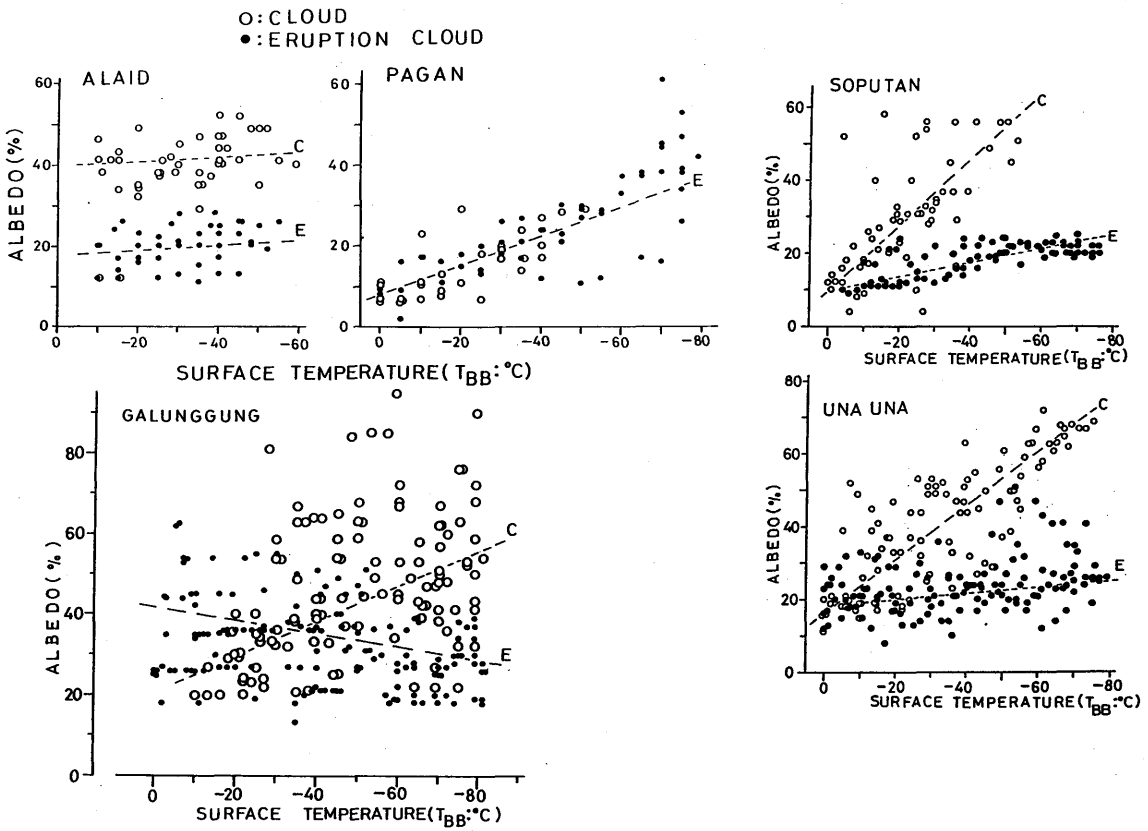

Fig. 5-1 Albedo in % v.s. suface-temperature in °C diagram for eruption cloud expressed by solid circle with letter E and atmospheric cloud by open circle with letter C, based on GMS's digital image data in cases of the eruption clouds from Alaid, Pagan, Soputan, Galunggung and Una Una volcanoes.

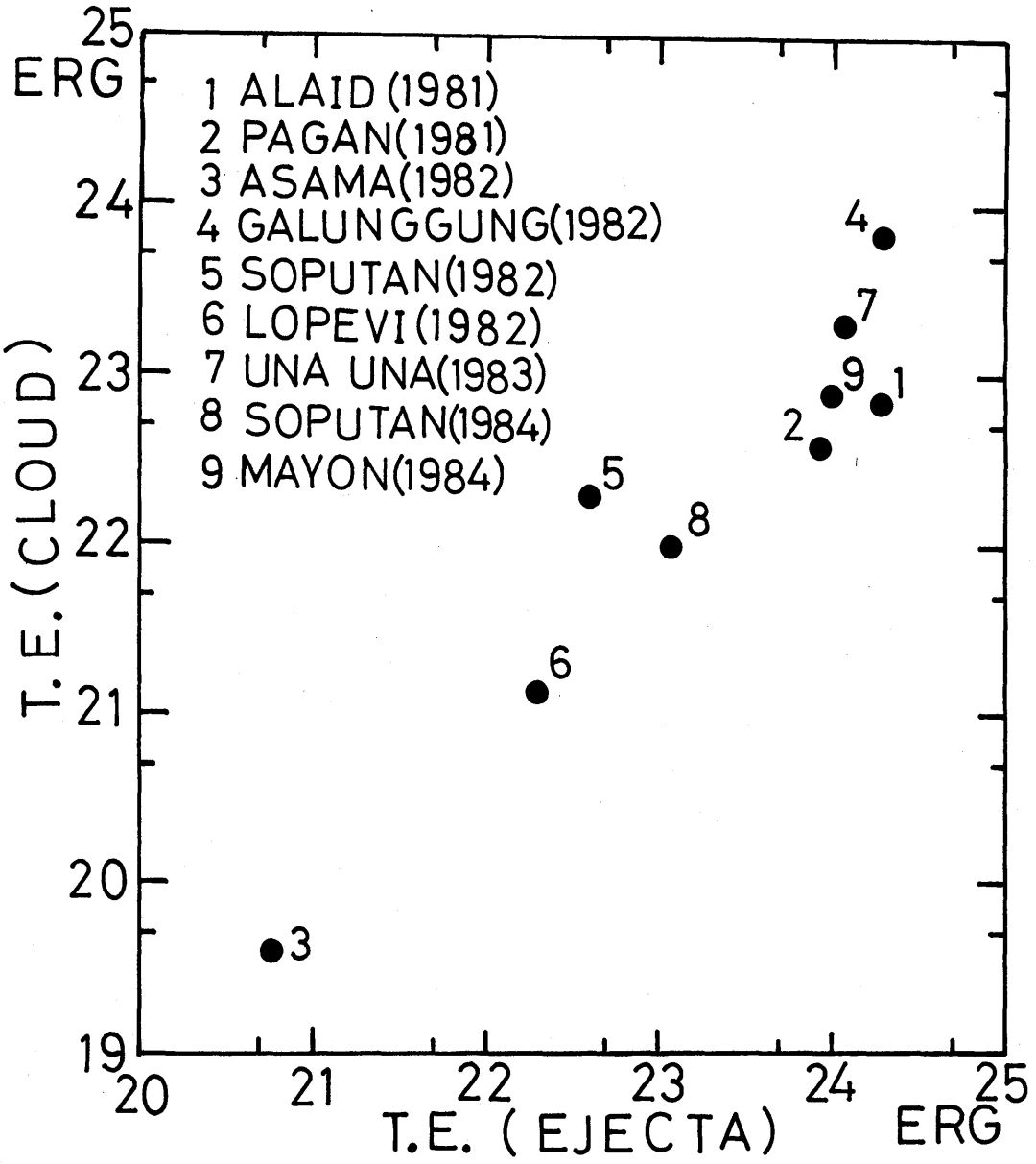

Fig. 5-2 Relationship between thermal energy releases by eruption cloud (T.E. (CLOUD)) and juvenile ejecta (T.E. (EJECTA)) for 9 eruptions as follows:

1 1981 Alaid	2 1981 Pagan	3 1982 Asama
4 1982 Galunggung	5 1982 Soputan	6 1982 Lopevi
7 1983 Una Una	8 1984 Soputan	9 1984 Mayon

where the scale of the vertical and horizontal axes in this figure are values for ten to the power in logarithmic scales.

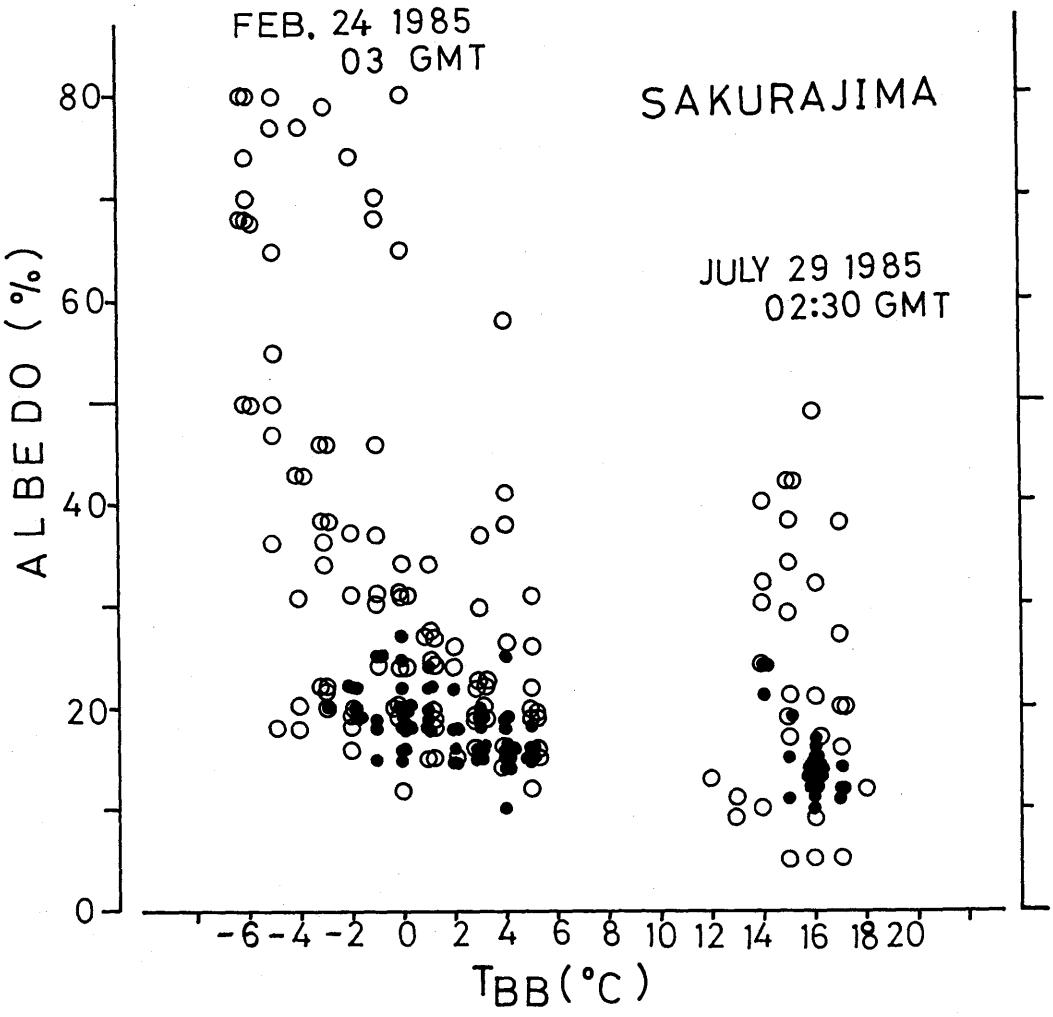

Fig. 5-3 Surface-temperature in °C v.s. albedo in % relationship between the Sakurajima eruption cloud (solid circle) and surrounding atmospheric cloud (open circle) detected by GMS images.

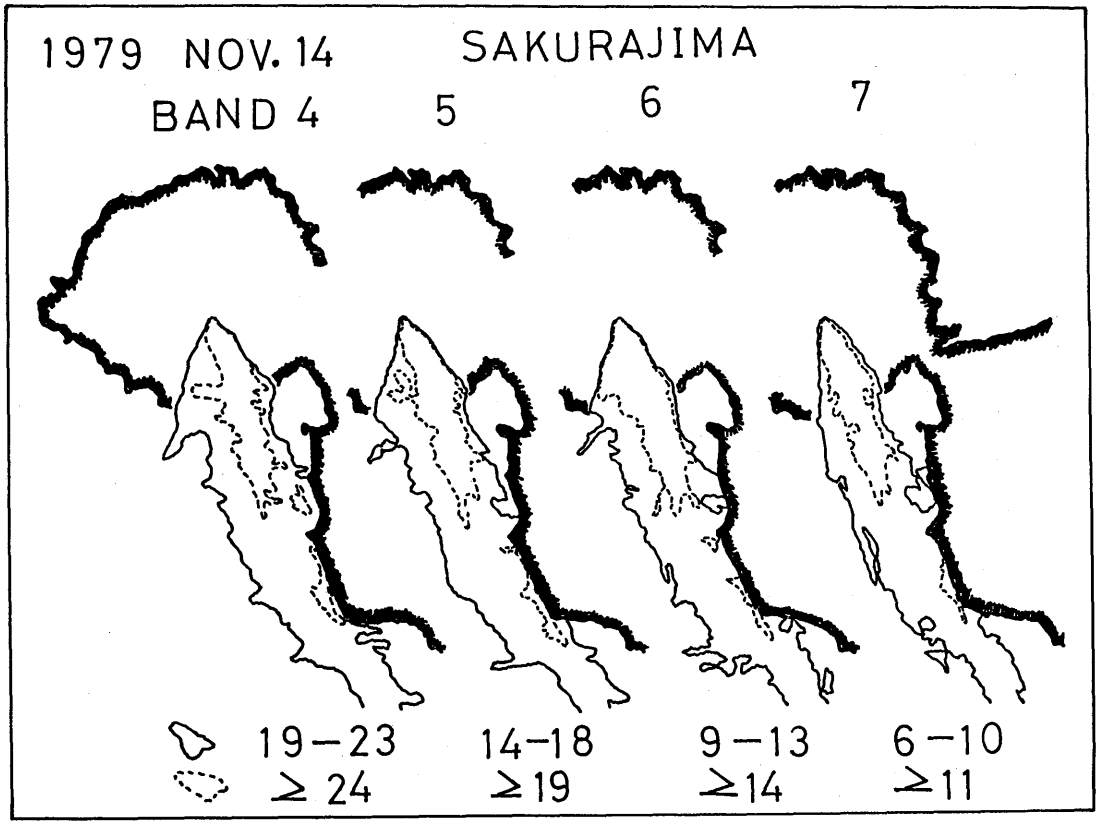

Fig. 5-4 Enhanced domains of the Sakurajima eruption cloud detected on November 14, 1979, on every 4 band images taken by LANDSAT MSS. Bold line means the shore line. Solid line and dotted one denote the extent of enhanced margin and bright-toned area of the eruption cloud, respectively. Numerals at the lower portion mean relative values of radiation-brightness assigned to a range of 0-127.

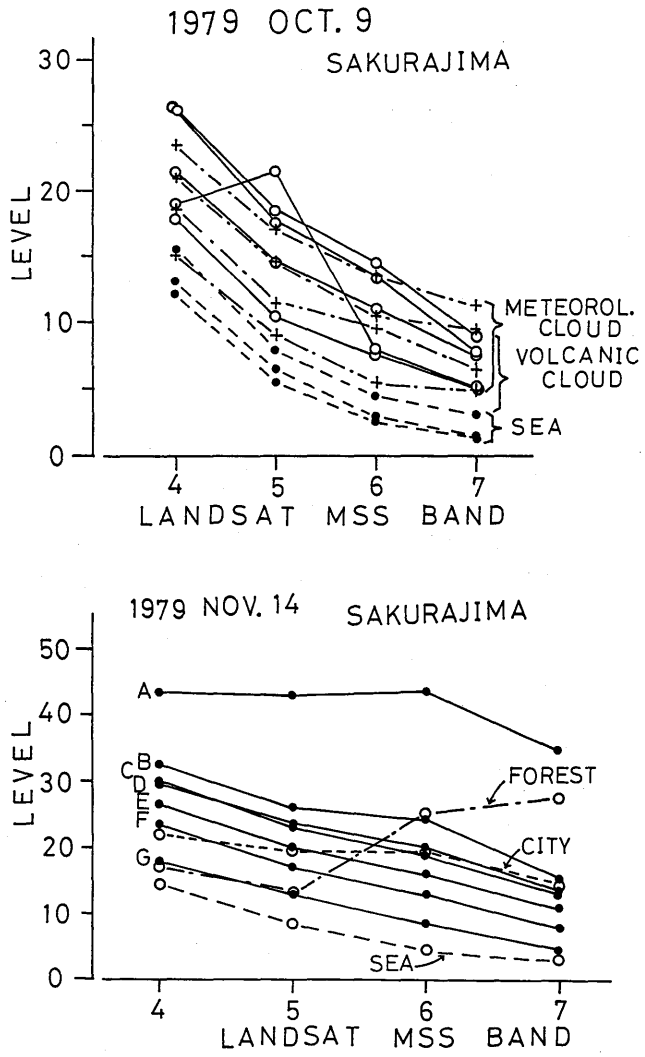

Fig. 5-5 Upper : Comparison between radiation-brightness patterns of eruption cloud (open circle), meteorological cloud (cross) and sea-surface (solid circle) in LANDSAT MSS image taken on October 9, 1979.

Lower : Comparison between radiation-brightness patterns of eruption cloud (solid circle), forest area (open circle with FOREST), city area (open circle with CITY) and sea-surface (open circle with SEA) in LANDSAT MSS taken on November 14, 1979.

LEVEL means relative radiation-brightness assigned to a range of 0-127. The eruption clouds in this figure are only the portions spread over the sea-surface.

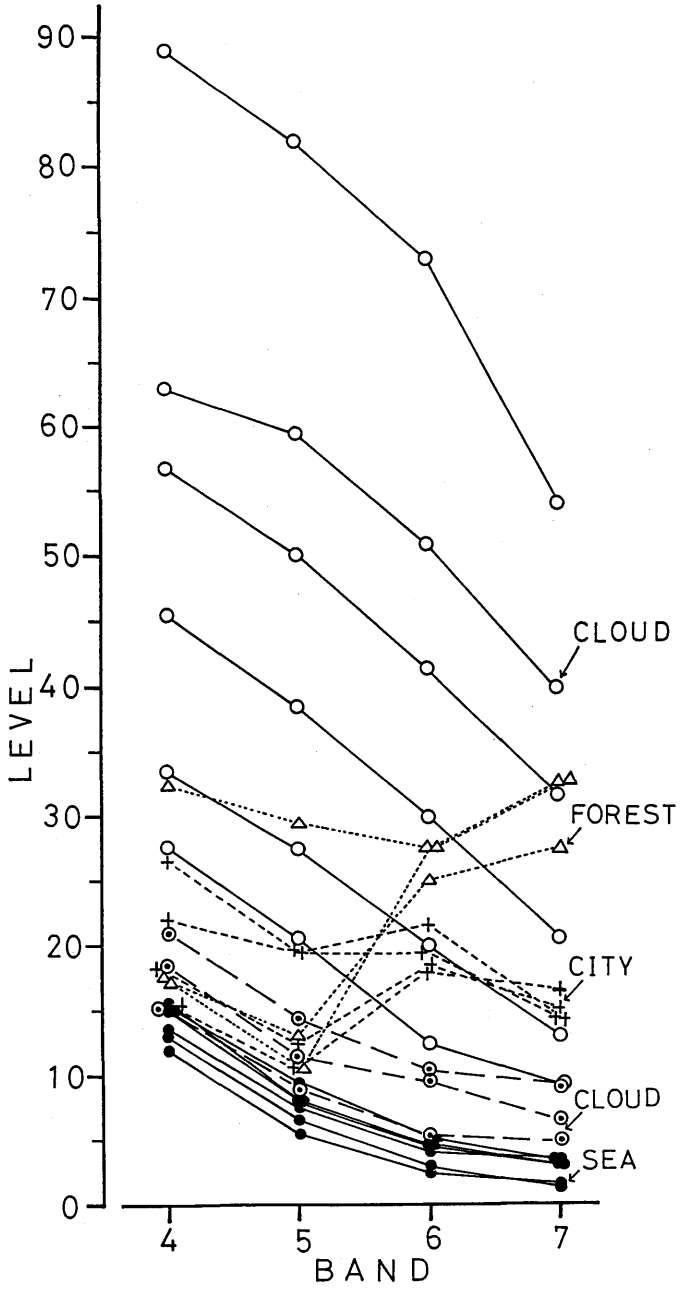

Fig. 5-6 Comparison between radiation-brightness patterns of various kinds of atmospheric cloud (open circle), forest area (triangle), city area (cross) and eruption cloud (double circle with CLOUD) and sea surface (solid circle) in LANDSAT MSS image taken on October 9, 1979. The eruption clouds in this figure are only the portions dispersed over the sea-surface.

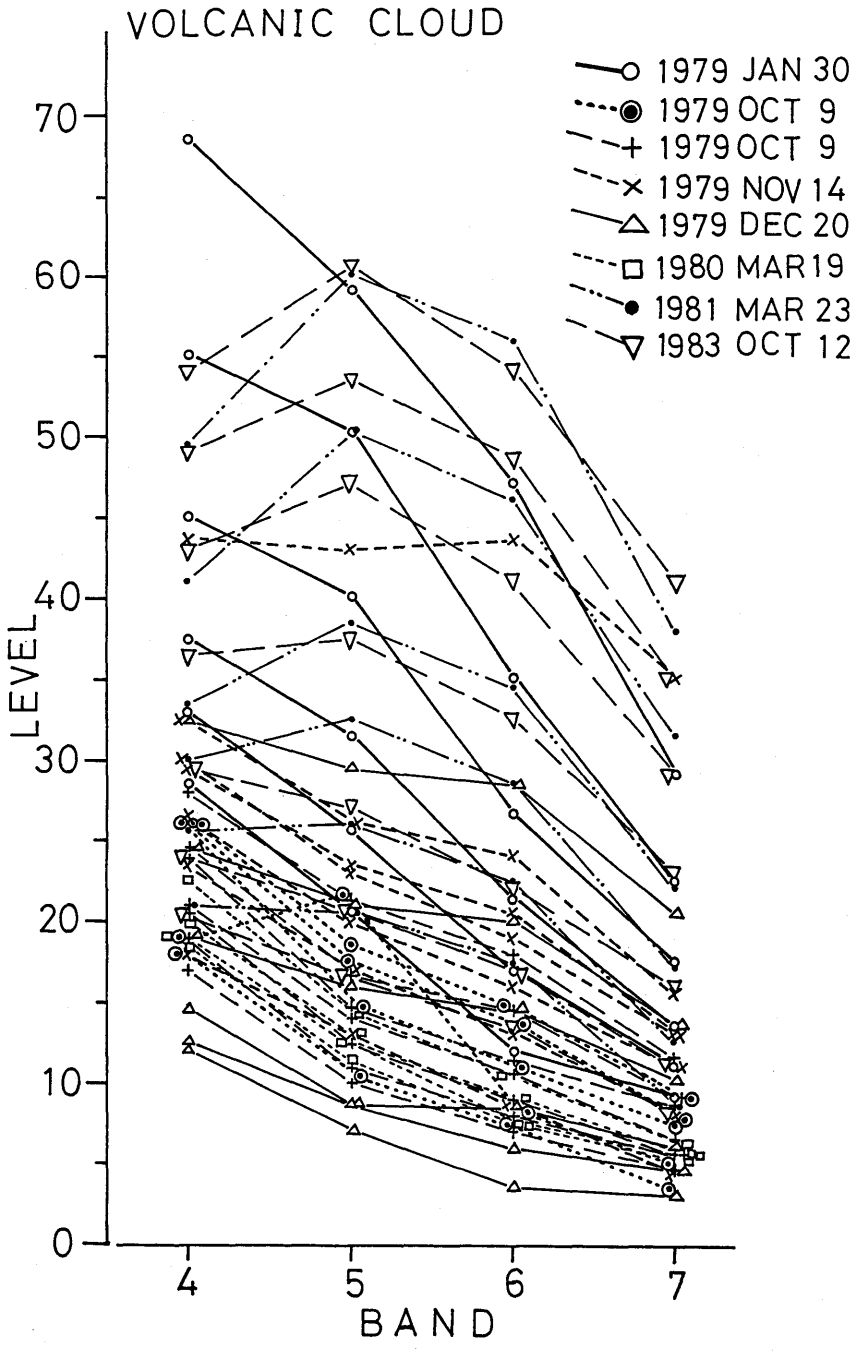

Fig. 5-7 Various radiation-brightness patterns of all of portions of eruption clouds detected in LANDSAT MSS images taken on January 30, October 9, November 14 and December 20, 1979, March 19, 1980, March 23, 1981 and October 12, 1983.